

Joint GSL-SEPM Research Conference

**External Controls on
Deep Water Depositional Systems:
Climate, Sea-level, and Sediment Flux**

Abstracts and Programme

March 27-29, 2006

Burlington House

London, UK

Conveners:

**Ben Kneller (Aberdeen), Ole Martinsen (Norsk Hydro), Bill McCaffrey (Leeds),
and Henry Posamentier (Anadarko Canada).**

Sponsors:

Anadarko

BP

Burlington

ConocoPhillips

Norsk-Hydro

Marathon

Shell

ORAL PROGRAM

MONDAY	MARCH 27	ORAL PROGRAM
9.00		Welcome and Introduction
		<u>Session 1: Overview</u>
9.20	Lambeck	Keynote: Sea level during glacial cycles: constraints on ice sheets and their rates of growth and decay during the past 140,000 years
10.00	Valdes	Keynote: Modelling Long Term Climate Change
10.40	break	
		<u>Session 2: Modern systems: big rivers</u>
11.10	Blum	Keynote: Fluvial responses to climate and sea-level change: implications for sediment delivery to the shelf margin and beyond
11.50	Dupont	Terrestrial input in the Congo fan system reveals Pleistocene climate changes expressed in vegetation records from tropical East Atlantic sediments.
12.20	Marsset	Climate control on the architecture of the Zaire Turbidite System?
12.40	Ducassou et al	The Nile deep-sea turbidite system: characterization and evolution of sedimentary processes during Late Quaternary
13.00	lunch	
14.00	Clift et al	The deep-water clastic sedimentary record of evolving climate and tectonics in the Arabian Sea
14.20	Schwenk & Spieß	The architecture of the Bengal Fan as response to tectonic and climatic changes in the Himalayan
14.40	Twichell et al	The effects of submarine canyon and proximal fan processes on the depositional systems of the distal Mississippi Fan
15.10	Maslin et al	Keynote: Heinrich event, Sea-Level and Avulsion Events on the Amazon Fan
15.50	Wood	Comparing and contrasting gravity processes in two large-scale margin depositional systems: the Orinoco and Amazon of northeastern South America
16.10	break	
		<u>Session 3: Modern systems: climate and tectonics</u>
16.40	Suter	Keynote: Shelf Margin Systems: Interface between Shallow Water Sediment Sources and Deep Water Sinks
17.20	Strachan et al	Submarine incision and renewed sediment influx during the Holocene: a case study from the Santa Monica Basin, California
17.40	Wynn et al	Timing and relation to climate/sea-level of giant landslides and turbidity currents on the Northwest African continental margin, from Morocco to Senegal
18.10		Wine Reception
19.30	close	
TUESDAY	MARCH 28	
8.30		Registration tea and coffee
		<u>Session 1: Modern systems: climate and tectonics (continued)</u>
9.00	Nakajima & Itaki	Late Quaternary terrestrial climatic changes recorded in deep-sea turbidites along the Toyama Deep-Sea Channel, central Japan Sea
9.20	Alonso	Late Glacial And Holocene Stratigraphy Of Four Small Turbidite Systems In The SW Mediterranean (Alboran Sea)

9.40	Garcia et al	Glaciomarine sedimentation of the Central Bransfield Basin shelf
10.00	Iorio	Utility of Palaeomagnetic Secular Variation in Late Pleistocene and Holocene Cored Sediment from the Gulf of Salerno, Eastern Tyrrhenian margin
10.20	Bozzano et al	Late Glacial And Holocene Depositional Patterns Of The Almeria Channel Levees (Sw Mediterranean)
10.40	break	
11.10	Gamberi & Marani	The influence of the age of back-arc basins on sediment influx and deep-sea clastic deposition: the Vavilov and the Marsili basins (Tyrrhenian Sea)
11.30	Weaver	Sedimentary processes throughout the North Atlantic. Glacial versus interglacial controls and comparisons between the eastern and western North Atlantic.
		<i>Session 2: Processes</i>
11.50	Paola	Keynote: Mass balance controls on offshore sediment delivery: experimental results
12.30	Dadson et al	Hyperpycnal River Flows from an Active Mountain Belt
12.50	Boyd	Highstand Sand Transport to Deep Water by Longshore Transport, Tidal and Gravity Processes
13.10	lunch	
14.10	Carvajal et al	Shelf Growth: Highstand versus Lowstand Sediment Delivery from Shelf Margins
14.30	Moscardelli & Wood	Morphometry of Mass-Transport Complexes in Offshore Trinidad
14.50	Munachen	Turbidity Current Generation from Submarine Debris-Flows: Flux Dynamics and Depositional Processes
15.10	Salles et al	Integrating basin-scale forcing parameters in density currents process-based modeling
15.30	Falcini et al	A simple three layers model for the eulerian behaviour of a turbidite current as a function of the Richardson number: sedimentological implication for the interpretation of the turbidite facies
15.50	break	
		<i>Session 3: Pre-Pleistocene Earth: the outcrop record</i>
16.20	Bralower	Keynote: Ancient Global Warming Events and their Implications for Sequence Stratigraphy and Evolution
16.40	Talling et al	Sediment Flux To Basin Plains, Bed Volumes, And External Controls On The Geometry Of Individual Turbidite Beds
17.20	Felletti et al	Sustained quasi-steady turbidity current: outcrop evidence from the Pliocene peri-Adriatic foredeep (Cellino Fm., Central Italy)
17.40	Stanzione	Tectonic and paleotopography control on turbidite sedimentation in confined basin: the lower Messinian wedge top sedimentation of the Laga Formation (Central Italy)
18.00	close	
		CONFERENCE DINNER

WEDNESDAY	MARCH 29	
8.30		Registration tea and coffee
		<u>Session 1: Pre-Pleistocene Earth: the outcrop record (continued)</u>
9.00	Martinsen	External controls on deep-water depositional systems in British Carboniferous Basins: responses to Gondwanan glaciations and evolving basin bathymetry
9.20	Eschard et al	Factors controlling sedimentation in the basin floor fan and the slope fans of the Pab Formation (Maastrichtian, Pakistan) : lessons from a stratigraphic modelling approach
9.50	Flint et al	Controls on Sediment flux, Routing and Storage and the impact on the Stratigraphic Development of Deepwater Basin Floor and Slope Systems, Karoo Basin, South Africa
10.10	break	
10.40	Gardner	Evaluating Extrinsic Controls on the Permian Record of Deep-Water Sedimentation in the Delaware Basin, West Texas, USA
11.10	Plink-Björklund	How do sediment flux and sea level changes control deepwater deposition? Implications from Eocene Central Basin of Spitsbergen
		<u>Session 2: Pre-Pleistocene Earth: the subsurface record</u>
11.40	Long et al	Tectono-stratigraphic History of Greater Mississippi Canyon, U. S. Gulf of Mexico
12.00	Lockhart et al	The Depositional Architecture of a Tithonian Lowstand Systems Tract in the Exmouth Sub-Basin, Western Australia
12.20	Lien et al	Deep water depositional systems along the Norwegian margin; external controls on reservoir development
12.40	lunch	
		<u>Session 3: Synthesis</u>
13.40	Smith & Burgess	Multi-source basins and approaches to stratigraphic prediction
14.00	Elliott & Pulham	The Role of Shelf-Edge Failures and Exceptional Sediment Gravity Flow Events in Submarine Fan Sedimentation and Stratigraphy
14.20	Legarth & Bjerrum	A numerical investigation of phosphate remobilization during sea-level change – implications for offshore phosphate and TOC deposition
14.40	break	
15.10	Bjerrum & Legarth	Modelling global organic carbon burial in response to sea level changes
15.30	Perlmutter	Cyclostratigraphy: Analysis of Precession-Scale Climate, Sediment & Sea Level Cycles to Understand Stratigraphic Variability
16.00	Nelson et al	Tectonic, volcanic, sedimentary, climatic, sea level, oceanographic, and anthropogenic controls on turbidite systems
16.30		concluding remarks
17.00		close

POSTER PROGRAM

1	Albianelli et al	<i>Climate control on the Pliocene deepwater deposits of the Periadriatic basin, central Italy</i>
2	Arzola	<i>Glacial-interglacial sedimentation in the deep continental margin off Portugal</i>
3	Bersezio et al	<i>Statistical analysis of stratal patterns and facies changes: deconvolving controls on the depositional architecture of deep-sea confined clastic units</i>
4	Ercilla et al	<i>Morpho-sedimentary features of the distal Cap Ferret Fan (Bay of Biscay, NE Atlantic Sea)</i>
5	Estrada	<i>The Plio-Quaternary Magdalena Turbidite System</i>
6	Foldager	<i>Inverse numerical modelling of mixed siliciclastic and carbonate sequence-stratigraphic systems, using the Metropolis algorithm in a Monte Carlo Inversion algorithm</i>
7	Frenz	<i>Sources and timing of the Agadir Basin turbidite fill, NW Africa</i>
8	Gamberi	<i>The impact of margin shaping processes on the architecture of deep-sea depositional systems: the Sicilian and Sardinian margins (Tyrrhenian Sea)</i>
9	Gutiérrez-Pastor et al	<i>Holocene turbidite history in the Cascadia Subduction Zone shows the potential to develop paleoseismic methods for the Sumatra and other subduction zones</i>
10	Lobo et al	<i>Plio-Quaternary development of small-scale submarine valleys in the northern margin of the Alboran Sea in relation with sea-level changes</i>
11	Maponi & Salusti	<i>On Forced Instabilities Of Density – Turbidity Marine Currents</i>
12	Nelson et al	<i>Holocene Turbidite Paleoseismic Record Of Great Earthquakes On The Cascadia Subduction Zone: Confirmation By Onshore Records And The Sumatra 2004 Great Earthquake</i>
13	Normark et al	<i>Late Quaternary (MIS 1-3) turbidite deposition in the California Continental Borderland: Comparison of closed and open basin settings</i>
14	Tropeano et al (a)	<i>The Offlap Break Position Vs Sea Level: A Discussion</i>
15	Tropeano et al (b)	<i>Sedimentary response to low- and high-frequency relative sea-level changes during the Quaternary filling of a foreland basin (Bradanic Trough, southern Italy)</i>

TABLE OF CONTENTS

ORAL PROGRAM	2
POSTER PROGRAM	5
TABLE OF CONTENTS	6
ORAL ABSTRACTS	12
Late Glacial And Holocene Stratigraphy Of Four Small Turbidite Systems In The SW Mediterranean (Alboran Sea)	12
<i>Alonso, B., Ercilla, G., Bozzano, G., Casas, D., and Lebreiro, S.</i>	12
Modelling global organic carbon burial in response to sea level changes	14
<i>Bjerrum, C.J.*, and J. J. F. Legarth, J.J.F.</i>	14
Fluvial responses to climate and sea-level change: implications for sediment delivery to the shelf margin and beyond	16
<i>Blum, Mike and Hattier-Womack, Jill</i>	16
Highstand Sand Transport to Deep Water by Longshore Transport, Tidal and Gravity Processes	17
<i>Boyd, R.¹, Ruming, K.¹, Sandstrom, M.², and Schroder-Adams, C.³</i>	17
Late Glacial And Holocene Depositional Patterns Of The Almeria Channel Levees (SW Mediterranean)	18
<i>Bozzano, G.*, Alonso, B., Ercilla, G., Casas, D., Estrada, F., and García, M.</i>	18
Ancient Global Warming Events and their Implications for Sequence Stratigraphy and Evolution	20
<i>Bralower, Timothy J.</i>	20
Shelf Growth: Highstand versus Lowstand Sediment Delivery from Shelf Margins	21
<i>Carvajal, C., Petter, A., Uroza, C., and Steel, R.</i>	21
The deep-water clastic sedimentary record of evolving climate and tectonics in the Arabian Sea	22
<i>Clift, P.¹, Schwab, A.¹, Calves, G.¹, Giosan, L.², Blusztajn, J.², Tabrez, A.³, Danish, M.³, Inam, A.³, Alizai, A.⁴</i>	22
Hyperpycnal River Flows from an Active Mountain Belt	23
<i>Dadson, S.^{1,2}, Hovius, N.¹, Pegg, S.¹, Dade, W.D.³, Horng, M.J.⁴, and Chen, H.⁵</i>	23
The Nile deep-sea turbidite system: characterization and evolution of sedimentary processes during Late Quaternary	25
<i>Ducassou E., Migeon S., Mulder T., Gonthier E., Murat A., Bernasconi S., Duprat J., Capotondi L. and Mascle J.</i>	25
Terrestrial input in the Congo fan system reveals Pleistocene climate changes expressed in vegetation records from tropical East Atlantic sediments	26

<i>Dupont, L.</i>	26
The Role of Shelf-Edge Failures and Exceptional Sediment Gravity Flow Events in Submarine Fan Sedimentation and Stratigraphy	28
<i>Trevor Elliott, T.¹, and Pulham, A.²</i>	28
Factors controlling sedimentation in the basin floor fan and the slope fans of the Pab Formation (Maastrichtian, Pakistan) : lessons from a stratigraphic modelling approach	29
<i>Eschard, R.^{1*}, Euzen, T.¹, Granjeon, D.¹, and Lopez, S.</i>	29
A simple three layers model for the eulerian behaviour of a turbidite current as a function of the Richardson number: sedimentological implication for the interpretation of the turbidite facies	31
<i>Falcini, F.^{1*}, Milli, S.¹, Moscatelli, M.², Stanzione, O.¹, and Salusti, E.³</i>	31
Sustained quasi-steady turbidity current: outcrop evidence from the Pliocene peri-Adriatic foredeep (Cellino Fm., Central Italy)	34
<i>Felletti, F.¹, Carruba, S.², and Casnedi, R.²</i>	34
Controls on Sediment flux, Routing and Storage and the impact on the Stratigraphic Development of Deepwater Basin Floor and Slope Systems, Karoo Basin, South Africa	36
<i>Flint, S., Hodgson, D., King, R., van Lente, B., Wild, R., and Potts, G.</i>	36
Inverse numerical modelling of mixed siliciclastic and carbonate sequence-stratigraphic systems, using the Metropolis algorithm in a Monte Carlo Inversion algorithm	37
<i>Foldager, R.*</i>	37
The impact of margin shaping processes on the architecture of deep-sea depositional systems: the Sicilian and Sardinian margins (Tyrrhenian Sea)	38
<i>Gamberi, F.</i>	38
The influence of the age of back-arc basins on sediment influx and deep-sea clastic deposition: the Vavilov and the Marsili basins (Tyrrhenian Sea)	39
<i>Gamberi, F., and Marani, M.P.</i>	39
Glaciomarine sedimentation of the Central Bransfield Basin shelf	41
<i>García, M.^{1*}, Anderson, J.B.², Ercilla, G.¹, and Alonso, B.¹</i>	41
Valuing Intrinsic and Extrinsic Controls on the Permian Record of Deep-Water Sedimentation in the Delaware Basin, West Texas, USA	43
<i>Gardner, M. H. ¹, Melick, J. J. ¹, Borer, J. M. ², Kling, E. ², Baptista, N. ³, and Romans, B. ⁴</i>	43
Channel Avulsion Patterns In Some Major Deep-Sea Fans—External Versus Internal Controls	45
<i>Kolla, V.¹, and Posamentier, H.W. ²</i>	45
Sea-level change during glacial cycles: constraints on ice sheets and their rates of growth and decay during the past 140,000 years with results from arctic Eurasia and the Mediterranean.	46
<i>Kurt Lambeck,</i>	46

A numerical investigation of phosphate remobilization during sea-level change – implications for offshore phosphate and TOC deposition	47
<i>Legarh, J.J.F. *, and Bjerrum, C.J.</i>	<i>47</i>
Utility of Palaeomagnetic Secular Variation in Late Pleistocene and Holocene Cored Sediment from the Gulf of Salerno, Eastern Tyrrhenian margin	48
<i>Liddicoat^a, J., Iorio^b, M., Budillon^b, F., Tiano^c, P., Incoronato^c, A., Coe^d, R., D'Argenio^b, B., and Marsella^b, E.....</i>	<i>48</i>
Deep water depositional systems along the Norwegian margin; external controls on reservoir development	50
<i>Lien, T. *</i>	<i>50</i>
The Depositional Architecture of a Tithonian Lowstand Systems Tract in the Exmouth Sub-Basin, Western Australia.....	51
<i>Lockhart, D.¹, Stark, C.J.², Rosser, J³, Burns, F.E.² and Gamarra, S³.....</i>	<i>51</i>
Tectono-stratigraphic History of Greater Mississippi Canyon, U. S. Gulf of Mexico	53
<i>Long, M.S.¹*, Helsing, C.E.¹, Berman D.C.¹, Deemer, D.L.², and Albert, R³</i>	<i>53</i>
On Forced Instabilities of Density – Turbidity Marine Currents	55
<i>Maponi, P. ¹, and Salusti, E².....</i>	<i>55</i>
Climate control on the architecture of the Zaire turbidite system?	56
<i>Marsset, T.¹*, Droz, L.², Dennielou, B.¹, Savoye, B.¹, and Bez, M³.....</i>	<i>56</i>
External controls on deep-water depositional systems in British Carboniferous basins: responses to Gondwanan glaciations and evolving basin bathymetry	58
<i>Martinsen, Ole J.</i>	<i>58</i>
Heinrich event, Sea-Level and Avulsion Events on the Amazon Fan.....	59
<i>Maslin, M.¹*, Knutz, P.C.², and Ramsay, T³.....</i>	<i>59</i>
Cyclostratigraphy: Analysis of Precession-Scale Climate, Sediment & Sea Level Cycles to Understand Stratigraphic Variability.....	60
<i>Perlmutter, M.¹, Moore, T.², and Urwongse, T³.....</i>	<i>60</i>
Morphometry of Mass-Transport Complexes in Offshore Trinidad.....	61
<i>Moscardelli, L.¹, and Wood, L².....</i>	<i>61</i>
Turbidity Current Generation from Submarine Debris-Flows: Flux Dynamics and Depositional Processes	63
<i>Munachen, S.E.</i>	<i>63</i>
Late Quaternary terrestrial climatic changes recorded in deep-sea turbidites along the Toyama Deep-Sea Channel, central Japan Sea	65
<i>Nakajima, T.¹, and Itaki, T².....</i>	<i>65</i>
Tectonic, volcanic, sedimentary, climatic, sea level, oceanographic, and anthropogenic controls on turbidite	

systems	66
<i>Nelson, C.H.¹, Escutia, C.¹, Goldfinger, C.², Gutiérrez-Pastor, J.¹, Karabanov, E.³</i>	<i>66</i>
Mass balance controls on offshore sediment delivery: experimental results.....	68
<i>Paola, C.</i>	<i>68</i>
How do sediment flux and sea level changes control deepwater deposition?	69
Implications from Eocene Central Basin of Spitsbergen	69
<i>Plink-Björklund, P.</i>	<i>69</i>
Facies architecture and sediment composition of Middle-Upper Jurassic base-of-slope successions, central Apennines, Italy	70
<i>Rusciadelli, G.</i>	<i>70</i>
Integrating basin-scale forcing parameters in density currents process-based modeling	71
<i>Salles, T., Lopez, S., Euzen, T., and Eschard, R.....</i>	<i>71</i>
The architecture of the Bengal Fan as response to tectonic and climatic changes in the Himalayan	73
<i>Schwenk, T., and Spieß, V.....</i>	<i>73</i>
Multi-source basins and approaches to stratigraphic prediction.....	74
<i>Smith, R.D.A., and Burgess, P.M.</i>	<i>74</i>
Tectonic and paleotopography control on turbidite sedimentation in confined basin: the lower Messinian wedge top sedimentation of the Laga Formation (Central Italy)	75
<i>Stanzione, O.¹, Milli, S.¹, Moscatelli, M.², and Falcini, F.¹</i>	<i>75</i>
Submarine incision and renewed sediment influx during the Holocene: a case study from the Santa Monica Basin, California	77
<i>Strachan, L.J.^{1*}, Schimmelmann, A.², Lange, C.³, Kneller, B.⁴, and McCaffrey, W.⁵</i>	<i>77</i>
Shelf Margin Systems: Interface between Shallow Water Sediment Sources and Deep Water Sinks.....	78
<i>Suter, John R.</i>	<i>78</i>
Sediment Flux To Basin Plains, Bed Volumes, And External Controls On The Geometry Of Individual Turbidite Beds.....	79
<i>Talling, P.J.¹, Amy, L.A.¹, and Wynn, R.B.².....</i>	<i>79</i>
The effects of submarine canyon and proximal fan processes on the depositional systems of the distal Mississippi Fan.....	81
<i>Twichell, D.C.¹, Schwab, W.C.¹, Nelson, C.H.², and Kenyon, N.H.³</i>	<i>81</i>
Modelling Long Term Climate Change.....	83
<i>Valdes, Paul</i>	<i>83</i>
Sedimentary processes throughout the North Atlantic. Glacial versus interglacial controls and comparisons	

between the eastern and western North Atlantic	84
<i>Weaver, P.P.E., and Benetti, S.....</i>	<i>84</i>
Influences on deep-marine sedimentation along the continental margins of northeastern South America: Orinoco and Amazon systems	86
<i>Wood, Lesli J., and Moscardelli, Lorena</i>	<i>86</i>
Timing and relation to climate/sea-level of giant landslides and turbidity currents on the Northwest African continental margin, from Morocco to Senegal.....	87
<i>Wynn, R.B.* and the UK-TAPS group.....</i>	<i>87</i>
POSTER ABSTRACTS	89
Climate control on the Pliocene deepwater deposits of the Periadriatic basin, central Italy.....	89
<i>Albianelli, A.¹, Cantalamessa, G.², Di Celma, C.², Didaskalou, P.², Lori, P.², Napoleone, G.¹, and Potetti, M.²</i>	<i>89</i>
Glacial-interglacial sedimentation in the deep continental margin off Portugal	91
<i>Arzola, R.....</i>	<i>91</i>
Statistical analysis of stratal patterns and facies changes: deconvolving controls on the depositional architecture of deep-sea confined clastic units.....	92
<i>Bersezio, R., Felletti, F., Micucci, L., and Riva, S.</i>	<i>92</i>
Morpho-sedimentary features of the distal Cap Ferret Fan (Bay of Biscay, NE Atlantic Sea)	93
<i>Ercilla, G., and Marconi Team.....</i>	<i>93</i>
The Plio-Quaternary Magdalena Turbidite System	95
<i>Estrada, F.*, Alonso, B., and Ercilla, G.....</i>	<i>95</i>
Sources and timing of the Agadir Basin turbidite fill, NW Africa	97
<i>Frenz, M., Wynn, R.B., and Masson, D.G.</i>	<i>97</i>
Holocene turbidite history in the Cascadia Subduction Zone shows the potential to develop paleoseismic methods for the Sumatra and other subduction zones	98
<i>Gutiérrez-Pastor, J.¹*, Nelson, C.H.¹, Goldfinger, C.², and Johnson, J.³.....</i>	<i>98</i>
Plio-Quaternary development of small-scale submarine valleys in the northern margin of the Alboran Sea in relation with sea-level changes.....	100
<i>Lobo, F.J.¹, Fernández-Salas, L.M.², Ercilla, G.³, Alonso, B.³, García, M.³, Escutia, C.¹, Maldonado, A.¹, and Gómez, M.⁴</i>	<i>100</i>
Holocene Turbidite Paleoseismic Record Of Great Earthquakes On The Cascadia Subduction Zone: Confirmation By Onshore Records And The Sumatra 2004 Great Earthquake	102
<i>Nelson, C.H.¹, Goldfinger, C.², Gutiérrez-Pastor, J.¹, and Johnson, J.E.³</i>	<i>102</i>
Late Quaternary (MIS 1-3) turbidite deposition in the California Continental Borderland: Comparison of closed	

and open basin settings	104
<i>Normark, W.R.¹, Piper, D.J.W.², Romans, B.W.³, Covault, J.A.³, and McGann, M.¹</i>	<i>104</i>
The Offlap Break Position Vs Sea Level: A Discussion.....	105
<i>Tropeano, M.^{1*}, Pomar, L.², and Sabato, L.¹</i>	<i>105</i>
Sedimentary response to low- and high-frequency relative sea-level changes during the Quaternary filling of a foreland basin (Bradanic Trough, southern Italy)	106
<i>Tropeano, M., Sabato*, L., Cilumbriello, A., and Pieri, P.</i>	<i>106</i>

ORAL ABSTRACTS

Late Glacial And Holocene Stratigraphy Of Four Small Turbidite Systems In The SW Mediterranean (Alboran Sea)

Alonso, B., Ercilla, G., Bozzano, G., Casas, D., and Lebreiro, S.

CSIC, Instituto de Ciencias del Mar, Passeig Maritim de la Barceloneta, 37-49, 08003 Barcelona.

The contribution of this work is to define the Last glacial and Holocene stratigraphy of four turbidite systems (TSs) of the Northern Alboran Sea (SW Mediterranean), in order to explain their depositional history and controlling factors. This work is based on sedimentological analysis and radiocarbon dating (^{14}C) of gravity cores (< 3 m long) recovered from water depths between 100 m to 1,624 m.

Four small turbidite systems (Almeria, Sacratif, Calahonda, and Guadiaro) each tens of kilometres long are developed in the complex morphostructural setting of the Northern Alboran Sea (SW Mediterranean) (Figure 1). They have similar primary architectural elements (canyons, channel-levee systems, and lobes) (Alonso and Ercilla, 2003).

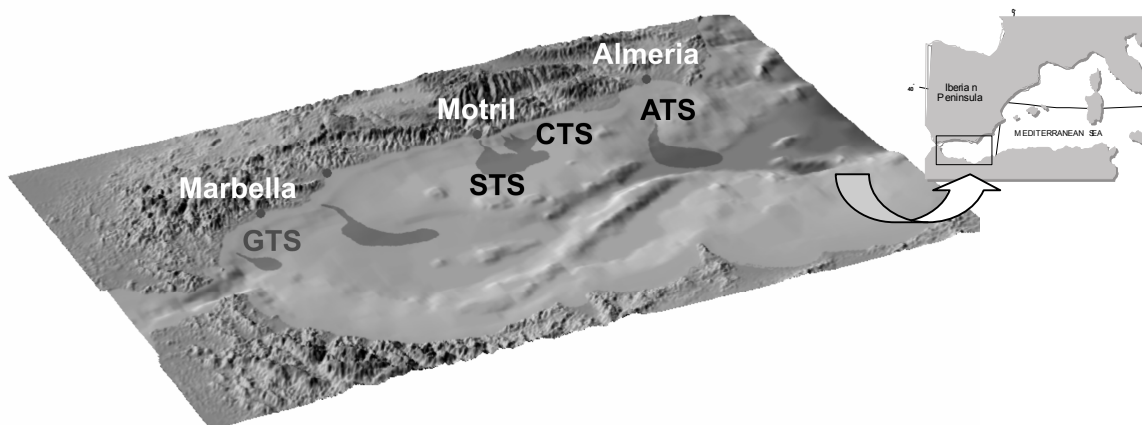


Figure 1. Location map of the four studied turbidite systems developed in the Northern margin of the Alboran Sea. Legend: ATS, Almeria; CTS, Calahonda, STS Sacratif; and GTS, Guadiaro.

The Almeria TS develops on the Almeria Margin (120 m to 1800 m water depth) and Alboran Trough (> 1800 m water depth). It is fed by the Andarax River, a relatively long submarine canyon (55 km) and several tributaries valley systems (Dalias, Andarax and Gata) that erode the shelf and slope deposits (Garcia et al., 2005). The course of the Almeria Canyon is affected by the Serrata and Cape of Gata faults and its axial gradient changes are largely controlled by the morpho-tectonic setting (Woodside and Maldonado, 1992). The Calahonda TS develops from Motril slope (200 m water depth) to base of slope (850 m water depth). It is fed by ephemeral rivers, several gullies that are eroding the shelf margin deposits, and four small slope canyons. The Sacratif TS develops from Motril shelf to Motril Basin (890 m water depth). It is fed by the Guadalfeo River and two important canyons that erode the shelf deposits. The Guadiaro TS develops from the Marbella slope to base of slope (800 m water depth). It is fed by the Guadiaro River and by a short slope canyon (7 km).

The main sediment types defined into the four mentioned TSs are the following: hemipelagites, hemiturbidites, turbidites (Ta to Te divisions), debrites, and shelf-spillower deposits. The core chronostratigraphies indicate that the oldest ages dated in this study are the following: (1) 20.0 ka in the Almeria TS; (2) ^{14}C dating data are not available in the Calahonda and Sacratif TS but the cores record at least Holocene time by correlation with others cores of the Alboran region; and (3) 9.4 ka in the Guadiaro TS.

The vertical distribution of sediment types and dated layers (^{14}C ages) allow us to establish the recent depositional history of the TSs. It could be divided into three periods: A, B, and C.

(A) During the last sea level fall and lowstand period (at least from 20.0 to 14.3 ka), the shelf was dominated by shoreface erosion processes resulting from the seaward shifting of the coastline. Simultaneously, turbidity flows predominated on the TSs and locally shelf spillover flows also occurred on the proximal parts (canyons heads). Hemipelagic settling occurred at the end of this period on deepest sector of the TSs.

(B) During the transgressive period (14.0 to 6.5 ka) the hemipelagic settling is a predominant processes on the TSs which are interrupted by some turbidite and debrites events; in particular, at least three turbidite events have been identified (after 12.4 ka, before 10.5 ka and after 8.1 ka) in the Almeria TS, and one turbidite event (9.4 ka) and debrites (after 8.3 ka) in the Guadiaro TS and,

(C) During the highstand period (6.5 kyr to present) hemipelagic settling has been predominant except in the Sacratif TS where turbidity currents seem to be occurred. In spite of the hemipelagic settling different turbidite events have been identified. In this sense, the most recent turbidity flow occurred after 1.9 ka in the Almeria TS, and two turbidity flows are identified, one between 6.5 and 3.1 ka and the most recent between 1.4 and 1.3 ka in the Guadiaro TS. The variability of these turbidite events displayed by the cores could be related in addition to local factors which are relatively different in the four TSs such as sediment source (e.g. river vs coastal erosion; single canyon vs multiple canyons and gullies) oceanography (small-scale variation of geostrophic currents and littoral drift), physiography (differences of the wide of the margins, location of head canyon on shelf or on slope-), and neotectonism.

- Alonso, B., and Ercilla, G., 2003. Small turbidite systems in a complex tectonic setting (SW Mediterranean Sea): Morphology and growth patterns. *Marine and Petroleum Geology*, 1225-1240.
- Garcia, M., Alonso, B., Ercilla, G., Gràcia, E., et al., 2005. The tributary valley systems of the Almeria canyon (Alboran Sea, SW Mediterranean): Sedimentary architecture. *Marine Geology*, in press.
- Woodside, J.M., and Maldonado, A. 1992. Styles of compressional neotectonic in the eastern Alboran Sea. *Geo-Marine Letters*, 12 (2/3), 116-116.

Founding was provided by the projects SAGAS (CTM2005-08071-C03-02/MAR) and WESTMED (01-LEC-EMA22F).

Modelling global organic carbon burial in response to sea level changes

Bjerrum, C.J.*, and J. J. F. Legarth, J.J.F.

Geological Institute, University of Copenhagen, Øster Voldgade 10, DK-1350 Kbh. K., Denmark.

** Corresponding author: cjb@geol.ku.dk*

For a long time various sedimentological, biological and geochemical changes in the rock record have been related to sea-level changes. The relationship between sea level and deposition of organic carbon has in particular been investigated for greenhouse periods in the Mesozoic where economically important hydrocarbon source rocks were deposited during global anoxic events. Correlation of global and local proxy data (e.g. $\delta^{13}\text{C}$ or productivity indicators) to sea-level curves are attempted for the events because it could increase our understanding of process relations. However, despite three decades of research on the correlations, there has been very little quantification of the first order influence that sea level change has on nutrient inventory, marine productivity and burial of organic carbon. Here we will present a model aimed at quantifying the burial of organic carbon as a function of sea-level rise. The biogeochemical model explicitly considers the seafloor – surface area distribution of Earth as a function of elevation and the burial efficiency as a function of sedimentation rate (Bjerrum et al., in review). We quantify how imposed land-area flooding as in the Cretaceous, influences the cycle of the nutrient phosphate and burial of organic carbon.

In the model total burial of marine organic carbon is more efficient under high sea level for a given dissolved inorganic phosphate (DIP) concentration, because burial primarily depends on the area of the shelf with its high sedimentation and associated burial efficiency. As a result the residence time of DIP in the ocean is only 60% of the present residence time for a shelf area comparable to that of the Late Cretaceous. In the final steady state, the DIP and new production of organic matter (NP) in the open ocean are reduced when the biologically reactive phosphorus flux (FpIN) to the ocean from land is held constant. Such a reduction reduces the oxygen demand in respiration and results in a significant oxygenation of the global ocean. Global organic carbon burial decreases by 30% because the burial-ratio of organic C to reactive P is smaller for a reduced rain of organic carbon to the sea floor and for an increase of the oxygen concentration.

During transient sea-level rise we find coastal erosion may increase FpIN to the ocean on a global scale by 10 to 30% as indicated by our sequence architecture modelling (see abstract by Legarth and Bjerrum). In turn this increased flux results in a reduction of the oxygen concentration on the shelf and in intermediate water masses and thereby a modest increase of the C:P burial ratio. Such changes result in small carbon isotope events (+0.4 to 0.8 permil) (Figure 1). Redox related feedbacks can only cause significant carbon isotope events when the ocean prior to the sea-level rise is sufficiently close to the “edge of anoxia”, caused by a high steady state background FpIN to the ocean. Such threshold behaviour may explain the different conclusions reached by other researchers on the relation between eustatic sea level and organic productivity and burial. Thus, in the model, ocean anoxic events can be triggered by sea-level rise only during periods of intense continental weathering.

Low and falling sea-level is found more readily to result in ocean anoxia in the model. This result may be understood by noting that the oxygen demand in the ocean is greater during low sea level, because DIP and new organic production are higher when the shallow water area is less extensive.

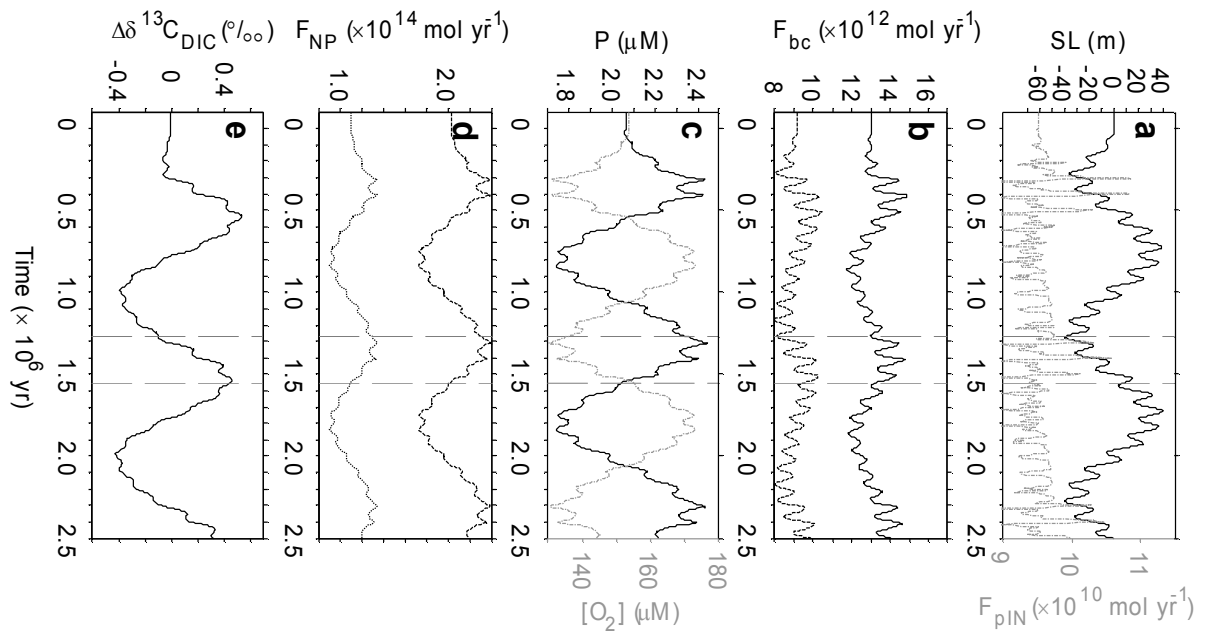


Figure 1. Typical transient model results for sea-level changes where only small redox feedbacks are triggered. a. Sea level (black line). Biologically available phosphate flux into ocean (F_{pIN}) is dependent on weathering in response to CO_2 -climate changes and dependent on coastal and flood plain sedimentation/erosion (grey dash-dotted line). b. Burial of organic carbon in the global ocean (F_{bc}) (solid line) and on the shelf (dashed line). c. Mean ocean dissolved inorganic phosphate (DIP) (black line) and thermocline oxygen concentration (grey dash-dotted line). d. New production in low latitude (dashed line) and high latitude (stippled). e. Change in carbon isotope composition of dissolved inorganic carbon ($\Delta\delta^{13}C_{DIC}$). Variation in shelf area and DIP liberated from coastal erosion cause DIP changes resulting in notable changes in organic carbon burial and there by $\delta^{13}C_{DIC}$. The background F_{pIN} changes from coastal erosion and flood plain deposition during sea-level changes is from sequence architecture modeling (see abstract by Legarth and Bjerrum) and here overprinted by weathering changes due to CO_2 -climate feedbacks.

Fluvial responses to climate and sea-level change: implications for sediment delivery to the shelf margin and beyond

Blum, Mike and Hattier-Womack, Jill

*Department of Geology and Geophysics
Louisiana State University
Baton Rouge, Louisiana 70803
mike@geol.lsu.edu*

River systems are the conveyor belts that deliver sediments eroded from the hinterland to the shelf margin and beyond. Accordingly, coastal-plain and cross-shelf incised valleys provide the physical link between processes that control sediment production, and processes that control dispersal to the continental margin and deep basin.

Hinterland drainage area, relief, and lithology represent the first-order controls for the volume of sediment delivered to continental margins. Over the relatively short time scales represented by high-frequency depositional sequences, multiples of 10^4 to 10^5 years, these variables remain relatively steady, and might be viewed as conditioning a background order of magnitude sediment flux for specific river systems and depositional basins. Superimposed on this background rate is an unsteadiness that reflects climate change and associated changes in runoff in hinterland source regions, but the rates and directions of change in sediment supply will vary regionally. Although difficult to quantify, both older research and current empirical models converge to suggest the variability in sediment supply due to climate change may be ~10-30%. Contrary to many views expressed in the literature, sediment yield through the vast midlatitudes was likely less during cooler and drier climates typical of glacial periods, when compared with warmer and wetter interglacials like the Holocene.

If sea level were held constant, river systems would modulate climate-controlled unsteadiness in sediment supply through changes in storage along valley axes. However, over the relatively short time scales represented by high-frequency depositional sequences, climate and sea-level change are directly coupled. Sea-level change has little effect on the total volume of sediment delivered to the margin, but does play a paramount role in determining the proximal to distal location of the river mouth point source through which sediment is dispersed to the shelf and beyond: incised valleys form and channels extend across emergent shelves to deliver sediments to the shelf margin during sea-level fall, and channels shorten and valleys fill during sea-level rise such that much sediment is sequestered farther updrift. In addition to changes in the location to which sediments are dispersed into the basin, for some basins sea-level fall may also result in the merging of drainage basins that, in a highstand world, discharge separately to the coastal oceans. This is especially critical to deep basins, as total sediment yield during sea-level fall and lowstand may decrease due to climate change, but the merging of drainages may result in significant point source increases.

Coastal-plain and cross-shelf incised valleys are the key stratigraphic elements of the fluvial conveyor belt, and form during sea-level fall and lowstand as river systems extend across newly emergent shelves. Contrary to earlier models that envisioned incision and complete sediment bypass within incised valley systems during periods of relative sea-level fall, falling stage to lowstand fluvial deposition is actually common in well-studied Quaternary analog systems, and there is no process-based reasoning that would suggest otherwise for the pre-Quaternary record. Studies of Quaternary analog systems show that multiple episodes of channelbelt formation and incision take place within extended valleys, which likely reflects climate-controlled unsteadiness in the relationship between discharge regimes and sediment supply, and is not causally linked to sea-level change per se. Models for falling stage and lowstand systems tracts should therefore incorporate significant fluvial channelbelt deposits that are likely connected to, and feeding, shelf-margin deltas and linked downslope depositional systems, as well as the unsteadiness in sediment delivery to the deep basin that reflects climate changes in hinterland source regions.

Highstand Sand Transport to Deep Water by Longshore Transport, Tidal and Gravity Processes

Boyd, R.¹, Ruming, K.¹, Sandstrom, M.², and Schroder-Adams, C.³.

1. University of Newcastle, NSW, Australia.
2. Australian School of Petroleum, Adelaide, South Australia.
3. Carleton University, Ottawa, Ontario, Canada.

How does sand reach the deep sea? Current models using a sequence stratigraphic approach predict sand delivery by river systems to the edge of the continental shelf during times of low sea level and then by gravity processes to deep water. Here we demonstrate a new approach in which waves, tides and the geometry of the continental margin combine to supply deep water sands at sea-level highstand. This new approach has been developed on the SE Queensland margin of Australia through a combination of high-resolution multibeam and seismic surveying, ROV dive traverses, bottom sediment and microfaunal sampling, and current meter data.

These techniques have imaged the distal end of a 1500 km longshore transport system forming the largest coastal sandy barrier in the world (Fraser Island - 205 km³), and then prograding a 30 km subaqueous spit across the continental shelf to the shelf break. Here strong tidal currents create large migrating submarine dune fields with individual bedforms up to 12 m high. The multibeam 3D and insitu ROV imagery shows the dunes migrate at up to 20 m per year over the shelf break (Figure 1), create a range of gravity slumps and slides before funnelling beach and nearshore sands onto the upper continental slope through a network of 35 submarine gullies up to 40 m deep and 300 m wide.

The sand then continues for a further 40 km seaward down the continental slope, over a 300 m high carbonate platform escarpment, through a major gully and canyon system to over 4000 m water depth where it deposits beach sands containing estuarine foraminifera and mangrove roots.

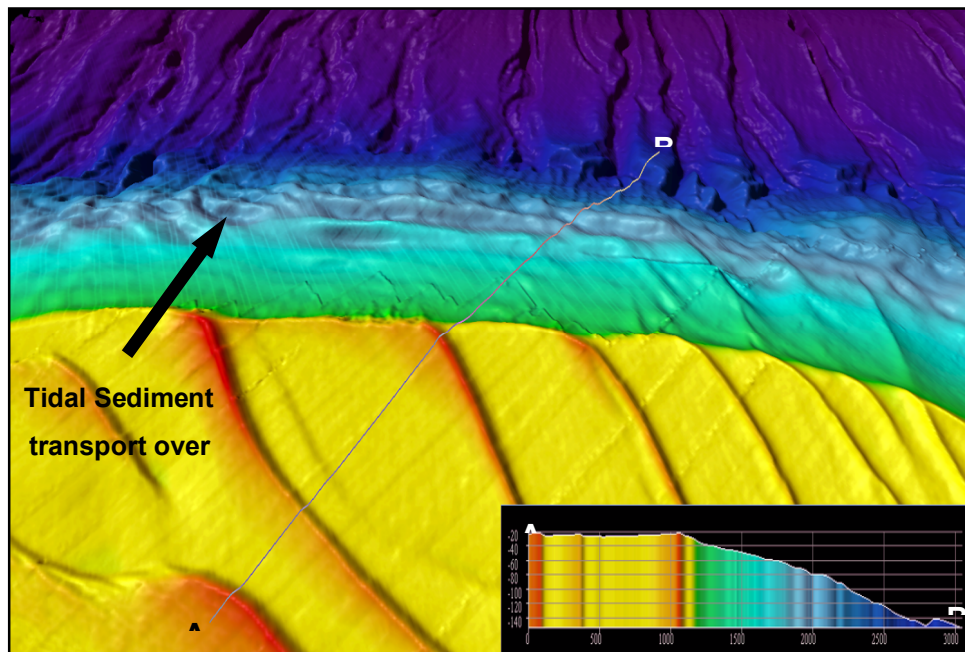


Figure 1. This shows a vertical multibeam image and A-B cross section of the shelf edge near Fraser Island, SE Queensland. Tidal bedforms up to 12 m high are migrating out of the Hervey Bay estuary (bottom) to the shelf break (centre of image) in 20 m water depth. Here they discharge large volumes of sand to the upper slope where it is funneled into gully systems beginning in around 120 m depth and continuing a further 40 km seaward to 4500 m depth on the Tasman Abyssal Plain.

Late Glacial And Holocene Depositional Patterns Of The Almeria Channel Levees (SW Mediterranean)

Bozzano, G. *, Alonso, B., Ercilla, G., Casas, D., Estrada, F., and García, M.

CSIC, Instituto de Ciencias del Mar, Passeig Marítim de la Barceloneta, 37-49, 08003 Barcelona, Spain.

* Corresponding author:: grazi@icm.csic.es

We performed a sedimentological study of the Almeria channel levee complex in order to determine the controlling factors of the sediment transfer from shallow to deep waters. In the Alboran Sea (SW Mediterranean), the Almeria Canyon incises the narrow continental shelf at a water depth of 100 m and then routes along the slope until, at least, 1200 m water depth. The Almeria Channel is the downward continuation of the Canyon and reaches depths of more than 1800 m (Fig. 1) (Alonso and Ercilla, 2003). The system is fed by a complex structure of tributary valleys (gullies and levee channels) whose dynamics is governed by sea level fluctuations and seasonal sediment supply (García et al., 2005).

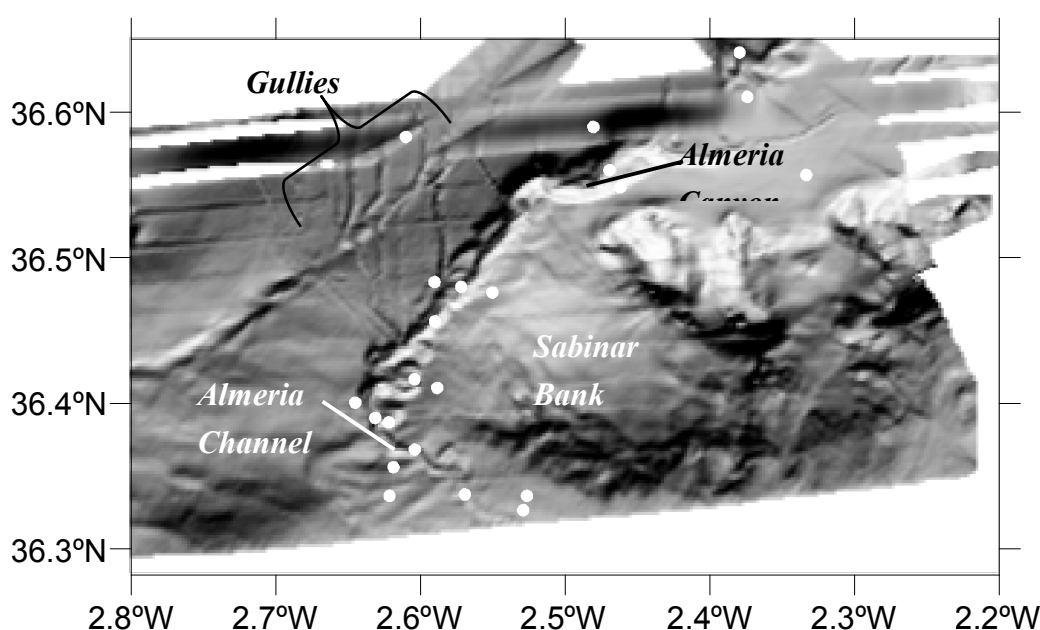


Figure 1. Shaded relief of the Almeria turbidite system. White spots show the location of the sediment cores used in this study.

Sediment physical properties, such as P-Wave Velocity (PW), Density (D) and Magnetic Susceptibility (MS), were obtained at 1-cm resolution step on 26 sediment cores located within the Almeria turbidite system. In addition, calcium carbonate content, grain size parameters and sand-fraction composition were analysed on discrete sediment samples from a focussed number of these sediment cores. A common age model was elaborated on the base of radiometric dating (^{14}C) and stratigraphic correlations using the continuous MS logs. MS records were also used as additional proxy of the sediment composition.

We found differences in the sediments of the eastern and western Almeria channel levees. The western levee shows a common sedimentary sequence made of turbidites at the bottom (20-12.8 cal kyr BP) evolving into hemiturbidites (12.8-6.5 cal kyr BP) and hemipelagic deposits (6.5-2 cal kyr). This sedimentary sequence is not recognisable in the sediments of the eastern levee. Differences in the depositional patterns distinguish also the distal and proximal sectors of the western levee. In the distal sector (>1500m water depth), Holocene deposits are characterized by fairly constant MS values, whereas in the proximal sector (800-1000 m water depth) are characterized by variable MS values. Both eastern and western levees sediments are overlaid by a recent turbidite event (younger than 2 cal kry) found at the top of different cores, which has been interpreted as a general reactivation of the system in the late Holocene (Estrada et al., 2004). We believe that regional sea level changes mainly control the sediment transfer to the Almeria channel levees. In addition, external factors, such as the tributary gullies of the Almeria Canyon to the west and the volcanic seamounts (Sabinar bank) to the east, locally contribute in shaping the depositional pattern in the region.

- Alonso, B., Ercilla, G., 2003. Small turbidite systems in a complex tectonic setting (SW Mediterranean Sea): morphology and growth patterns. *Marine and Petroleum Geology*, 19, 1225-1240.
- Estrada, F., Alonso, B., Ercilla, G., Garcia, M., 2004. Recent sedimentary evolution of the Almeria Channel (SW Mediterranean Sea). Second Euromargins Conference, Barcelona, 11-13 November.
- García, M., Alonso, B., Ercilla, G., Gràcia, E., 2005. The tributary valley system of the Almeria canyon (Alborán Sea, SW Mediterranean): sedimentary architecture. *Marine Geology*. In press.

Acknowledgement: Funding was provided by the projects SAGAS (CTM2005-08071-CO3-02/MAR) and WESTMED (01-LEC-EMA22F).

Ancient Global Warming Events and their Implications for Sequence Stratigraphy and Evolution

Bralower, Timothy J.

Department of Geosciences, Pennsylvania State University, University Park, PA 16802

The geologic record offers unique opportunities to investigate the effects of abrupt global warming on marine and terrestrial ecosystems. Such studies complement those focused on the ecological effects of modern global warming by providing a complete and long-term perspective of biotic responses. The last decade has seen advances in our understanding of biotic effects of abrupt climate events including Oceanic Anoxic Events (OAEs) in the Jurassic and Cretaceous (~185 to 90 Ma) and hyperthermal events in the early Paleogene, such as the Paleocene/Eocene thermal maximum (PETM at 55 Ma). This presentation will provide an overview of the response of marine calcareous plankton groups (nannoplankton and planktonic foraminifera) during these events.

The OAEs and PETM involved transformations in surface water habitats that affected plankton groups in profound ways. These changes include increases in temperature and changes in thermal structure, changes in salinity, modifications in nutrient and trace element cycling, and fluctuations in alkalinity. In every case, changes in surface habitats resulted in *transient* plankton communities. For example, the abrupt PETM event corresponded to an equally short-lived but major change in nannoplankton and planktonic foraminiferal population structure in open-ocean and coastal locations. In addition, the environmental changes often resulted in *long-term* biotic consequences involving increases in the rates of evolutionary turnover (combined increases in rates of evolution and extinction). For example, during OAEs two highly successful groups of plankton were decimated; the nannoconids were nearly eradicated during OAE1a (early Aptian), and the rotaliporids became extinct during OAE2 (Cenomanian/Turonian boundary). In other cases only species that were rare went extinct. Although we have a poor understanding of ancient plankton ecology, it appears that the extinctions were selective and targeted more specialized and often deeper-dwelling species. Not unexpectedly, transient assemblage changes included specialists and generalists. Nannofossil and planktonic foraminiferal records from the OAEs and PETM highlight a surprising effect of abrupt climate events, that niches opened through extinction were filled with almost no time lag. This is different from major extinction events such as the Cretaceous/Tertiary boundary where many new species did not evolve for several million years. Perhaps the quick recovery of organisms after abrupt climate events reflects the rapid return of marine habitats to relative stability.

Shelf Growth: Highstand versus Lowstand Sediment Delivery from Shelf Margins

Carvajal, C., Petter, A., Uroza, C., and Steel, R.

University of Texas at Austin.

Although sand can be partitioned into deepwater by a variety of processes, the most effective mechanism for delivery to deepwater slope and basin floor is from shelf-edge deltas. This sand delivery also involves repeated regressive and transgressive deltaic transits, resulting in shelf aggradation of up to 200m in a single cycle, during a time interval of only a few 100ky. Rates of accretional growth on shelf margins are documented up to 61 km/my, depending on supply rate, basinal water depth, presence/absence of large growth faults in shelf-edge area, and shelf-edge trajectory.

Conventional models of shelf-margin building involve preferential accretion when relative sea level is low, and a series of early and late growth phases, with or without slope bypass, can be identified. Lowstand growth of margins can generate prominent sequence boundaries, and is best achieved when accommodation (A) (through low or high amplitude relative sea-level changes) tends to drive deltas to the shelf-edge. There is increasing evidence that shelf margins can also show sand-prone growth and basin-floor fan development during highstand of sea level, if a strong sediment supply (S) drives deltas to the shelf-edge. In this case there are no sequence boundaries developed, the shelf-edge trajectory rises during progradation, the margin is more strongly affected by autogenic processes and the linkage between shelf-edge deltas, slope channels and fans is simpler than in the lowstand model. Thus, accommodation- and supply-driven accretion represent end-member scenarios, and a given shelf-margin may show elements of both as A and S vary through time.

The deep-water clastic sedimentary record of evolving climate and tectonics in the Arabian Sea

Clift, P.¹, Schwab, A.¹, Calves, G.¹, Giosan, L.², Blusztajn, J.², Tabrez, A.³, Danish, M.³, Inam, A.³, Alizai, A.⁴.

1. School of Geosciences, University of Aberdeen, Meston Building, Aberdeen, AB24 3UE, United Kingdom.

2. Department of Geology and Geophysics, MS#22, Woods Hole Oceanographic Institution, Woods Hole, MA 02543, USA.

3. National institute of Oceanography, Clifton, Karachi, Pakistan.

4. Geological Survey of Pakistan, St. 17/2, Gulistan-e-Jauhar, Karachi, Pakistan.

The Indus River drains some of the highest terrain on Earth and is also affected by the rains of the Asian summer monsoon, resulting in a huge clastic flux to the ocean that has built the second largest sediment mass in the world in the Arabian Sea. Newly released 2D and 3D seismic reflection data from the proximal Indus Fan can be tied to industrial wells on the Pakistan Shelf and used to reconstruct the deep-sea record of continental erosion. The age resolution of the deep-sea record will be improved by future Integrated Ocean Drilling Program (IODP) operations that are planned to drill a complete section on the uplifted edge of the fan along the Murray Ridge. Seismic stratigraphy now allows the identification of two peaks in clastic flux, one spanning the Early and Middle Miocene (24–11 Ma) and the other in the Plio-Pleistocene (since 3 Ma). These periods appear to be linked with climate variations. The Miocene pulse coincides with tectonic activity in the mountain sources and a strengthening of the summer monsoon rains. The Late Miocene, in contrast, has reduced rates of sedimentation linked to drier climatic conditions across south Asia. The Plio-Pleistocene is again a time of stronger monsoon rains, coupled with intensified and expanded glaciation in the mountains. Although parallel-bedded distal turbidites linked to channel levee complexes dominate the upper part of the mid fan stratigraphy, there is also evidence for debris flow sedimentation, large coherent slump blocks, as well as meandering channels in the sub-surface. These are more strongly developed in the Lower-Mid Miocene and Plio-Pleistocene sections. Erosive channels on the upper mid fan show complex histories of multi-stage erosion and fill. Sand waves are observed at a number of levels, interbedded with turbidite units.

The modern clastic load of the river is somewhat more than the average rates of sedimentation in the Pleistocene, even after accounting for anthropogenic influences (250 vs. 205 million tons/yr). This implies that there is only limited buffering of sediment flux between the mountains and the deep ocean, and also that erosion rates varied strongly between glacial and interglacial periods. We suggest that deglaciation was a time of strongest sediment transport to the ocean, as the climate warmed and wetted after colder, drier glacial conditions. The Indus River itself appears to be disconnected from the deep sea fan at the start of the Holocene, when sedimentation was focused in the incised valley and on the Pakistan Shelf. The fan is mantled by a relatively carbonate-rich sediment at that time. The Indus delta has migrated west from the Rann of Kutch to its present position since 14 Ka. At the same time the submarine delta has been building a cliniform that is prograding towards the head of the canyon. Isotopic data indicate that the sediment in the modern canyon reflects reworking of material originally deposited there during the Last Glacial Maximum around 20 Ka.

Hyperpycnal River Flows from an Active Mountain Belt

Dadson, S.^{1,2}, Hovius, N.¹, Pegg, S.¹, Dade, W.D.³, Horng, M.J.⁴, and Chen, H.⁵

1. Department of Earth Sciences, University of Cambridge, Downing Street, Cambridge, CB2 3EQ, UK.

2. Now at Centre for Ecology and Hydrology, Maclean Building, Crowmarsh Gifford, Wallingford, OX10.

3. Department of Earth Sciences, Dartmouth College, Hanover, NH 03755, USA.

4. Water Resources Agency, Ministry of Economic Affairs, Hsin-Yi Road, Taipei, Taiwan.

5. Department of Geoscience, National Taiwan University, No. 1, Sec. 4, Roosevelt Road, Taipei, Taiwan.

Rivers draining the tectonically-active island of Taiwan commonly discharge suspended sediment to the ocean at hyperpycnal concentrations ($>40 \text{ kg m}^{-3}$), typically during typhoon-driven floods. During the period 1970–1999, between 99–115 Mt yr⁻¹ of sediment was discharged at hyperpycnal sediment concentrations from Taiwan to the sea. This amount represents 30–42% of the total sediment discharge from Taiwan to the ocean. The spatial distribution of hyperpycnal discharge broadly mirrors the pattern of total sediment discharge and rivers draining catchments having recent earthquakes and weak rocks, such as the Choshui and Erhjen, discharge up to 50–70% of their sediment at hyperpycnal concentrations. Following the Chi-Chi earthquake, the frequency of hyperpycnal flows increased, owing to an earthquake-driven increase in sediment supply. Landslides triggered by the Chi-Chi earthquake have resulted in an increase in the concentration of suspended sediment in rivers for a given water discharge; in turn, the threshold flood discharge required to generate hyperpycnal flow has decreased and so hyperpycnal flows are occurring more frequently. Our findings suggest that, if hyperpycnal plumes evolve into bottom-hugging gravity currents descending to and ultimately debouching in the deep-sea, earthquakes may be recorded as bundles of turbidites.

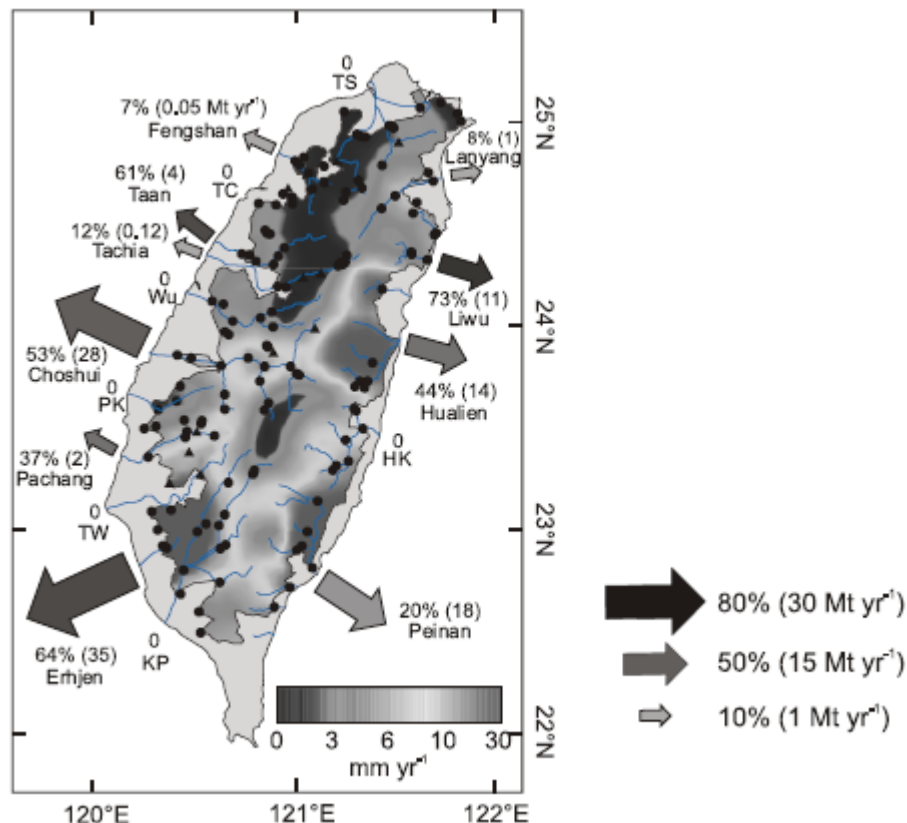


Figure 1. Hyperpycnal discharges to the ocean from Taiwan 1970–1998 based on measured hydrometric data. The coloured map shows decadal average erosion rates for reference [from Dadson et al., 2003, *Nature*, 426:648–651]. Arrows indicate rivers for which at least one hyperpycnal discharge was measured (Table 1). The size of each arrow is proportional to the annual average hyperpycnal sediment discharge to the ocean (also given in brackets); its shade is proportional to the percentage that the hyperpycnal amount represents of the total annual sediment discharge (also given on figure). These estimates are probably conservative, because they are based on measured data only. River names are given beneath arrows. Rivers labeled “0” had

no recorded hyperpycnal sediment discharge between 1970–1998. The names of these rivers are abbreviated: TS, Tanshui; TC, Touchien; PK, Peikang; TW, Tsengwen; KP, Kaoping; HK, Hsiukuluan. Black circles indicate hydrometric stations used to construct the erosion map; triangles indicate locations of water supply reservoirs. No data are available in the grey shaded area. (Source: Dadson et al., JGR. In press).

The Nile deep-sea turbidite system: characterization and evolution of sedimentary processes during Late Quaternary

Ducassou E., Migeon S., Mulder T., Gonthier E., Murat A., Bernasconi S., Duprat J., Capotondi L. and Mascle J.

The Nile deep-sea turbidite system is the largest sedimentary accumulation within the Eastern Mediterranean. Its global morphology and geometry are controlled at a regional scale by tectonics (crustal and salt tectonics). However, during Quaternary, the Nile River has known several hydrologic regimes linked to climate oscillations. These variations are enhanced because the Nile River drains a large drainage basin including several climatic zones. Consequently, climate forcing is essential to understand the different construction phases of this deep-sea turbidite system.

The aim of this work is to reconstruct the evolution of this deep-sea system during the last 250,000 years, in particular the westernmost province called Rosetta fan.

The Nile deep-sea turbidite system is compound of four geomorphological provinces, from west to east: Western (Rosetta), Central, Eastern (Damietta) and Far eastern. Each province is characterized by different deposition and sedimentary dispersal modes.

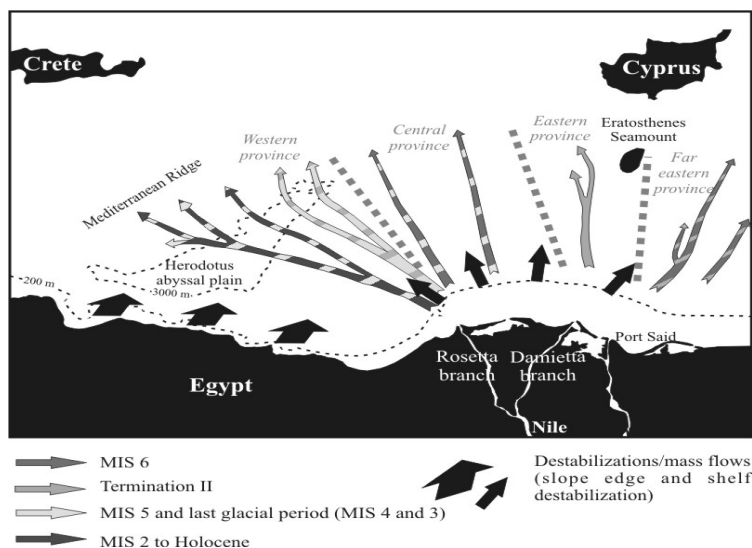
Forty sedimentary cores have been collected all over these four provinces during five oceanographic cruises between 1984 and 2004. The detailed study of these cores allowed to reconstruct sedimentary and palaeoceanographical processes for the last 250,000 years. The analysis of lithological facies, dominantly fine-grained sediments, is constrained by an accurate stratigraphy based on tephrochronology, sapropels, planktonic foraminifer ecostratigraphy, stable and radiogenic isotopes (Ducassou et al., submitted).

Observation of bathymetry and acoustic imagery show typical morphologies of deep-sea turbidite systems including channel-levee and depositional lobe complexes. Observations of sediment cores show a wide range of transport and deposition processes. In addition, data clearly show the migration of these complexes, the presence of large upslope destabilizations and deformed morphologies due to salt tectonics.

Observation of sedimentary facies on indurated thin sections, analysis of sediment sources and the use of the stratigraphic framework confirms the general migration of turbidite systems from the far eastern province to the western province in less than 100,000 years. The turbiditic activity (significant between 160,000 and 125,000 years BP) in far eastern and eastern provinces stops around 125,000 years BP. This change coincides with a tectonic event on the Nile drainage basin.

The Rosetta system became active approximately at 130-125 ky during the relative sea-level rise correlated with Termination II. The system is active from marine isotopic stage 5 to 1 (Holocene). Channel-levee systems were active during relative sea-level highstands. During these periods, main sediment load is supplied by frequent and intense Nile floods. Significant supplies are recorded in distal lobes and in channel and levee upstream parts until the middle of Holocene

Periods of rise or fall of sea level fit with major destabilization phases on fan slope and on the western Egyptian shelf. Thus relative sea-level variations seem to be an important forcing parameter for the deep-sea fan construction and morphology.



Terrestrial input in the Congo fan system reveals Pleistocene climate changes expressed in vegetation records from tropical East Atlantic sediments

Dupont, L.

University of Bremen.

Marine sediments from the Congo deep-sea fan system accumulate material and information from one of Africa's large inland basins that is covered, at present, mainly with lowland rain forest and swamp forests. The sediments provide a record of monsoon related hydrologic and vegetation change. During the mid-Pleistocene, global ice volume variations increased and changed from a 41- to a predominant 100-ka rhythm. This was coupled to an intensification of African aridity and trade-wind strength.

The distribution of pollen in modern marine sediments is used to reconstruct pathways of terrigenous input to the ocean and provides a record of vegetation change on the continent. Generally, a good latitudinal correspondence exists between the distribution patterns of pollen in East Atlantic surface sediments and the occurrence of the source plants in Africa. North of 10°S and along the coast, pollen and spores arrive from rain forest and dry deciduous forest mainly through river discharge, while woodland, savannah, and desert are the main sources for wind-blown pollen in sediments farther out and south of 10°S (Fig. 1).

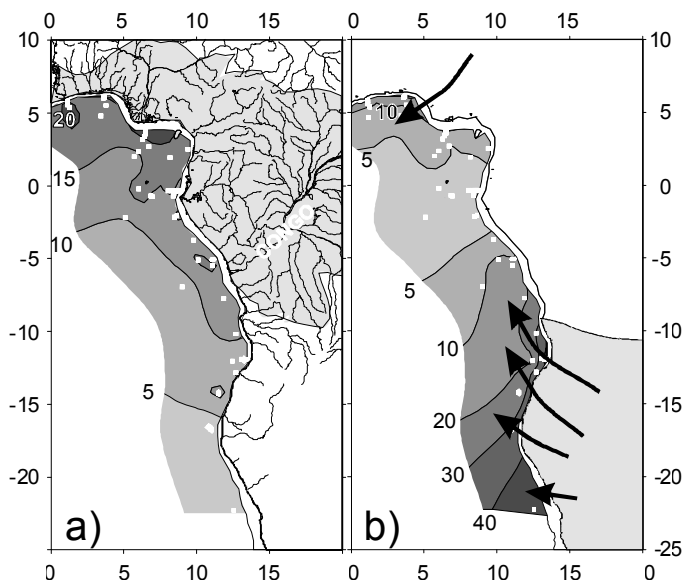


Figure 1. Pollen distribution in East Atlantic marine surface sediments in percentages based on the total number of pollen and spores. a) Lowland forest elements. The shading of the continent indicates areas of the rain forest to deciduous forest being the main source area of lowland forest pollen. Major rivers are denoted. b) Grass pollen. The shading of the continent indicates areas of the savannah to desert south of 10°S being the main source area of grass pollen. Arrows indicate the prevailing off-shore wind directions.

Multiproxy studies were carried out on cores located north and south of the Congo River undersea canyon. Pollen records are compared with other terrestrial signals (iron, clay minerals, biomarkers). The differentiated responses of mangroves, grasslands and swamps, lowland rain forest, and Afromontane forest to environmental fluctuations give insight in several aspects of Pleistocene climate cycles. a) Increased erosion of mangrove peat during periods of rapid sea-level rise supplies the deep sea sediments with enhanced amounts of mangrove materials such as indicated by taraxerol and pollen of mangrove trees (Fig. 2). b) The record of lowland forest pollen indicates extension of the rain forest as a response to increased precipitation in periods of strong monsoons corroborated by clay mineral fluctuations. c) During drier periods, grass and sedge pollen percentages are high indicating an opening of the canopy in large areas of the Congo basin, fitting nicely with evidence of increased C4 vegetation by stable carbon isotopes of alkanes (higher plant waxes). d) Podocarpus pollen percent maxima register the extension of the Afromontane forest during cool and humid, but not too arid, periods.

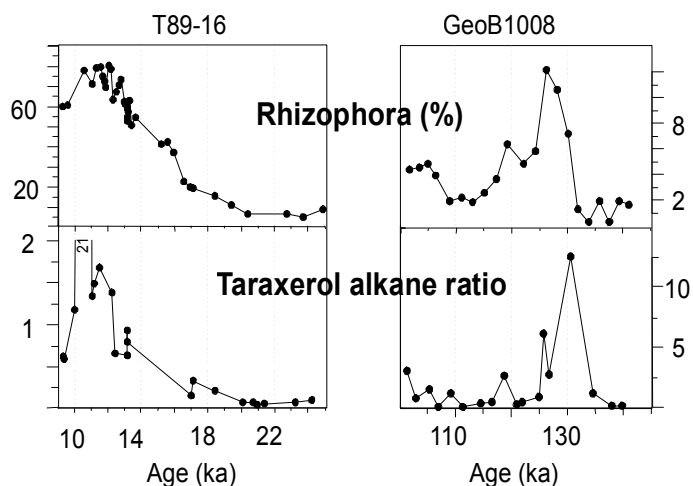


Figure 2. Relative abundances of Taraxerol vs alkanes (terrestrial wax components) and Rhizophora (mangrove tree) pollen percentages increase during periods of sea-level rise during the last (left) and the penultimate (right) deglaciation. The record shows increased erosion of coastal mangrove peat transferring both pollen and leaf material of mangrove trees to the deep ocean.

- Dupont, L.M. & Wyputta, U., 2003. Reconstructing pathways of aeolian pollen transport to the marine sediments along the coastline of SW Africa. *Quaternary Science Reviews*, 22: 157-174.
- Dupont, L.M., Donner, B., Schneider, R. & Wefer, G., 2001. Mid-Pleistocene environmental change in tropical Africa began as early as 1.05 Ma. *Geology*, 29: 195-198.
- Dupont, L.M., Schmäser, A., Jahns, S. & Schneider, R., 1999. Marine-terrestrial interaction of climate changes in West Equatorial Africa of the last 190,000 years. *Palaeoecology of Africa*, 26: 61-84.
- Schefeuf, E., 2003. Paleo-environmental effects of the Mid-Pleistocene transition in the tropical Atlantic and equatorial Africa. *Geologica Ultraiectina*, 223: 187p. (Thesis University of Utrecht).
- Schefeuf, E., Schouten, S., Jansen, J.H.F. & Sinnighe Damsté, J.S., 2003. African vegetation controlled by tropical sea surface temperatures in the mid-Pleistocene period. *Nature*, 422: 418-421.
- Schneider, R.R., Price, B., Müller, P.J, Kroon, D. & Alexander, I., 1997. Monsoon related variations in Zaire (Congo) sediments load and influence of fluvial silicate supply on marine productivity in the east equatorial Atlantic. *Paleoceanography*, 12: 463-481.
- Versteegh, G.J.M., Schefeuf, E., Dupont, L., Marret, F., Sinnighe Damsté, J. & Jansen, F., 2004. Taraxerol and Rhizophora pollen as proxies for tracking past Mangrove ecosystems. *Geochimica et Cosmochimica Acta*, 68: 411-422.

The Role of Shelf-Edge Failures and Exceptional Sediment Gravity Flow Events in Submarine Fan Sedimentation and Stratigraphy

Trevor Elliott, T.¹, and Pulham, A.².

1. Liverpool University, UK

2. Earth Sciences Associates C&T Inc., Colorado, USA

Major submarine fan systems tend to be linked to delta systems and, more specifically, to lowstand, shelf edge deltas. The mechanisms of sediment transfer from the shelf-edge delta to the submarine fan are traditionally ascribed to sediment gravity flows initiated by gravitational failures of unspecified magnitude and/or hyperpycnal underflows. Analysis of a range of complementary data sets identifies a critical role for large scale, shelf-edge failures in delta-driven submarine fans. These failures initiate exceptional sediment gravity flow events, often linked debris flow/high volume turbidity currents, that regionally resculpt the fan surface to the outer part of the mid fan, and possibly beyond. These flows are net erosional across most the fan surface and only become depositional at the fan fringe. Following a major failure event the shelf-edge delta progrades into a slump scar minibasin and strives to heal the topography created by the failure. Multiple, smaller volume turbidity currents are initiated during this phase and these flows are net depositional on the resculpted fan surface. Lowstand fan sedimentation is therefore a response to a bimodal suite of sediment gravity flow processes involving high magnitude/low frequency events that are net erosional across much of the fan, and lower magnitude/high frequency events that are net depositional. The depositional record of the outermost fringe of the fan system provides a critical test of this hypothesis.

Factors controlling sedimentation in the basin floor fan and the slope fans of the Pab Formation (Maastrichtian, Pakistan) : lessons from a stratigraphic modelling approach

Eschard, R.^{1*}, Euzen, T.¹, Granjeon, D.¹, and Lopez, S.

1. Institut Français du Pétrole, 1,4 av. de bois Préau, 92506 Rueil-Malmaison, France.

** Corresponding author : Remi.eschard@ifp.fr*

Basin floor fans and slope fans present major differences in their internal architecture associated to changes of the margin dynamics and of the variation of external forcing factors, which themselves have an impact on flow hydrodynamic. We will illustrate these changes from the Pab Sandstone in Pakistan, where a complete depositional system of deltaic and turbiditic sediments is preserved in outcrops. These sediments were deposited during the Late Maastrichtian on the Indo-Pakistani passive margin. The architecture of the basin floor fans and slope fans and of their platform deltaic equivalent will be first described from an outcrop regional transect. The results of a stratigraphic simulation will be then presented, restoring the gross geometry of the depositional sequences and quantifying the variation of the main forcing parameters (slope angle and depositional profile, evolution of the sediment supply through time, eustasy...). The simulation outputs will challenge a discussion about the parameters controlling the dynamic of a high-transport efficiency channel-lobe systems and a low-transport efficiency slope fan connected to a delta.

The Maastrichtian margin geometry has been restored in the Pab and Laki range outcrops (southern Pakistan), from the delta to the deep basin. Three superposed turbiditic systems overlapped slope carbonates and completely pinch out on the platform margin. The oldest turbiditic system (Lower Pab) was a sand-rich basin floor fan which was sourced by a single canyon incised in the carbonate slope sediments. The fan consisted of three stacked channel complexes passing to lobes basinward. Each of the channel complex has a multi-storey internal architecture, resulting from the amalgamation of dozens of individual turbiditic channels. Overflow deposits were also well-developed laterally to the channels. The whole basin floor fan backstepped through time. In the platform setting, an unconformity has been determined on top of platform carbonates and was probably associated to a network of fluvial incised valleys connected to the main canyon.

The basin floor fan was overlain by a mud-rich slope fan formed of hemipelagites, interbedded with small, narrow channel-levees of limited extension and thin lobes. At that time, the canyon was almost filled with sediments and the slope also aggraded. In the platform setting, transgressive shoreface backstepped testifying of a major relative sea level rise which drowned the shelf. The sediment supply to the basin decreased as the platform was drowned and the main basin-floor fan was abandoned. The minor amounts of clastic sediments still arriving in the basin setting constructed a mud-rich slope fan deposited during the transgression.

The younger turbiditic system (Upper Pab) consisted of poorly organized prograding lobes passing upward to conglomeratic scour and fill channels. The lobes had a tabular geometry and consisted of coarse-grained material presenting pseud-HCS structures. The channels present a massive infill of conglomerates with limited overflow sediments. Periods of fan abandonment were also marked by the development of shale units of regional extension. No feeder canyon has been found, and the hypothesis of a feeder system consisting of multiple slope channels is preferred. The fan rapidly thinned out basinwards and most of the sediments was trapped at the slope apron. In the platform setting, a sand-rich braided delta rapidly prograded up to the shelf break, directly supplying the slope fan with clastic material. The margin aggraded at the same time.

Transport efficiency was limited, the dominant mechanism of gravity flows being associated to hyperpycnites and floods events. The Upper Pab turbiditic system is interpreted as a low-efficiency sand-rich slope fan deposited on the slope apron. The fan prograded at the same time than the delta on the platform before the complete abandonment of the clastic system during the Paleocene transgression.

A stratigraphic simulation was then performed using the Dionisos software. This diffusion-based model is able to simulate turbiditic systems taking into account long-term low-energy transport diffusion, short-term high-energy flows and slope collapses. Basin parameters (subsidence, sediment supply, eustasy etc.) are first inferred, then iteratively fitted to the data by inversion.

The lessons we learnt from outcrop studies and from the simulations are the following:

Tectonism : the abrupt arrival of clastic sediments in the deep basin was probably related to the tectonic uplift of the margin. During Upper Maastrichtian, the thermal doming associated to the Deccan trap emplacement first was associated to a major erosion of the shield and an increase of the sediment supply.

The erosion increased during the late Maastrichtian, a sand-rich delta prograding till the shelf break and feeding the Upper Pab slope fan. The amount of reworked volcanic material increased. After the main volcanic event just before the K/T boundary, a rapid thermal subsidence occurred and induced the Paleocene transgression and the abandonment of the fan.

Margin topography: the uplift of the margin first induced a steep margin with a well-defined fault-controlled shelf-break during the Lower Pab basin floor fan. Depositional slope was steep. Sediments transited through canyons and accumulated in the Lower Pab basin floor fan while the slope was starved with clastic sediments. In contrast, during the deposition of the Upper Pab slope fan, the large amount of fine-grained material aggraded the margin which evolved to a ramp geometry. The canyons were filled with sediments and the system evolved to a multiple point source channel feeders as the delta reached the shelf break.

Eustasy : the transgression which drowned the platform before the progradation of the Upper Pab delta and slope fan was associated to a brutal reduction of the sediment supply arriving on the platform. A eustatic sea-level rise was imposed in the stratigraphic simulation to reproduce the backstepping and then the aggradation of the delta, and the deposition of slope fans.

Climatic cycles : a high frequency cyclicity is observed either in the Lower Pab basin-floor fan (channel complexes being separated by hemipelagic sediments) and in the Upper Pab slope fan (periods abandonment during the progradation of the slope fan). This high frequency fluctuation was related to the rapid variation of the sediment supply through time. This variation can either be due to the autocyclic lateral shifting of the source of sediment or to global changes of the sediment supply. This last explanation would be preferred as a similar sequence hierarchy can also be found in the deltaic sediments on the platform, suggesting global changes of the sediment supply which affected the whole margin.

Changes in the flow hydrodynamic : a change in the nature of the turbidity currents can be observed between the lower Pab and upper Pab turbiditic systems. The Lower Pab depositional processes were characterized by turbidity currents transporting sediments over very long distances basinward. High transport capacity of the basin-floor fan was enhanced by 1) the high slope angle, 2) the flow confinement in the canyon, 3) a muddy substrate which erosion increased flow buoyancy and 4) an irregular morphology which favoured turbulence. In contrast, the low-transport capacity of the slope fan was in relation with a smoother ramp morphology and the hydraulic connection of the turbiditic flows to the delta mouth favouring hyperpycnal flows. Sediments were trapped at the slope apron.

A simple three layers model for the eulerian behaviour of a turbidite current as a function of the Richardson number: sedimentological implication for the interpretation of the turbidite facies

Falcini, F.^{1*}, Milli, S.¹, Moscatelli, M.², Stanzione, O.¹, and Salusti, E.³.

1. Dipartimento di Scienze della Terra, University di Roma "La Sapienza", P.le Aldo Moro 5, 00185 Roma, Italy

2. CNR, Istituto di Geologia Ambientale e Geoingegneria, Via Bolognola 7, 00138 Roma, Italy.

3. Dipartimento di Fisica – INFN – Università di Roma "La Sapienza", P.le Aldo Moro 5, 00185 Roma, Italy.

* Corresponding author : federico.falcini@uniroma1.it

In this study, experimental data (Ellison and Turner, 1959) and analytical-numerical solutions for turbidity current (Stacey and Bowen, 1988) are analysed and compared with field observation data. This approach tentatively provides a simple scheme of the behaviour of a turbidity current flowing down inclines of constant slope.

The main features of the turbidity currents that appear from our analysis are: the erosive power (where available material is present) due to the turbulence generated by the high shear stress in the basal layer, between the bottom and the turbidity current itself; the entrainment at the leading edge of the current which may generate a turbid dilute cloud over the turbidity current itself; the Bingham flow behaviour in the middle layer of the current (namely the main part of the flow) which is able to transport the sediments.

In order to provide a simple analytical model which take into account the main characteristics above described, a three layer model for a turbidite current is here presented (Fig. 1). The behaviour of the three layers is represented as a function of the Richardson number defined as:

$$Ri = \frac{-g \cos \theta \frac{\partial \rho}{\partial z}}{\rho \left(\frac{\partial u}{\partial z} \right)^2}, \quad (1)$$

where z is the vertical axis (positive upward); $\rho(z)$, g , and θ represent the density, the gravity acceleration, and the angle of the slope respectively; $u(z)$ is the velocity. The density is considered directly proportional to the concentration of sediments $C(z)$.

Solutions for Eq. 1 can be determined for each layer of the current (Fig. 1). In detail, the balance between the numerator and denominator of Eq. 1 is studied for the three layers. Following Fig. 1, in the upper layer

$$\frac{\partial \rho}{\partial z} \approx 0$$

(namely layer 3) the low gradient of the density ($\frac{\partial \rho}{\partial z} \approx 0$, i.e. low stratification) yields $Ri \ll 1$, due to the entrainment (i.e. turbulent mixing) between the turbidity current and the environment water. A turbulent flow occurs and no horizontal transport of sediments is present (i.e. mean kinetic energy less than turbulent kinetic energy).

Viceversa, in the middle layer (layer 2 in Fig. 1) $Ri \gg 1$ because of the high gradient of the density

$$\left(\frac{\partial \rho}{\partial z} \gg 0, \text{ namely high stratification} \right) \text{ and the lack of velocity shear } \left(\frac{\partial u}{\partial z} \approx 0 \text{ and } u(z) \approx \text{const, like a Bingham fluid for high concentrations} \right).$$

In this layer the transport of sediment occurs.

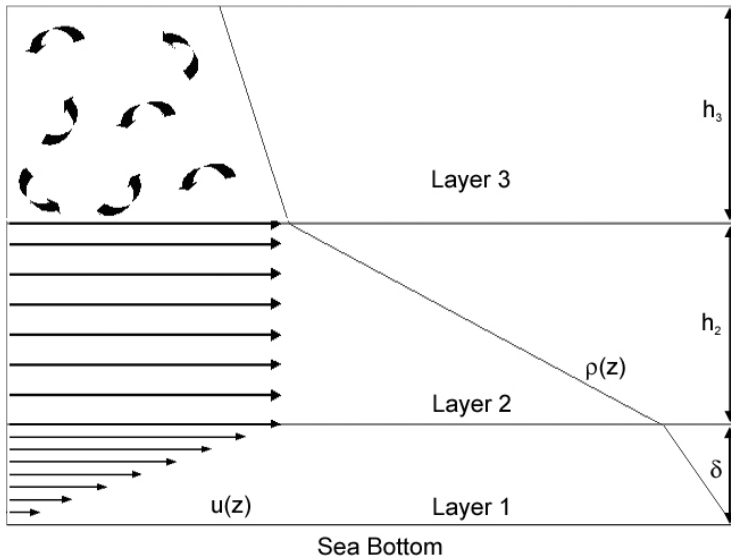


Fig.1. Three layer model for turbidity current where $\delta \ll h_2, h_3$. The stick diagram of the velocity profile $u(z)$ and the density profile $\rho(z)$ are shown.

The behaviour of the basal layer (layer 1 in Fig. 1) is more complex. It is able to erode or deposit sediments depending to the environment parameters (i.e. available material, grain size, slope) and to the values of velocity and concentration of the turbidity current (Parker, 1982). The velocity shear (due to the bottom

stress) being greater than the stratification ($\rho \left(\frac{\partial u}{\partial z} \right)^2 > g \frac{\partial \rho}{\partial z}$, i.e. $Ri < 1$), erosion of available sediments occurs. When the concentration of sediments contrasts the turbulence in Ri becomes ≈ 1 and erosion equals deposition. Finally, under condition of severe density gradient (i.e. high stratification), damping of the

turbulence ($\rho \left(\frac{\partial u}{\partial z} \right)^2 < g \frac{\partial \rho}{\partial z}$, i.e. $Ri > 1$) may cause a net loss of sediments during the deceleration of the current.

The results of this study emphasize the flow conditions when deposition occurs. In fact, according to the previously described model, loss of sediments in the basal layer occurs in laminar condition ($Ri > 1$). Then, turbiditic “massive” sandstones formation may be formed by a rapid temporal upward aggradation of sediments below the flow (probably due to a topography control), rather than by en masse deposition at the cessation of the flow (Kneller and Branney, 1995; Baas, 2004).

Consequently, the thickness of the recorded deposits are linked to the deposition duration time of the sustained turbidity current rather than the height of the current itself.

The presence of a crude lamination found in many turbiditic sandstones, bed originally interpreted as massive, observed into the Laga basin (Central Apennine, Italy), seem to confirm these results (Fig. 2).

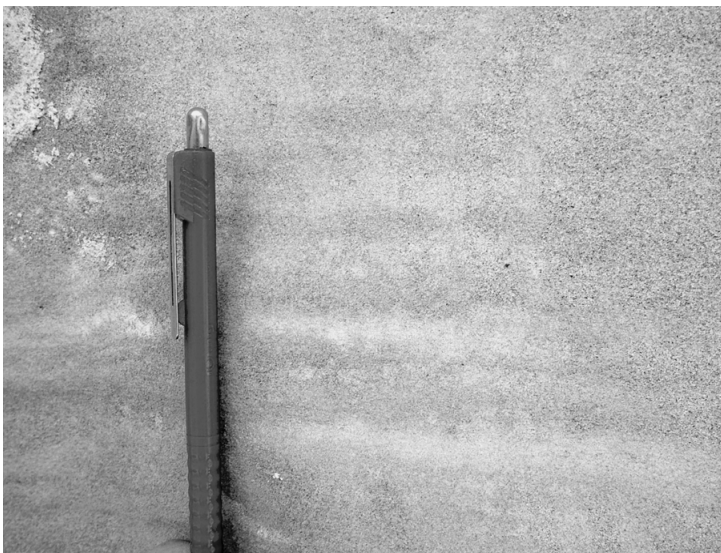


Fig. 2. Crude lamination found in a turbiditic sandstone bed originally interpreted as “massive sandstone” (Laga Basin, Central Apennine, Italy).

- Baas, J.H. (2004) Conditions for formation of massive turbiditic sandstones by primary depositional processes. *Sedimentary Geology*, 166, 293-310.
- Ellison, T.H. and Turner, J.S. (1959) Turbulent entrainment in stratified flows. *Journal of Fluid Mechanics*, 6, 423-448.
- Kneller, B.C. and Branney, M.J. (1995) Sustained high-density turbidity currents and the deposition of thick massive sands. *Sedimentology*, 42, 607-616.
- Parker, G. (1982) Conditions for the ignition of catastrophically erosive turbidity currents. *Marine Geology*, 46, 307-327.
- Stacey, M.W. and Bowe, A.J. (1988) The Vertical Structure of Density and Turbidity Currents: Theory and Observation. *Journal of Geophysical Research*, 93, 3528-3542.

Sustained quasi-steady turbidity current: outcrop evidence from the Pliocene peri-Adriatic foredeep (Cellino Fm., Central Italy)

Felletti, F.¹, Carruba, S.², and Casnedi, R.²

1 Dipartimento Scienze della Terra, Università di Milano, via Mangiagalli 34, 20133 Milano, Italy.

2 Dipartimento di Scienze della Terra, Università di Pavia, via Ferrata 1, 27100 Pavia, Italy.

The aim of this work is to investigate the nature of the numerous, very thick deep-water sheet-sandstones that dominate the lower portion of the Cellino Formation (Central Italy).

The studied turbidite system (about 2,500 m thick) represents the Lower Pliocene turbiditic filling of the outer Abruzzo sector of the Periadriatic foredeep. The foredeep was affected by compressional deformation linked to the overall migration of the chain-foredeep system toward the east. Tectonic activity was mostly coeval with the sedimentation and propagated towards the foreland; thrusting became progressively younger from W to E. The Cellino Basin has been intensely explored, being the site of hydrocarbon-bearing sands. The turbidite beds can be distinctively resolved in the well logs and correlated to the measured sedimentary sections on outcrop. Based on well log correlation, tens of individual beds up to 23 m thick have been traced along the axis of the basin over distance in excess of 100 km and, perpendicularly to the basin, over distance of 30-40 km (Carruba et al. in press), with sand volumes on the order of a few 10³ Km³ (10 – 80 Km³).

Palaeocurrent data taken from basal flute structures indicates southerly-directed flows, parallel to the depocentral axis of the basin. The thickest beds show a basin-wide extension, onlapping the basin margins without significant thickness variation.

The internal organization of the studied megabeds provides evidence for occurrence of long-lived flows and suggests deposition by gradual aggradation from sustained currents (sustained turbidity current; Kneller and Branney, 1995). The following features have been argued to be characteristic for sustained currents: (i) turbidite beds of extraordinary volume and thickness, (ii) very thick massive basal division (0.5 – 6 m thick), (iii) very frequent alternation of structureless and laminated intervals associated to internal scour surfaces, (iv) thick massive mudstone cap (1-10 m) that terminates the vertical organization of the sedimentary structures, (v) crudely developed grain-size profile that is overall upward fining (normally graded), (vi) abundant organic matter, (vii) extensive water-escape features.

The very thick massive basal division observed in the studied megabeds can be explained with progressive aggradation and absence of traction at the depositional flow boundary. The very frequent alternation of structureless and laminated intervals observed within the studied deposits, and their internal scour surfaces reflect temporal variation in flow velocity and sediment flux within the same current, as indicated by the discontinuity of the scour surface and the constant grain size above and below the surfaces. The graded upper part of the studied megabeds (a thick massive mud cap terminates the vertical organization of the sedimentary structures) represents the deposits of the waning stage of the current.

Assuming a quasi-steady flow scenario we can explain the nature of the numerous very thick megabeds within the Cellino Fm considering that the determining factors of the thickness of the studied deposits are the confinement of the basin and the rate and the duration of deposition, which may proceed as long as the current maintains a flux of grains towards the site of deposition.

The origin of these large-volume turbidity currents and their high rate of occurrence can be related to an interaction of many factors and external controls, which are typical of the ancient foredeep basins (Mutti et al., 2003).

Our data suggest that the studied megabeds could be originated from catastrophic floods and sediment failures during relative falling- and low-stand stage of sealevel forced by dramatic tectonic uplift of basin margins. Where the mountains fronts are close to shoreline, floods would be able to carry the majority of sediment load directly to the sea; the final depositional area of the ancient fluvial system that probably fed the Cellino basin lies in the deep water, far away from river mouths, and it is recorded by basinal turbidite sandstones and megabeds.

Although an understanding of climatic controls is extremely difficult on the basis of available data, high-frequency climatic pulses (that provided the water through which sediments were periodically flushed to the Periadriatic foredeep by flood-related process) could explain the amount of stacked megabeds. In this model, lower-frequency tectonically-forced cycles of uplift/denudation account for sediment availability through time. Consequently, the lower portion of the Cellino Formation could correspond to a stage of a single uplift/denudation cycle. In this stage, the tectonically active Cellino basin reaches its highest instability because the elevation of drainage basins is maximum and its proximity to the shoreline minimum.

Carruba S., Casnedi R., Perotti C.R., Tornaghi M. and Bolis G., 2005, Tectonic and sedimentary evolution of the Lower Pliocene Periadriatic foredeep in central Italy. *International Journal of Earth Sciences*, in press (DOI 10.1007/s00531-005-0056-4)

Kneller B., and Branney M.J., 1995, Sustained high density turbidity currents and the deposition of thick massive sands. *Sedimentology*, v. 42, pp 607–617.

Mutti E., Tinetti R., Benevelli G., Mavilla N., di Biase D., Fava L., Angella S., and Cavanna G., 2003, Deltaic, mixed and turbidite sedimentation of ancient foreland basin. *Marine and Petroleum Geology*, v. 20, pp 733-755.

Controls on Sediment flux, Routing and Storage and the impact on the Stratigraphic Development of Deepwater Basin Floor and Slope Systems, Karoo Basin, South Africa

Flint, S., Hodgson, D., King, R., van Lente, B., Wild, R., and Potts, G.

Stratigraphy Group, Department of Earth and Ocean Sciences, University of Liverpool, Liverpool L69 3GP, U.K.

Integration of sedimentological, stratigraphic, structural, petrographic and geochemical studies on the Permian Karoo deepwater succession and the Cape Fold Belt allows assessment of the relative effects of different external controls on the resultant deepwater stratigraphy of the Tanqua and Laingsburg depocentres. The petrography, whole rock geochemistry and Sm/Nd isotopic signatures of the sandstones in both depocentres is the same and indicates a single mainly granitic source area, possibly in Patagonia. The Cape Fold Belt was not, therefore, an emergent feature at this time.

Deposition of deepwater clastics was earlier in the Laingsburg depocentre than the Tanqua depocentre, and was initiated by the 230m thick Vischkuil Formation, a succession of mudstone interbedded with fine-grained turbidites with three phases of mass transport complex emplacement. The overlying 850m thick Laingsburg Formation shows a long-term progradational trend, from basin floor to upper slope sediments. Facies distributions and thickness changes observed by Sixsmith (2000) and Grecula (2000) suggest that episodic tectonic deformation of the seabed was contemporaneous with deposition. At this time the Tanqua depocentre accumulated over 600 m of hemipelagic mudstone and minor thin siltstone turbidites. Sediment was supplied to the early Karoo basin via the long-lived De Doorns Synform, which was a structural low in the early, still subaqueous, Cape Fold Belt and acted as a point source 'palaeo-canyon'. Restoration of the CFB structures indicates an average rate of 9mm y⁻¹ for the northward migration of the deformation front. Sand supply to the Laingsburg depocentre was terminated by tectonic uplift of the De Doorns Synclinorium, causing a regional (100 km)-scale switch in sediment delivery in favour of the Tanqua depocentre. This tectonically driven progressive avulsion resulted in the fining-upward profile of the Laingsburg succession and a corresponding coarsening-upward motif preserved in the Tanqua stratigraphy, also manifest in the progressive increase in volume of the four successive Tanqua basin floor fans.

The Karoo deepwater to shelf section is interpreted as a 3rd-order sequence. Initiation of major deepwater sand supply is marked by the MTCs of the Vischkuil Formation, which we interpret as a 3rd order falling stage systems tract with a low order sequence boundary at the base of Fan A complex. The Laingsburg Formation represents the late lowstand to early transgressive systems tract, capped by an 80 m-thick condensed shale TST/maximum flooding surface. Progradational shelf-edge delta cycles form the 3rd order highstand systems tract. Within the 3rd order late LST, Laingsburg Units B-F, and then Tanqua Fans 1 – 4 represent higher frequency sequences. Each Tanqua basin floor fan has been divided into regionally mappable high frequency intrafan sequences that are arranged in a progradational-aggradational-retrogradational stacking pattern. Although unsupported by absolute age control, careful mapping of the physical stratigraphic units and surfaces has allowed the establishment of a sequence hierarchy scheme dominated volumetrically by individual lowstand components, which stack into sequence sets and composite sequences. The progradational-aggradational-retrogradational stacking pattern means that moving down dip in any basin-floor fan system, the lowermost sandstone preserved is progressively younger, whilst the uppermost sandstone is progressively older. This stacking pattern exerts an important predictable control on seal geometries and the distribution of lithofacies and architectural elements at reservoir scale.

In the Karoo system we can distinguish 'lower order' and 'higher order' external controls on the stratigraphic evolution of the deepwater succession. The long-term sediment supply pathway and regional progressive re-routing of this supply from Laingsburg to Tanqua were controlled by the early tectonic development of the Cape Fold Belt. This tectonic modulation of the sediment delivery system explains the non-coeval fining-upward Laingsburg and coarsening-upward Tanqua successions within the same 3rd order LST, and the later contemporaneous progradation of shelf-edge delta cycles of the 3rd order HST as the SW Karoo Basin margin evolved from a bypass- to an accretion-dominated system. The higher order, still predictable, controls on stacking patterns and facies distributions within fans are interpreted to have been glacio-eustatic sea-level cycles in the Permian icehouse global climate regime.

Inverse numerical modelling of mixed siliciclastic and carbonate sequence-stratigraphic systems, using the Metropolis algorithm in a Monte Carlo Inversion algorithm

Foldager, R.*

Geological Institute, University of Copenhagen, Øster Voldgade 10, 1350 Copenhagen K, Denmark

** Corresponding author : foldager@geol.ku.dk*

Inverse numerical stratigraphic modelling is a quantitative technique that extracts values of model parameters – such as tectonic movement, sea-level changes, sediment supply and basin topography – from real stratigraphic data, seismic profiles, well-logs and outcrops.

The technique comprises of:

- A robust forward stratigraphic model that is fast enough to make it possible to be run many times in the inversions loop algorithm.
- A ‘misfit’-function that describes the quantitative difference between observed stratigraphic data and the forward modelled data.
- An inverse algorithm.

First step in the project is a base-level controlled 2D siliciclastic stratigraphic model that is used in a Metropolis algorithm in a Monte Carlo Inversion (Metropolis et al., 1953; Mosegaard and Sambridge, 2002; Foldager, 2004;).

Second step in the project is the development phase of a 3D combined siliciclastic/carbonate numerical model for use in a Monte Carlo Inversion algorithm. The 3D forward model uses a combination of geological ‘first principles’ (Posamentier and Allen, 1999) and the same modelling approach that is applied in other 3D models (Ritchie et al., 1999; Warrlich et al., 2002). The 3D model is a conceptual model, which uses that shear stress acting on the sediment, comes from three different sources: currents, wave activities and slope gradient. The overall model behaviour is that sediment is eroded or bypassed at high levels of shear stress and deposited at low levels of shear stress. Both forward models, the 2D and the 3D, are working within the borders of the sequence stratigraphic frame.

The combination of forward sequence stratigraphic modelling and numerical inversion in a Monte Carlo Inversion technique has many advantages. In normal forward stratigraphic models it is still the geologist who is making the manipulations on the model parameters to make them fit the observed data parameters. Making this search for a solution of fit between observed stratigraphic data and calculated stratigraphic data, is done by the use of a Monte Carlo Inversion Algorithm. Applying his technique, one benefits twice in the sense that the modelled parameters come with error-uncertainties and are more objective than when modelled solely by the geologist.

Foldager, R., 2004. Numerisk modelleret sekvensstratigrafi - teori, forsøg og eksempler. Unpublished Master Thesis, University of Copenhagen, Copenhagen, Denmark, 114 pp.

Metropolis, N., Rosenbluth, A.W., Rosenbluth, M.N., Teller, A.H. and Teller, E., 1953. Equations of state calculations by fast computing machine. *Journal of chemical physics.*, 21: 1087–91.

Mosegaard, K. and Sambridge, M., 2002. Monte Carlo analysis of inverse problems. *Inverse Problems*, 18(3): R29.

Posamentier, H.W. and Allen, G.P., 1999. Siliciclastic sequence stratigraphy - concepts and applications. *Concepts in sedimentology and paleontology*, 7. SEPM (Society for Sedimentary Geology), Tulsa, Oklahoma, U.S.A., 210 pp.

Ritchie, B.D., Hardy, S. and Gawthorpe, R.L., 1999. Three-dimensional numerical modeling of coarse-grained clastic deposition in sedimentary basins. *J. Geophys. Res.*, 104(B8): 17759–17780.

Warrlich, G.M.D., Waltham, D.A. and Bosence, D.W.J., 2002. Quantifying the sequence stratigraphy and drowning mechanisms of atolls using a new 3-D forward stratigraphic modelling program (CARBONATE 3D). *Basin Research*, 14(3): 379-400.

The impact of margin shaping processes on the architecture of deep-sea depositional systems: the Sicilian and Sardinian margins (Tyrrhenian Sea)

Gamberi, F.

ISMAR, Sezione Istituto Geologia Marina di Bologna.

Multibeam bathymetric data, providing the details of the seafloor geomorphology, are influential for expanding our knowledge on deep-sea depositional systems. As a matter of fact, the recent extensive acquisition of multibeam data has shown that a higher variability in the style of deep-sea deposition along continental margins occurs than was previously thought. In particular, multibeam data have greatly contributed to enhancing our perception of the wide range of architecture and of component geomorphic elements that characterise present-day depositional systems along different stretches of continental margins.

Moreover, the possibility of a direct study of the land and shallow water areas can lead to the establishment of a straightforward link between the processes acting in the source and transfer areas and the geometry of the observed deep-sea depositional systems. Such a study has been carried out on two portions of the Tyrrhenian Sea margin where multibeam bathymetric data have been recently collected.

The Tyrrhenian Sea, located in the Mediterranean Basin, is enclosed by the islands of Sardinia and Corsica to the west, by the Italian peninsula to the east and Sicily to the south. The setting of Tyrrhenian region is the result of a complex recent geological history, characterised by the interplay of compression and orogenic processes and extension, arc volcanism and back-arc basin opening. As a consequence, the single margins of the Tyrrhenian Sea present highly variable geological features. In particular, since extensional tectonics has migrated with time toward the E-SE, a remarkably contrasting present-day geological setting characterises the Sardinian and Sicilian margins, located respectively to the west and to the south-southeast of the Tyrrhenian sea.

In Sicily, extensional tectonics is still active and dissects the Maghrebic chain in a series of horsts and grabens, both perpendicular and parallel to the margin with high differential vertical movements and an uplift rate as high as 1 mm/year. A network of parallel, intermittent discharge rivers with small drainage basins develops; rivers run perpendicular to the margin in the tectonically depressed areas and enter the coastal region at intervals of less than 10 km. In addition, along the whole northeastern Sicilian margin, the shelf is always very narrow. On the slope, canyons face most of the river entry points; in general, the canyons are followed downslope by leveed channels. At the base-of-slope an apron consisting of laterally coalescing deposits of leveed channels is formed. However, in the eastern portion of the northern Sicilian margins, where the rivers have very small drainage basins and the rate of uplift is higher, a destructional apron consisting of a large mass wasting complex is developed.

The eastern Sardinian margin, on the contrary, is a passive margin where extensional tectonics has been quiescent since the Early Pliocene, and is in general characterised by a negligible rate of uplift. Rivers have larger drainage basins than in the Sicilian margin and their feeding points to the coastal system are widely spaced at around 30 km. Furthermore, a wide shelf is present along the whole eastern Sardinian margin and in the northern area reaches a width of around 20 km. On the slope, the major canyons, being connected with the river entry points are widely spaced. Therefore, at the base-of-slope they feed isolated depositional bodies in the form of a series of small, radial or elongated fans developed at the mouth of the canyons. Large canyons also develop in the central part of the Sardinian margin where there are no large rivers; here they are likely due to slope instability following the uplift of the region because of recent volcanic activity.

A strict application of the sequence stratigraphy models, would lead one to interpret the small fans of the Sardinian margin and the slope apron of the Sicilian one as representing deposition during different stands of sea level. On the contrary, the study shows that the differences in the present-day Sicilian and Sardinian depositional systems are mainly due to the features of the sediment delivery systems developed in the two margins. Thus, the research shows that the distinct setting of each margin is a primary factor in controlling the architecture of the depositional systems and that it must be considered when predictive models for the distribution of deep-sea deposits are applied.

The influence of the age of back-arc basins on sediment influx and deep-sea clastic deposition: the Vavilov and the Marsili basins (Tyrrhenian Sea)

Gamberi, F., and Marani, M.P.

ISMAR, Sezione Istituto Geologia Marina di Bologna.

The Vavilov and the Marsili basins are two separated depocenters, at a water depth of around 3500, in the center of the Tyrrhenian Sea. The Vavilov basin, the oldest backarc basin of the Tyrrhenian region supra-subduction system, formed around 6 Ma ago behind a volcanic arc that is presently inactive and dismembered. Successively, around 2 Ma ago, the Marsili back-arc basin and the presently active Aeolian volcanic arc developed to the southeast. The Vavilov and Marsili basins thus, represent successive stages in the evolution of back-arc basins, and are therefore characterised by different tectonic and volcanic regimes and by contrasting margin settings. Multibeam bathymetric data, long range and deep towed sidescan sonar images, high- and very-high resolution seismic lines and seafloor sampling are available over the two basins. They allow us to compare the depositional processes at the scale of the basin fill and to decipher the smaller scale depositional architectural elements of the recent depositional systems of the two basins.

The Vavilov basin is bound to the west by the D'Ancona Ridge and by the De Marchi seamount that represent structural barriers to the Sardinia Valley, the main submarine sedimentary pathway that collects siliciclastic sediments from the Sardinian passive margin. Thus, the main sedimentary entry points are located on the northern and eastern sides of the Vavilov basin where submarine canyons and slope failures that dissect the structurally controlled intraslope basin of the Campanian and margin, can directly feed sediments to the Vavilov basin plain. At the base of the Campanian slope, small depositional lobes are present at the mouth of the major canyons. However, no large fans develop in the Vavilov Basin and the salient features of its recent sedimentary infill are, 4 basin-wide Acoustic Transparent Layers (ATLs). The two lowermost ATLs lie between 50 and 10 m below the seafloor; they have a cumulative thickness in the range of 45 m, with only slight thickness variations over the small-scale intrabasinal highs (tens of metres) and abrupt terminations against the hundreds of metres high basin-bounding structural blocks. The two uppermost ATLs are thinner, and are present over two distinct depocentres in the eastern and western part of the Vavilov Basin; they thin out considerably over the small-scale intrabasinal highs and gradually pinch out towards the structural highs that bound the basin. The basin-wide ATLs, highlight that whatever the entry point, sedimentary processes consisting of flows that spread and deposit over the whole basin are responsible for much of the recent sedimentary infill of the Vavilov Basin. Furthermore, the differences in the distribution, in the geometry of terminations and in the interaction with the small scale intrabasinal highs, that distinguish the 4 ATLs point to variable characteristics of the flows responsible for the ATLs' deposition. The volume of the deepest ATL is around 150 km³. ATLs with similar volumes have already been reported in the deep basins of the Eastern and the Western Mediterranean Sea in very different geodynamic settings. As a consequence, the finding in the Vavilov Basin further strengthens the evidence that ATLs are a common element of the recent stratigraphic successions of the deep-sea basins of the Mediterranean region, regardless of the structural and geodynamic context.

The Marsili basin is flanked by the active Aeolian arc and by the rapidly uplifting Apenninic and Calabrian arc. From the Calabrian margin, the Stromboli Canyon cuts through the Aeolian Arc and reaches the Marsili Basin; it funnels a large input of siliciclastic and volcanoclastic material that enters the western portion of the Marsili basin. As a result, of the large clastic input, a deep-sea fan spans almost the whole western portion of the Marsili basin, with a length of 40 km and a width of 20 km. Much of the fan is characterised by a strongly reflective, rough seafloor highlighting that it is mainly floored by coarse-grained sandy or gravelly material and by highly disorganised depositional bodies, with small lateral continuity as confirmed by the highly variable sedimentary facies observed in the cores. Different architectural elements characterise the deep-sea fan. To the south, a leveed channel is evident down to a depth of around 3200 m where it connects to a lobe measuring a length of around 9 km and a width of around 4,5 km. The central portion of the fan is occupied by a valley that reaches the deeper portion of the basin down to a depth of 3400 m; it measures a maximum width of 4.5 km and is characterised by intrachannel longitudinal bars and marginal terraces. The valley feeds a depositional lobe that in the distal portion of the fan interacts with tectonic features at the base of the Marsili volcano. In the northern portion of the fan, another main channel is present; it has well developed levees with a well layered sequence, indicative of finer-grained material as compared with the other architectural elements that make up the Marsili fan.

The differences in the recent depositional setting of the Vavilov and Marsili Basins can be mainly ascribed to the different ages of the two basins that in turn has a considerable impact on the sediment influx to the basins. The Marsili basin faces the active portion of the supra-subduction Tyrrhenian region, where a large

production of clastics is fostered by the high rate of uplift and the active volcanism; as a consequence, a coarse-grained deep sea fan develops in the eastern part of the Marsili basin. On the contrary, the Vavilov faces the Sardinian passive margin and is experiencing a reduced sediment influx from the coastal areas also because of the structural setting of the surrounding margins; the filling of the basins occurs through basin-wide thick layers resulting from sediment flows that are likely triggered by the failure of the adjacent slopes.

Glaciomarine sedimentation of the Central Bransfield Basin shelf

García, M.^{1*}, Anderson, J.B.², Ercilla, G.¹, and Alonso, B.¹.

1 Instituto de Ciencias del Mar (CMIMA)- CSIC- Passeig Maritim de la Barceloneta, 37-49. 08003 Barcelona. Spain.

2 Department of Earth Science, Rice University, Houston, TX 77251, USA.

** Corresponding author : mgarcia@icm.csic.es*

The Bransfield Basin is a narrow NE-SW oriented basin, confined between the northern Antarctic Peninsula and the South Shetland Islands (Fig. 1a). The Bransfield Basin developed in a complex tectonic setting, as a roll-back basin after the end of the spreading of the Phoenix-Antarctic Ridge during the middle Pliocene (Galindo et al., 2004), and its geological complexity is enhanced by the cyclical glaciomarine sedimentary processes affecting the basin since its opening. The aim of this work is to better define the morphology and seismic stratigraphy of the glaciomarine record in the Central Bransfield SE shelf. The data used include swath bathymetry and single-channel seismic reflection profiles obtained in the MAGIA99 cruise and swath bathymetry obtained in the GEBRA93 cruise (Gràcia et al., 1996; Prieto et al., 1999), both on board B.I.O. Hespérides, as well as bathymetry datasets made public by the University of Texas.

The CBB SE margin consists of a gently seaward sloping shelf, a relatively steep narrow slope and a flat basin (Fig. 1a). The shelf shallows and narrows towards the NE. The upper shelf is dissected by prominent troughs. The shelf edge occurs at depths of 800 to 1000 m and has a WSW-ENE orientation and a sinuous shape. The narrow (4 to 6 km) and steep (5.5° to 8.5°) slope reaches depths of about 1400, and the basin deepens towards the NE reaching depths of 1900 m (Gràcia et al., 1996). The swath bathymetry reveals the existence of glacial-related morphologic features on the lower shelf, off the mouth of troughs, such as the S-N to SW-NE oriented channel-like features that cut the CBB shelf and reach the shelf edge. Their morphology and similarity with features described on the Antarctic continental shelf (Welner et al., 2001; Heroy and Anderson, 2005) allow their interpretation as mega-scale glacial lineations. This indicates that the ice-sheet reached the shelf edge during the Last Glacial Maximum and together with the facies identified in the seismic record provides a basis for interpretation of older units and bounding unconformities.

Five seismic units (S1a to S1e, from the youngest to the oldest units) have been identified overlying a prominent unconformity (Fig. 1b). The seismic unit below the unconformity includes highly deformed strata and both crystalline and sedimentary basement. In contrast, the five seismic units above the unconformity show no signs of deformation and are generally conformable, or they onlap on the inner shelf, while they downlap in prograding wedges near the shelf edge. The units terminate at or near the shelf edge and are bounded by erosional surfaces with considerable relief. This, plus the facies character of the units, implies a glacial and glaciomarine origin. The five seismic units form part of the regional seismic unit S1 described by Jeffers and Anderson (1990). The unconformity at the base of the seismic units can be interpreted as the beginning of the predominance of glaciomarine processes in the basin, and the highly deformed sediments below it would be interpreted as syn-rift deposits. This would agree with the interpretations of Banfield and Anderson (1995), Prieto et al. (1999) and Galindo-Zaldívar et al. (2004).

The four older seismic units (S1b to S1e) are characterised by the presence of channel-like incisions, interpreted as either melt-water channels or tunnel valleys, and lens-shaped bodies of chaotic reflectors, interpreted as till deposits. In contrast, the most recent seismic unit S1a is characterised by layered seismic reflectors and few chaotic intervals. Chaotic reflectors interpreted as slide deposits occur at the shelf-edge. This may be indicative of the predominance of a less severe climatic setting during deposition of the younger seismic unit.

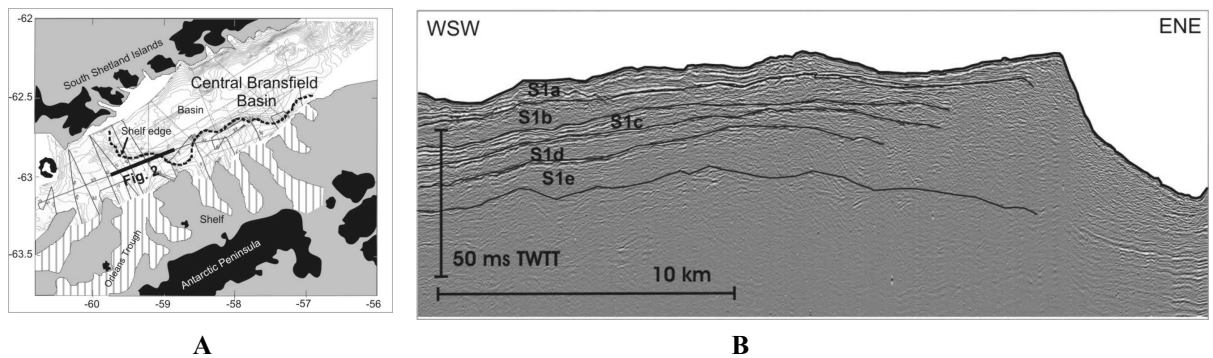


Figure 1. (A) Location map and morphology of the Central Bransfield Basin. (B) Seismic reflection profile on the CBB shelf showing the five seismic units (S1a to S1e). See location in the map.

- Banfield, L.A., Anderson, J.B., 1995. Seismic facies investigation of the late Quaternary glacial history of Bransfield Basin, Antarctica. In: Cooper, A.K., Barker, P.F., Brancolini, G. (Eds), *Geology and Seismic Stratigraphy of the Antarctic margin*. AGU Antarctic Research Series 68, 123-140.
- Galindo-Zaldívar, J., Gamboa, L., Maldonado, A., Nakao, S., Bocha, Y., 2004. Tectonic development of the Bransfield Basin and its prolongation to the South Scotia Ridge, northern Antarctic Peninsula. *Marine Geology* 206, 267-282.
- Gràcia, E., Canals, M., Farrán, M., Prieto, M.J., Sorbias, J., GEBRA Team, 1996. Morphostructure and Evolution of the Central and Eastern Bransfield Basins (NW Antarctic Peninsula). *Marine Geophysical Researches* 18, 429-448
- Heroy, D.C., Anderson, J.B., 2005. Ice-sheet extent of the Antarctic Peninsula region during the Last Glacial Maximum (LGM)- Insights from glacial geomorphology. *GSA Bulletin*, 117, 1497-1512
- Jeffers, J.D., Anderson, J.B., 1990. Sequence stratigraphy of the Bransfield basin, Antarctica: implications for tectonic history and hydrocarbon potential. In St. John, B. (Ed), *Antarctica as an Exploration Frontier – Hydrocarbon Potential, Geology, and Hazards*. American Association of Petroleum Geologists, *Studies in Geology* 31, 13-30.
- Prieto, M.J., Ercilla, G., Canals, M., de Batist, M., 1999. Seismic stratigraphy of the central Bransfield Basin (NW Antarctic Peninsula); interpretation of deposits and sedimentary processes in a glacio-marine environment. *Marine Geology* 157, 47-68
- University of Texas bathymetry dataset website: www.marine-geo.org
- Wellner, J.S., Lowe, A.L., Shipp, S.S., Anderson, J.B., 2001. Distribution of glacial geomorphic features on the Antarctic continental shelf and correlation with substrate: implications for ice behavior. *Journal of Glaciology*, 47 (158), 397-411.

Valuing Intrinsic and Extrinsic Controls on the Permian Record of Deep-Water Sedimentation in the Delaware Basin, West Texas, USA

Gardner, M. H. ¹, Melick, J. J. ¹, Borer, J. M. ², Kling, E. ², Baptista, N. ³, and Romans, B. ⁴

Montana State University (1), Colorado School of Mines (2), PDVSA (3), and Stanford University (4)
Corresponding address: Montana State University, Department of Earth Sciences, 200 Traphagen Hall, Bozeman, Montana, 59715

Linking basin-restricted subaqueous flows to extrinsic controls governing their initiation is difficult. Even though the influence of extrinsic controls (eustasy, tectonics, and climate) is best resolved in the basinal strata, intrinsic controls (i.e., gradient, grain-size population, topography and flow run-out length) have a more profound effect on deep-water sedimentation patterns. Source-to-sink correlations relating tectonic, eustatic and climatic forcing to deep-water facies, lithology, sedimentary bodies, and stratigraphic cycles were analyzed from 590 sedimentological profiles and detailed (20m) mapping of continuous shelf-to-basin outcrops (255-km² area) correlated (355 well logs and 3300 km of 2D seismic) across the 33,500-km² Delaware Basin.

The record of extrinsic forcing, resolved in basinal strata, is obscure outside of the basin, and is only confidently isolated from intrinsic controls restricted to the basin through complete basin analysis. Tectonic movements controlled the southwest to southeast, clockwise, onset of Brushy Canyon and lower Cherry Canyon Formation clastic sediment, sourced from at least seven shelf feeders encircling this foreland basin. Basin-restricted siltstone intervals correlated throughout the basin help define a threefold hierarchy of stratigraphic cycles within this lowstand systems tract (LST) of a 3rd-order composite sequence (2-4 my). Although along-strike variations in sediment supply change the thickness, lithology and architecture of these basinal cycles, stratigraphic changes in multiple criteria permit regional correlation that reflects eustasy. Repetitive, multi-scale and organized clustering of varve-like laminations, present in carbonate, evaporite and clastic strata, reflect precipitation-modulated climate.

In this study, as with most others, an incomplete record outside of the basin make separating extrinsic from intrinsic controls on sedimentation difficult; therefore, we are required to draw our conclusions from a record deposited solely below the physiographic break of two older carbonate ramps. Overlying an organic-rich siltstone (4m thick, TOC >6%) that drapes highstand carbonate mass transport deposits (MTDs), sandy basinal strata (350m thick) resemble the basin-floor and slope fans of an LST. The basal siltstone drape records either a basin-restricted marine deepening event, separating highstand and lowstand strata with no shelf record, or it is the correlative conformity to the shelf unconformity, as we interpret. In either case, the higher fidelity basinal strata record events not preserved in shelf-equivalent strata. Because condensed sedimentation records sediment starvation, but not necessarily sea level rise, this siltstone drape, most likely records the substantial time lag between unconformity initiation and significant sand bypass, and therefore suggests continuous sea-level fall between emplacement of highstand MTDs and LST sand deposition. Further complicating shelf-to-basin correlations, the MTDs created sea-floor topography that locally ponded and produced sandstone pinch-outs in the lower 80m of the succession.

Stratigraphic changes in multiple criteria correlated throughout the basin suggest an evolution in basin sedimentation recording eustatic control. Younger carbonate MTDs of the Cherry Canyon Formation incise the LST top and resemble those at the base; both of which record mass failure during highstand outbuilding of carbonate ramps. Siltstone, resembling the basal drape, also is found at the LST top. Condensed sedimentation, recorded by the basal siltstone drape, most likely correlates to continual sea-level fall spanning highstand and lowstand deposition, whereas the younger siltstone records the end of gradual sea-level rise and represents a downlap surface for the overlying Cherry Canyon LST. Strata in the upper 100m of the Brushy Canyon LST show an upward increase in shelf-derived carbonate allochems (+50%), a decrease in sand percent (-40%), and an increase in the thickness and organic richness of siltstones (+300%). This latter attribute suggests a decreased frequency of sandy subaqueous flow deposition. Equivalent source-distant strata in the upper LST, and derived from the same shelf feeder system, show a doubling in silty sandstone and feldspar that records hydraulic fractionation of grain size and mineralogy within these subaqueous flows. In this case, longitudinal fractionation was enhanced by more complete flow transformation enabled by transport along smoothed depositional profiles within the upper LST. Both slope expansion and back-stepping of aggradational upper-slope channels, record a shelfward shift in the locus of basinal sedimentation, while more elongate basin-floor thicks in this upper part reflect the decreased

sediment volume. These depositional patterns record a gradual eustatic sea-level rise and suggest that its onset commences within the LST. Organic-rich sand-poor basinal facies bracketing this LST occur during either eustatic rise or fall because they record sediment starvation that is only indirectly related to an extrinsic control.

The more complete deep-water record correlates to a fragmented shelf record, and this incongruity makes recognition of extrinsic controls from the record solely outside the basin challenging. As the ultimate sediment sink, extrinsic controls are best resolved from the basinal record, but intrinsic changes in gradient, grain-size population, topography, and run-out length, have a greater impact on subaqueous flow transport and deposition, which can be difficult to differentiate from extrinsic signatures without complete characterization of the basin.

Channel Avulsion Patterns In Some Major Deep-Sea Fans—External Versus Internal Controls

Kolla, V.¹, and Posamentier, H.W.²

1. *Reliance Industries Ltd, Mumbai, India*

2. *Anadarko Petroleum Corporation, Canada.*

We discuss here the anatomy and patterns of the most recent channel avulsions in the Amazon, Zaire, Indus and Bengal Fans, all located along passive margins and the factors affecting them. The channels in all these major fans are sinuous to very sinuous. In majority of cases, the process of avulsion consists of deposition of high-amplitude reflection packets (HARPs) of relatively continuous sheet deposits, overlain by leveed channels. The leveed channel patterns formed by fore- (seaward) or back- (landward) stepping avulsions are common in the western Amazon Fan and in the Northern and Central Zaire Fan. However, the most recent channels in the Indus and Bengal Fans and in the Southern Zaire Fan appear to form radial patterns, most of the main avulsions having occurred in relatively restricted areas.

Sufficient sediment supply by major river systems and its accessibility to a canyon or shelf edge are pre-requisites for the generation of sediment-gravity flows and evolution of channels in these fans. Thus, external factors such as climate, terrestrial drainage, hinterland topography and geology and sea levels ultimately affected the sediment supply and overall fan evolution. However, channel avulsions in the deep-sea fans studied appear to have been influenced by specific processes and events both external and internal to the depositional systems. The internal processes and factors that appear to have lead to channel instability and avulsion-threshold conditions are: channel sinuosity increase and lengthening, channel thalweg aggradation, differential channel fill and decrease in channel relief, bank cohesion, depositional and syn-tectonic topography, slumping and channel plugging. The external events consist of increased volumes and speeds of turbidity currents that may have acted as avulsion triggers, depending on the degree of development of avulsion-threshold conditions of channels. It is apparent that many of the internal factors themselves are ultimately influenced by external controls.

Depending on the data available, it is possible, in some cases, to point to certain controls as being more critical for the channel avulsion and evolution in the fans studied. It is evident that an initial sealevel fall was imperative to make canyons the active sediment conduits and thus cause the channel evolution in the Amazon, Indus and Bengal Fans. In the case of the Zaire Fan, the Zaire canyon and river mouth were apparently connected both during high and low stands of sealevel for much longer time than Quaternary. Thus, sea level fall was not necessary to cause channel evolution in the Zaire Fan. However, during the time intervals considered here, many sealevel falls and rises of varying magnitudes occurred and must have, together with climatic changes influenced the timing of avulsions, to a greater or lesser degree, in all the fans. Detailed isotope data suggest that, after the initial sealevel fall that may have initiated the recent channel evolution in the Amazon Fan, some avulsions coincided with sealevel falls, while others corresponded to sealevel rises (and climatic changes). In the case of the Bengal Fan, the most recent channel apparently formed during the rise of sealevel in Holocene. In all other cases, in the absence of detailed data, although we can speculate on the effects of sea levels in some instances, we cannot attribute a specific sealevel or climate change to a particular avulsion.

The main differences between the fan areas with the fore-and back-stepping and those with radial channel avulsion patterns are that in the former case the fan gradients are steeper with frequent breaks and the channel thalweg aggradation occurs along much of the depositional profiles, and that in the latter case, downdip of the avulsion nodes, the fan gradients are either flat or have possibly no breaks, and the channels are incised below the fan surface with no thalweg aggradation in the middle and lower fan regions. We believe that these differences, given other internal and external factors and events, resulted in the differences in the channel avulsion patterns in these areas.

Sea-level change during glacial cycles: constraints on ice sheets and their rates of growth and decay during the past 140,000 years with results from arctic Eurasia and the Mediterranean.

Kurt Lambeck,

*Research School of Earth Sciences,
The Australian National University,
Canberra 0200, Australia.
(email:kurt.lambeck@anu.edu.au)*

The evidence for sea-level change during the geological past is the observation of ages and elevations of palaeo-shorelines or of sediments whose depositional environments can be related to sea level. It is therefore a relative measurement and other than changes in ocean volume it includes contributions from land movements, from changes in the planetary gravity field, and from higher frequency climate and meteorological forcing of the ocean surface. Because of these other contributions sea-level change is spatially variable as well as variable in time. Departures from eustasy can exceed the eustatic change itself and in order to relate observations from one locality to that of another it is necessary to be able to evaluate these other contributions. Alternatively, observations of the spatial variability provide constraints on climate and tectonic processes. The challenge is to separate the various contributions to the sea-level signal.

On the time scale from $\sim 10^3 - 10^6$ years the dominant contribution to sea level change is from the cyclic growth and decay of ice sheets. This change is global and contains a broad spectrum of wavelengths that are determined by the dimensions and chronology of the ice sheets and by the earth's rheological response to changes in surface loading (ice and the concomitant changes in water load). The physics and mathematics of these changes are well understood and are largely predictable for known ice sheets and rheology. Alternatively, if a well-distributed database existed in time and space this could be inverted for load and rheological parameters. The other major contribution on the $\sim 10^6$ year time scale comes from tectonic movements and include slow subsidence or uplift associated with volcanic or sediment loading or with erosion. It also includes the very high frequency (seismic) changes associated with the crustal response to deeper mantle processes.

Neither the full ice history nor the rheology of the Earth can be assumed known from ab-initio assumptions and one of the challenges is to improve understanding of the ice and earth behaviour in the presence of incomplete observational data and tectonic contributions. Partial separation of the tectonic and glacial contributions can be achieved by examining sea level change over periods equal to or longer than the principal glacial cycle of $\sim 120,000$ years and by the assumption that the high frequency changes represent a white noise signal superimposed on long-term trends. The usual approach is to parameterize the ice history and earth response functions in some appropriate way and to invert the observational data base for critical parameters such as the effective viscosity of the mantle or ice thickness at the time of maximum glaciation. Through an iterative approach, using field data from areas far from the ice sheets to establish estimates of the ice volume change through time and to establish mantle rheology, and using field data from within former areas of glaciation to constrain the individual ice sheets, it becomes possible to effect a separation of parameters and to develop a model for the ice sheets over the last glacial cycle. This will be illustrated with results for the northern European glaciations over the past 140,000 years and from the Mediterranean. The resulting models are then used to reconstruct the geographic environment through time, including palaeo-topography and bathymetry.

A numerical investigation of phosphate remobilization during sea-level change – implications for offshore phosphate and TOC deposition

Legarth, J.J.F.*, and Bjerrum, C.J.

Geological Institute, Øster Voldgade 10, 1350, København K, Denmark.

** Corresponding author : jj.legarth@gmail.com*

Phosphorus (P) is generally considered as the ultimate limiting nutrient on geological timescales and the availability of P in the ocean constitutes a key control on primary production, ocean carbon cycling and hence atmospheric CO₂. Studies have until now primarily focused on quantifying the riverine and aeolian P-flux to the ocean. However, coastal erosion associated with base level changes presents a potentially significant and as yet un-quantified source of nutrients to the coastal zone. We will assess how the P flux to the ocean varies in direct response to changes in relative sea level. For this purpose we have developed a geometric sequence architectural process-response model into which a simple nutrient budget has been implemented. The model simulates the sequence architectural response of a wave-dominated passive margin to changes in the governing parameters e.g., sediment supply, subsidence and eustatic sea level change. The quantification of coastal and terrestrial erosion is linked to experimentally obtained geochemical data of phosphate speciation in the sedimentary environments. Estimates of the temporal change in the land to ocean P flux were quantified through an extensive sensitivity analysis and the chief controlling parameters identified.

A suite of different scenarios has been constructed to illustrate how these parameters affect the system on different time scales. The model indicates that coastal erosion on the basin scale has the potential to increase the coastal-to-ocean P-flux with up to 70% for short periods of ~5–15 kyr and up to 25–35 % for longer periods of ~35–50 kyr. The timing of maximum P release coincides with maximum rate of sea-level rise when the model is run with a single sinusoidal sea-level curve. When running the model with a composite sea level curve, the timing of maximum P-release is phase shifted (~440) back towards the onset of long term sea-level rise, on the composite sea-level curve. On short time scales the main factors governing erosion and thus P-release in response to a sea-level change is the shoreline/coastal plain geometry. On longer time scales subsidence exerts a progressively more dominant control.

Utility of Palaeomagnetic Secular Variation in Late Pleistocene and Holocene Cored Sediment from the Gulf of Salerno, Eastern Tyrrhenian margin

Liddicoat^a, J., Iorio^b, M., Budillon^b, F., Tiano^c, P., Incoronato^c, A., Coe^d, R., D'Argenio^b, B., and Marsella^b, E.

a Department of Environmental Science, Barnard College, Columbia University, NY, NY 10027

b Istituto Ambiente Marino Costiero – CNR, Calata Porta di Massa, Porto di Napoli, 80133 Naples, Italy (marina.iorio@iamc.cnr.it)

c Dipartimento di Scienze della Terra, Università degli Studi di Napoli “Federico II”, Largo S. Marcellino 10, 80138, Naples, Italy

d Earth Science Department, University of California, Santa Cruz, CA 95064

Cored marine sediment from the Gulf of Salerno (Fig. 1) in the western Mediterranean Sea records long-term change (secular variation) of Earth's magnetic field during the approximately last 40,000 years that has application in regional sedimentology, tephrochronology, and paleoclimate investigations. The record is from two six-metre gravity cores that were studied in their entirety. Ages are based on radiocarbon dates, and correlation of relative magnetic intensity to the North Atlantic Paleointensity Stack (NAPIS; Laj, et al., 2000) and South Atlantic Paleointensity Stack (SAPIS; Stoner, et al., 2002). One core (GS1201, 40° 28' 92" N, 14°42'24"E, 300 meter depth) is a continuous record to about 30,000 yrs B.P. (Buccheri, et al., 2002). The other core (GS1202, 40° 08' 34"N, 14° 43' 57"E, 243 meter depth) extends the record to about 40,000 yrs B.P. with a hiatus between about 14,000 and 24,000 yrs B.P. caused by slumping of shelf margin sediments (Trincardi et. al, 2003). Where the cores overlap in time, there is good agreement of palaeomagnetic directions (declination and inclination) and normalized field intensity (ARM/NRM). Core GS1201 confirms very well the palaeomagnetic record for the last 8,000 years in core C836 (40° 35' 59"N, 14° 40' 29"E; Iorio, et al., 2004), also from the Gulf of Salerno. There is evidence that sediment in Core GS1202 records the Mono Lake Excursion and Laschamp Excursion at approximately 34,000 yrs B.P. and 40,000 yrs B.P., respectively. Those brief departures from expected palaeomagnetic field behavior in the Brunhes Normal Chron are excellent chronologic markers in the Mediterranean region for the corollary investigations noted above.

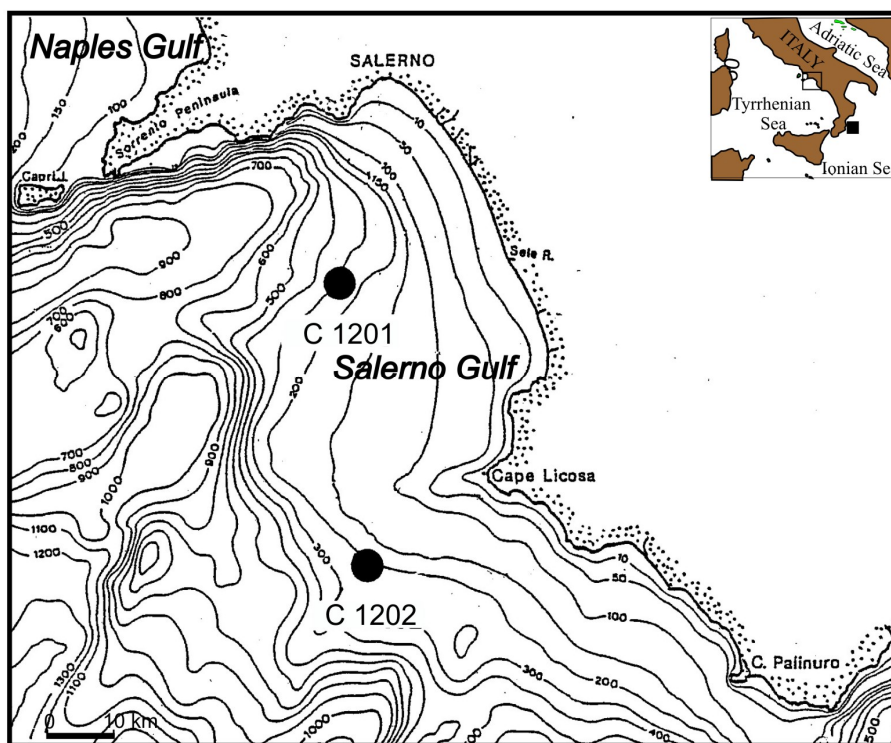


Figure 1. Location of the C1201 and C1202 cores in the Salerno Gulf. The two cores were collected in a water depth of ca. 300 and 243 m and are 40 km apart.

Buccheri, G., Capretto G., Di Donato, V., Esposito P., Ferruzza G., Pescatore T., Russo Ermolli E., Senatore M. R., Sprovieri M., Bertoldo M., Carella D., Madonia G. 2002: A high resolution record of the last

- deglaciation in the Southern Tyrrhenian Sea: environmental and climatic evolution. *Marine Geology*, 186, 447–470.
- Iorio M, L. Sagnotti, A. Angelino, F. Budillon, B. D'Argenio, J. Dinare's-Turell, P. Macri and E. Marsella 2004: High-resolution petrophysical and palaeomagnetic study of late-Holocene shelf sediments, Salerno Gulf, Tyrrhenian Sea. *The Holocene* 14,3, 426–435.
- Laj C., Kissel, C., Mazaud, A., Channell, J.E.T., Beer, J., 2000. North Atlantic paleointensity stack since 75 ka (NAPIS-75) and the duration of the Laschamp event. *Philosophical Transactions of the Royal Society, Series A* 358, 1009–1025.
- Stoner, J.S., Laj, C., Channell, J.E.T., and Kissel, C., 2002. South Atlantic (SAPIS) and North Atlantic (NAPIS) geomagnetic paleointensity stacks (0-80 ka): implications for inter-hemispheric correlation. *Quat. Sci. Rev.*, 21,1141-1151.
- Tricardi F., Cattaneo A., Correggiari A., Mongardi S., Breda A., Asioli A.: 2003. Submarine slides during relative sea level rise: two examples from the eastern Tyrrhenian margin. in: Locat J., Mienert J. (eds), *Submarine mass movements and their consequences: 1. International Symposium*, pp. 469-478.

Deep water depositional systems along the Norwegian margin; external controls on reservoir development

Lien, T.*

Norsk Hydro Research Centre, P.O. Box 7190, N-5020 Bergen, Norway.

** Corresponding author : trond.lien@hydro.com*

Several sandy deep-water depositional systems of Cretaceous and Palaeogene age occur along the Norwegian margin. These systems vary in their basin position, depositional geometries, scale, sand richness and area distribution related to the external and internal controls that were active during deposition.

Lower Cretaceous deep-water systems in the North Sea and in the Norwegian Sea were deposited during an early post-rift stage. They are characterised as slope systems where depositional geometries were strongly controlled by the underlying rift topography. The deposits are commonly sand to mud-rich, relatively thin and have a variety of depositional elements and facies. Middle Cretaceous systems in the North Sea and in the Norwegian Sea were deposited during a late post-rift stage. They are characterised as slope to basin floor systems with depositional geometries less controlled by the underlying rift topography. The depositional systems are commonly sand-rich, relatively thin, but of basin wide extent.

From the mid Late Cretaceous and onwards, the North Sea and the Norwegian Sea experienced a significantly different tectonic development, resulting in a markedly different deep-water deposition in the two areas. The North Sea remained in a post-rift stage with no significant latest Cretaceous deep-water sand deposition, while the Norwegian Sea passed into a new rift stage with deposition of thick sandy basin floor systems controlled by the newly created rift topography. Despite different tectonic regimes, the Paleocene systems in the North Sea and Norwegian Sea are relatively similar. The deposits are sand-rich basin floor systems of significant thickness related to basin margin uplift and structures along the basin margin largely controlled the location and depositional geometries. The Eocene transition into oceanic rifting in the Norwegian Sea, and basin margin subsidence in the North Sea, had a pronounced effect on the deepwater systems. The lack of major sediment source areas resulted in mud prone deposition and a general lack of significant reservoir development during the Eocene.

To understand the observed differences in the deep-water depositional systems, a hierarchy of external factors is evaluated where a combination of different factors are controlling the various depositional changes. On the large scale, changes in the main tectonic regime and associated basin changes seem to have the dominant control on the stratigraphic position, basin location and depositional geometry of the deep-water reservoirs. Different external factors are active at different tectonic stages, controlling the basin geometry, sediment source, transport routes and geometry of the depositional sink. By combining the tectonic development and the hierarchy of associated external factors linked to the tectonic stage, better understanding of the external controls on reservoir development can be achieved.

The Depositional Architecture of a Tithonian Lowstand Systems Tract in the Exmouth Sub-Basin, Western Australia

Lockhart, D.¹, Stark, C.J.², Rosser, J.³, Burns, F.E.² and Gamarra, S.³.

1. BHP Billiton Pty Ltd

2. Firmground Pty Ltd

3. Consultant

This study represents the results of detailed mapping of the Tithonian succession in the Exmouth Sub-basin, offshore Western Australia, using 3D seismic data, and integration with core and borehole image data from all well penetrations within the basin. The Macedon Member of the Lower Barrow Group in the Exmouth Sub-basin, was deposited on a ramp setting during regional rifting and uplift associated with the separation of India from Australia during the Tithonian. The Macedon-Pyrenees 3rd order sequence was deposited within a timeframe of 2.5my based on palynological dating.

Regional mapping of 3D seismic data, in association with a full scale review of core and high-resolution resistivity image logs from all well penetrations of the Macedon Member, enable the definition of fifteen 4th order sub-sequences within the 3rd order lowstand. Early and late lowstand deposits can also be delineated. Biostratigraphic data reveals a younging direction towards the east, with initial lowstand deposition focused in the west, progressively migrating towards the east during the late lowstand systems tract.

During the earliest lowstand, two active canyon systems (the Laverda and Eskdale canyons), located in the western part of the study area, were directly connected to major fluvial point sources most likely emanating from an alpine region to the south (similar to the Bounty Trough, offshore east coast of the South Island, New Zealand). It is hypothesized that these rivers were prone to driving hyperpycnal events into the canyons. The two well-defined seismic-delineated canyons extend from the uplifted eroded sub-crop edge in the south of the study area, and terminate in large-scale basin floor fan systems in the north. Although canyon gradients are relatively low (approximately 0.750), both canyons are linear and aligned in a SSW–NNE orientation.

The preliminary canyon fills penetrated by wells in the south consist principally of thick to very thickly bedded, clast-supported, imbricated conglomerates interbedded with granular, massive, horizontal and thickly bedded cross-stratified sandstones; deposited from traction carpets and high-density turbidites respectively. Minor matrix-supported conglomerates (debris flows) and laminated sandstones (low-density turbidites) also occur. Texturally, the sandstones are medium to coarse grained, ranging from poor to moderately well sorted. Well penetrations through the preliminary canyon fill in the north reveal a dominance of massive, medium to thick bedded, high-density turbidite sandstones, which are texturally more mature than those to the south of the study area. Reverse and normal graded beds are also common. No bioturbation is observed in core from either of the preliminary canyon fills. Towards the end of the early lowstand the Eskdale canyon system became inactive and all deposition is focussed on the Laverda canyon to the east. Subsequent filling of the canyon led to widespread unconfined splay deposits.

Late lowstand deposition was initiated as accommodation space increased in response to basin subsidence. Active fluvial systems ceased to feed directly into the established canyons. Sediment supply however was still relatively abundant and the late lowstand deposits are characterised by a series of backstepping 4th order sequences.

The 4th order sequences are characterised by a dominance of unconfined mass flow deposits forming a series of distal inner to outer shelf fans. Medium to thick bedded massive sandstones derived from high-density turbidites are dominant. These are capped by thin bedded, laminated sandstones reflecting either late stage low-density turbidite flows or discrete low density flow units. Core and FMI analysis indicate the presence of stratified hyperpycnal flow-derived sandstones within these sequences. Interbedded sand-rich siltstones are moderately to highly bioturbated with a dominance of *Phycosiphon* and *Chondrites* ichnofabrics; suggesting deposition of the hyperpycnal flows on the distal inner to outer shelf environment. Seismic-derived ramp gradients are consistent with these interpretations, while foraminiferal data suggest palaeobathymetries ranging from 50 – 100m.

As subsidence rates increased and relative sediment supply began to diminish towards the end of the late lowstand, the dominance of unconfined fan systems gave way to the development of channel-levees complexes, with a switch to an overall mud-dominated system. Sand deposition ceased to the west and

became focused to the east of the study area. High-density turbidites are confined to discrete channels, with levees consisting of moderately inclined ($\sim 5\text{-}15^\circ$) heterolithic beds. The end of the late lowstand and the onset of the 3rd order transgressive systems tract (Muiron Member) is characterised by glauconitic, very fine-grained sandstones to argillaceous siltstones reflecting the onset of distal outer shelf to slope sedimentation.

Tectono-stratigraphic History of Greater Mississippi Canyon, U. S. Gulf of Mexico

Long, M.S.^{1*}, Helsing, C.E.¹, Berman D.C.¹, Deemer, D.L.², and Albert, R.³

1. ExxonMobil Exploration Company, 222 Benmar Drive, Houston, TX 77060.

2. ExxonMobil Production Company, 800 Bell Street, Houston, TX 77252.

3. ExxonMobil Upstream Research Company, P.O. Box 2189, Houston, TX 77002

* Corresponding author : m.shane.long@exxonmobil.com

This paper describes the tectono-stratigraphic history of the Greater Mississippi Canyon area based on a multi-year study utilizing extensive seismic and well databases. Key 3rd-order sequence boundaries from the acoustic basement through the water bottom were interpreted over approximately 6,300 mi², providing the basis for generating regional paleogeographic maps. These data were used to better understand the distribution of reservoir/seal facies and thereby evaluate remaining hydrocarbon potential within the area.

One aspect that sets this study apart from previous reports is the documentation of a complete tectono-stratigraphic cycle that started with autochthonous, sheet-like evaporites (Middle Jurassic) that were loaded initially by future four-way turtles (Middle Jurassic – Middle Miocene) then three-way turtles (Lower Miocene – Pliocene) into increasingly mature salt stocks, tongues, then canopies (Upper Miocene – Pliocene). This allowed the cycle to be repeated as a second generation of future four-way turtles began forming directly over these salt canopies (Pleistocene).

This study also documents that where Mesozoic sediments are thick, Cenozoic sediments tend to be relatively thin and sand poor, and conversely, where Mesozoic sediments are thin, Miocene sediments tend to be relatively thick. This inverse relationship reflects the dependent nature of sediment accommodation on the presence or absence of underlying salt (i.e. where salt is evacuated at an early stage, limited accommodation space remains) and allows maps from any 3rd-order interval to be used as predictive tools for sediment trends within deeper or younger sections. The observations and methods developed during this study can be applied to similar settings where data are more limited.

Mesozoic History

The Gulf of Mexico began to open during the Late Triassic – Early Jurassic. As the Yucatán pulled away from North America, it left in its wake a ‘basin and range’ province defined by NW-SE trending strike-slip faults. Thousands of feet of Middle Jurassic Louann salt accumulated within grabens during prevailing arid conditions. This ‘basin and range’ fabric, coupled with the presence of salt, played a critical role in establishing the general location and orientation of subsequent sediment pathways and salt structures through the present day. Middle Jurassic – Upper Cretaceous fairways, trending NE-SW, transported sediment from as far as the ancestral Appalachians into the aforementioned grabens, developing large, fan-shaped depocenters. These depocenters loaded Louann salt into incipient pillows and stocks, then eventually inverted to form four-way turtles, representing structural highs through much of the Cenozoic. Collectively, they comprise a depositional system within Mississippi Canyon that is thickest and most amalgamated in the NE and thinnest and least amalgamated in the SE.

Although there are no Mesozoic penetrations within the study area, regional data record lithologies that vary from Middle Jurassic aeolian sands (Norphlet) to Upper Cretaceous chinks, marls, and shales. This succession not only records the deepening of the Gulf of Mexico, but also the climatic shift from arid conditions during the Middle Jurassic to relatively high global temperatures through much of the Cretaceous. Since the shelf edge was not well developed until the Lower Cretaceous, early clastic deposition (e.g. Norphlet, Cotton Valley, Hosston, etc.) likely extended into the study area over a ramp-like margin, representing an untested play.

Cenozoic History

Miocene – The Mesozoic interval is capped by a condensed section of shales and marls. These strata represent a 40 million year hiatus, during which a major shift in continental drainage patterns and provenance occurred. Active sedimentation returned to the area during the Early Miocene along fairways oriented W-E. These depositional systems transported sediment from the ancestral Rockies into lower slope depocenters in central and southern Mississippi Canyon. The rate of sedimentation increased dramatically during the Middle Miocene as fairways swept across the study area from W-E along NW-SE trending pathways, likely reflecting an east-ward shift of the ancestral Mississippi delta. For the first time since the

Mesozoic, major depocenters developed in central and eastern Mississippi Canyon. Sediment from both Lower and Middle Miocene fairways continued to deflate salt away from the center of active mini-basins towards the flanks, feeding increasingly mature, dominantly NW-SE-oriented salt stocks. As a consequence, accommodation in the center of these mini-basins became more limited, causing sediments to stack compensationally, resulting in an increasing number of future three-way turtles near ascending salt. Though the Upper Miocene experienced little change in fairway orientation, the rate of sedimentation decreased significantly, allowing salt to form coalesced tongues and canopies.

Plio-Pleistocene – Regional work indicates that by the Pliocene, the focus of sedimentation had shifted back to the west, causing the rate of deposition to further diminish within the study area. Only a few significant depocenters developed up-dip of ascending salt, allowing canopies to reach their maximum aerial extent. Otherwise, sand development was confined within relatively narrow, NW-SE-oriented channel complexes, reflecting upper-slope conditions over the area. However, during the Pleistocene, depositional rates were sufficient to overwhelm and eventually cover salt canopies. Sedimentation was largely restricted to a series of fan-shaped depocenters (future four-way turtles) directly overlying salt canopies in the SW portion of the study area, signifying the beginning of a second tectono-stratigraphic cycle.

On Forced Instabilities of Density – Turbidity Marine Currents

Maponi, P.¹, and Salusti, E.²

1. Dipartimento di Matematica e Informatica, Università di Camerino, Via Madonna delle Carceri, 962032 Camerino, Italy.

2. Dipartimento di Fisica – INFN, Università di Roma "La Sapienza", P.le Aldo Moro 2, 00185 Roma, Italy.

We here investigate the hydrodynamic stability properties of bottom currents when the water density is increased by entrainment of bottom sediments. To schematize this complex interaction, the water density variation, ultimately due to bottom erosion or deposition, is viewed here as a mere function of the current shear stress on the sea bottom.

We can sketch out a possible scenario for the general case. For a steady density current flowing geostrophically along isobath lines at the border of an oceanic shelf, a sudden external forcing can raise bottom sediments and so the bottom current increases its density. Such a complex interaction between the bottom particulate and the bottom current can produce an intense down-flow, crossing the oceanic shelf break, namely that a density/turbidity current develops.

This has been examined here with a further heuristic position, that the sediment concentration has been assumed here to be a function of the bottom stress. A complex equation is thus obtained, in which both time and space variability are considered in a realistic two-layer model of density currents down-flowing over an erodible bottom. On mathematical grounds, this consists in a linear heat-like equation based on hydrodynamic stability properties, with a peculiar type of non-linear “time-delayed” behavior. Our model appears suitable for inferring the start-point of violent perturbations, somehow reminiscent of the “ignition” in impulsive turbidity currents. Comparison with the experimental data suggests that the most interesting physical quantity is probably the “ignition” time t^* , i.e. the time necessary to an external forcing to generate non-linear explosive effects. In the early stage of this development t^* governs the response time to the forcing of the current in order to ensure an increased mixing with the bottom sediments. In particular we show here that all this happens in the presence of external perturbations over an erodible bottom of space-dimensions larger than $10 t^*$ times the dense water velocity.

In fact, after large perturbations start destabilizing the current, a scenario of violent mixing occurs, namely large masses of turbulent marine water with hydrologic characteristics intermediate between the two original waters may be generated and are then observed to reach the deepest layers, or to float at mid depth. In the end, a numerical study of the model equation supports the evidence of these effects.

Climate control on the architecture of the Zaire turbidite system?

Marsset, T.^{1*}, Droz, L.², Dennielou, B.¹, Savoye, B.¹, and Bez, M.³.

1. Ifremer, DRO/GM, BP 70, 29280 Plouzané.

2. UMR 6538, IUEM, Place Nicolas Copernic, 29280 Plouzané, France.

3. Total, 64018 PAU Cedex, France.

* Corresponding author : tmarsset@ifremer.fr

The ZaiAngo project (Ifremer/Total, 1998-2000) allowed to acquire a voluminous geophysical and geological data set including EM12 swath mapping, High and Very High seismic profiles and corings. These data highlighted the detailed architecture of the Quaternary Zaire (Congo) turbidite system (Savoye et al., 2000; Babonneau et al., 2002; Droz et al., 2003).

The Zaire turbidite system shows an internal structure well organized in relation with the current canyon (Babonneau et al., 2002). It consists of at least 80 channel/levees systems that are chronologically referenced and are grouped into three successive fans (Northern, Southern and Axial fans from the oldest to the youngest) (Fig. 1). From stratigraphic correlation with ODP leg 175 the age of the base of the Northern, Southern, Axial fans is 780, 540 and 210 Ka BP respectively. (Droz et al., 2003). This organization is linked the lateral shifting of depocenters (channel/levees systems and terminal lobes) in response to avulsion processes. In addition, the fan is characterised by longitudinal shifting of depocenters which are evidenced by the relative chronological evolution of several parameters with respect to the sedimentary source point (length of channels, location of bifurcation points and number of bifurcation points per channel). During the building history of the turbidite system, the sedimentation was characterised by successive progradation/retrogradation cycles which, from correlations with work of Gingele et al. (1998) could be linked to the climate variations via changes of the sedimentary input (quantity and/or nature and/or frequency) (Fig. 2).

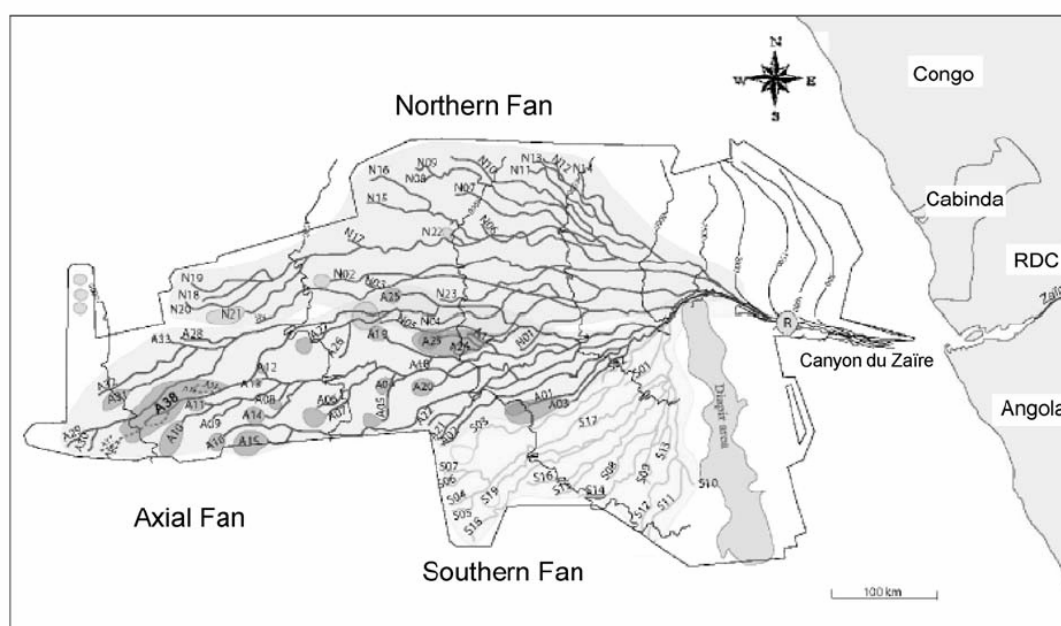


Figure 1: Map of the Quaternary Zaire turbidite system showing the 80 channel/levees systems chronologically referenced and grouped into three successive fans (Northern, Southern and Axial fans from the oldest to the youngest)

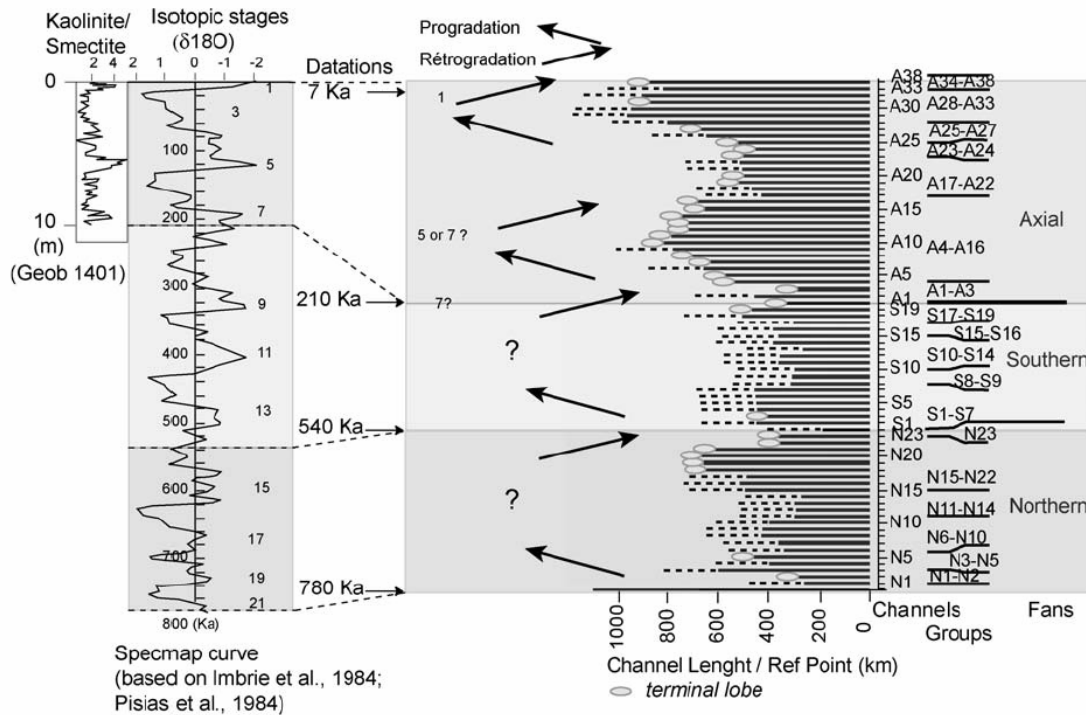


Figure 2: Progradation/ retrogradation cycles in the Zaire turbidite system and proposed correlation with SPECMAP and clay ratio of core Geob 1401 (Gingele et al., 1998). The study parameter here is the length of channel/levees system with respect to a reference point (R) located in the canyon (cf Fig. 1).

F

Babonneau, N., B. Savoye, M. Cremer, and B. Klein, 2002, Morphology and architecture of the present canyon and channel system of the Zaire deep-sea fan: *Marine and Petroleum Geology*, v. 19, p. 445-467.

Droz L., Marsset T., Ondréas H., Lopez M., Savoye B., Spy-Anderson F.L., 2003a. Architecture of an active mud-rich turbidite system: the Zaire fan (Congo-Angola margin southeast Atlantic): results from ZaiAngo 1 and 2 cruises. *AAPG*, 87, 7, 1145-1169.

Gingele F.X., Müller P.M., Schneider R.R., 1998. Orbital forcing of freshwater input in the Zaire Fan area – clay mineral evidence from the last 200 Kyr. *Palaeogeography, palaeoclimatology, palaeoecology* 138 p 17-26.

Savoye, B. et al., 2000, Structure et évolution récente de l'éventail turbiditique du Zaire: Premiers résultats scientifiques des missions d'exploration ZaiAngo 1 t 2 (Marge Congo-Angola): *Comptes Rendus de l'Académie des Sciences, Paris*, t. 331, p. 211-220.

Wefer, G., W. H. Berger, and C. Richter, eds., 2002, *Proceedings of the Ocean Drilling Program, Scientific Results*, 175, <http://wwwodp.tamu.edu/publications/175_SR/175sr.htm> Accessed July 9, 2002.

External controls on deep-water depositional systems in British Carboniferous basins: responses to Gondwanan glaciations and evolving basin bathymetry

Martinsen, Ole J.

Hydro Oil and Energy Research Centre, 5020 Bergen, Norway.

The Carboniferous basins of the British Isles show a tri-partite stratigraphic subdivision of deep-water depositional systems, largely controlled by eustatic sea-level changes as a response to Gondwanan glaciations, and an initially increasing then decreasing bathymetry as a response to crustal extension and decay.

The tri-partite stratigraphic division is expressed by (i) deep-water carbonates developed above shallow-water carbonates as deepening took place, (ii) time-transgressive black shale formations, locally with source potential, deposited during or shortly after extension climax, and (iii) shallowing-upward basin floor and slope deposits deposited as siliciclastic deposition gradually was introduced and eventually filled the basins.

The carbonate and particularly the clastic deep-water fill of the basins is punctuated by numerous fossil bands, also termed marine bands, each of which carry their own diagnostic species of goniatites. These bands can be correlated between basins, and some of them can be traced from western Ireland through Poland to the Urals. They record the boundaries between 10000-100000 year long cycles of deposition. The widespread nature of the bands, their diagnostic fossil species and that they separate mostly barren thick successions of widely variable sedimentary character suggest that they were controlled by eustatic changes of sea level, induced by glaciations in Gondwana. The bands form a high-resolution stratigraphy, only second to the Neogene record, and provide an excellent basis for correlation.

The clastic fill of the deep-water basins varies between mudstones, slumps and slides, and turbidite sand bodies in the form of either sheets or channels. In some instances, a systematic cyclicity akin to that described in Neogene and Recent submarine fan systems can be established. There, marine bands/condensed horizons are overlain by sand-rich turbidites, which are further overlain by mud-rich turbidites. This type of cyclicity is however in several instances apparently overprinted by high sedimentation rates and autocyclic responses. This cyclicity is apparently a result of eustatic influence on sediment supply. A similar type of cyclicity also occurs on a larger, basinal scale, but in that case probably reflects the overall fill of deep-basin bathymetry as a response to decaying subsidence and an increased rate of sediment supply.

The deep-water fill of the British Carboniferous basins is excellent outcrop examples of numerous critical aspects of deep-water sedimentation, which are highly applicable to subsurface settings globally.

Heinrich event, Sea-Level and Avulsion Events on the Amazon Fan

Maslin, M.^{1*}, Knutz, P.C.², and Ramsay, T³.

1. ECRC, Department of Geography, 26 Bedford Way, University College London, London, WC1H 0AP, UK.

2. Geological Institute, Østre Voldgade 10, DK-1350, Copenhagen, Denmark

3. Department of Earth Sciences, Marine & Environmental Geoscience Research Group Cardiff University, P.O. Box 914, CF1 3YE Cardiff, Wales

* Corresponding author : mmaslin@geog.ucl.ac.uk

The late Pleistocene Amazon deep-sea fan provides a 'modern' analogue to ancient fan systems containing coarse grained hydrocarbon reservoirs. This study shows that large sand lobes (~1 km³) formed during abrupt shifts in channel pathways are triggered by relatively small, millennial scale changes in marine transgression and regression (5-10 m) associated with Heinrich events. Relative sea-level also controls the architecture of the channel-levee distributive systems within the Amazon Fan. Transitions between multi-channel and single channel configurations are related to variations in the volume of sediment supply resulting in aggradation or erosion of channel floor and levee growth in the canyon-channel transition area. These results support the fundamental assumption of sequence stratigraphy that relative sea level controls sediment deposit.

Cyclostratigraphy: Analysis of Precession-Scale Climate, Sediment & Sea Level Cycles to Understand Stratigraphic Variability

Perlmutter, M.¹, Moore, T.², and Urwongse, T.³

1. Chevron, Exploration Technology Company, Houston, Texas, U.S.A.

2. Argonne National Laboratory, Argonne, Illinois, U.S.A.

3. Chevron, Information Technology Company, Houston, Texas, U.S.A

At precession-scale (~20 kyr), Northern and Southern Hemisphere insolation cycles are 10,000 years out of phase. Consequently, similar climatic successions in opposite hemisphere, and associated sediment yield cycles can be 10,000 years out of phase, as well. Prior to the Plio-Pleistocene, the common glacial condition was a unipolar icecap. Under this condition, precession-scale eustasy will tend to track the insolation cycle of the glaciated hemisphere. The result is that similar climatic successions in opposite hemispheres will have sediment yield cycles with distinctly different phase relationships to glacioeustasy. Such differences would not exist in an ice-free world.

To accurately forecast how this phase relationship influences stratigraphy, the impact of climate and elevation on sediment yield needed to be understood. We evaluated ~ 100 present day river drainage networks to develop a numerical model to forecast yield for specific climates and elevations. The model that was developed has an accuracy of 86% (data/model correlation). To evaluate the impact of climate change on stratigraphy during specific geologic intervals, we analyze the pattern of high frequency climate variability by building climate maps directly from paleoclimate indicators or by running paleoclimate models, such as FOAM (Fast Ocean Atmosphere Model). The paleoclimatic range for that time period combined with the average elevation for a drainage basin permits an estimate of a sediment yield cycle for a specific river system. Sediment yield cycles are then put in context with global sea level change. When evaluated in this manner, it is clear that the timing of sediment delivery by fluvial systems to continental shelves is regionally dependent and not necessarily correlated with a specific phase of glacioeustasy.

By taking into account the interaction of sediment yield and sea level, exploration areas that are prone to the development of sand-rich submarine fans can be evaluated and high graded. Understanding the inherent stratigraphic variability of a system will help improve depositional models and interpretation, and reduce the uncertainty associated with exploration analyses. In addition, recognition of hemispheric asymmetry in the stratigraphic architecture of a particular time interval demonstrates the occurrence of polar glaciation.

Morphometry of Mass-Transport Complexes in Offshore Trinidad

Moscardelli, L.¹, and Wood, L.².

1. Jackson School of Geosciences University of Texas at Austin

2. Bureau of Economic Geology University of Texas at Austin

Successive episodes of mass-transport complex (MTC) development in the deep marine environments off the coast of Trinidad and Venezuela affected areas of thousands of square kilometers during the Plio-Pleistocene. Sediment volumes in the range of hundreds of cubic kilometers have been displaced by these catastrophic events, which may have been associated with a variety of causes, including high sedimentation rates, earthquakes, high-frequency sea-level fluctuations and gas-hydrate dissociation (Fig. 1). A database that includes morphometric parameters from a variety of MTC's located in different geologic settings around the world has been built in order to analyze and compare geometry of the deposits in offshore Trinidad with similar events in different continental margins (Fig. 2). The objective is to establish whether systematic morphometric parameters characterize MTC deposits originating from these different drivers, parameters that may increase understanding of processes associated with MTC formation in our study area. A series of statistical plots involving external morphometric parameters, such as run-out distance and area of deposits, clearly show the existence of geometric relationships that are independent of lobe size, causal mechanism, and geographic location of MTC's (Fig. 2). Flow-efficiency values were calculated on the basis of area and volume of the deposits. These values were plotted against run-out distances, but despite the existence of some trends, a clear relationship between these two parameters was not observed. Morphometric data from several turbidite deposits were also included in this study. The objective was to investigate whether relationships between morphometric parameters such as run-out, area, and volume had the capacity to demonstrate differences between rheology and flow efficiency of turbidites versus MTC's. Preliminary results suggest that geometric and crude statistical relationships between run-out and area of the deposits are the same for MTC's and turbidites, but flow-efficiency relationships involving the volume of the deposits seem to behave differently. These observations define a fundamental difference between issues associated with scale of deposits and efficiency of processes responsible for their transport and deposition. Scale of the deposits will depend on sediment budget in the source area and controls on accommodation space in the basin, whereas flow efficiency is directly associated with the Newtonian character of flow in real turbidites versus laminar flow in MTC's.

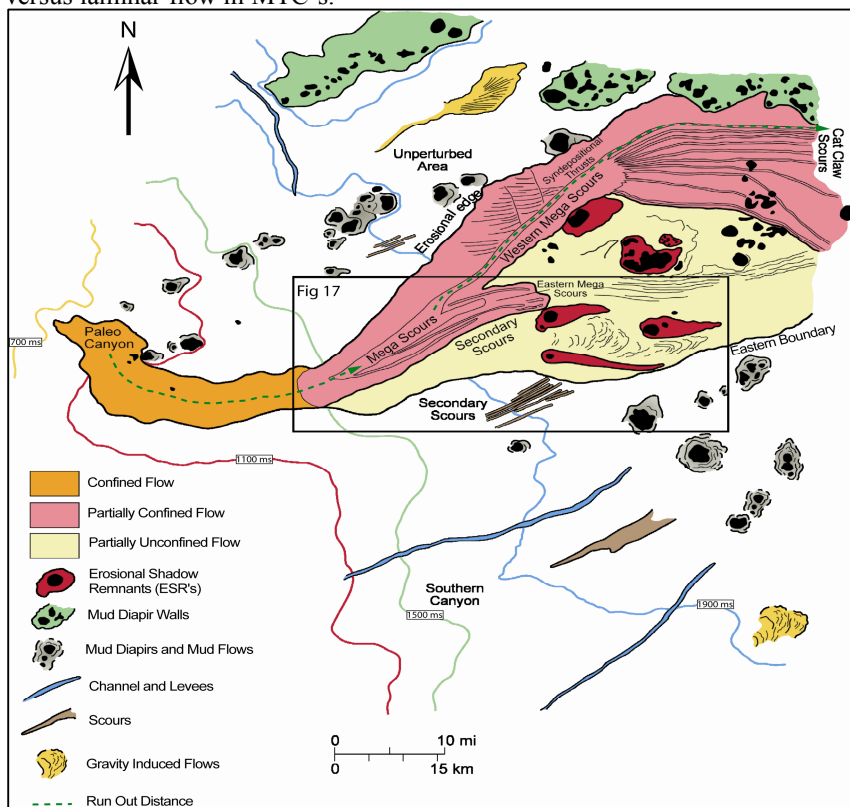


Figure 1. Geomorphological interpretation of basal erosional surface of MTC_1 offshore Trinidad. Several stratigraphic features that show significant basal incision located in core area (scours). Certain degree of flow confinement was necessary in this area for observed incisions to be generated. Peripheral part of mass-

transport complex shown in yellow. Flow in this area interpreted as partly unconfined because of absence of deep grooves or incisions. However, presence of erosional shadow remnants is evidence of flows' large-scale lateral erosive energy.

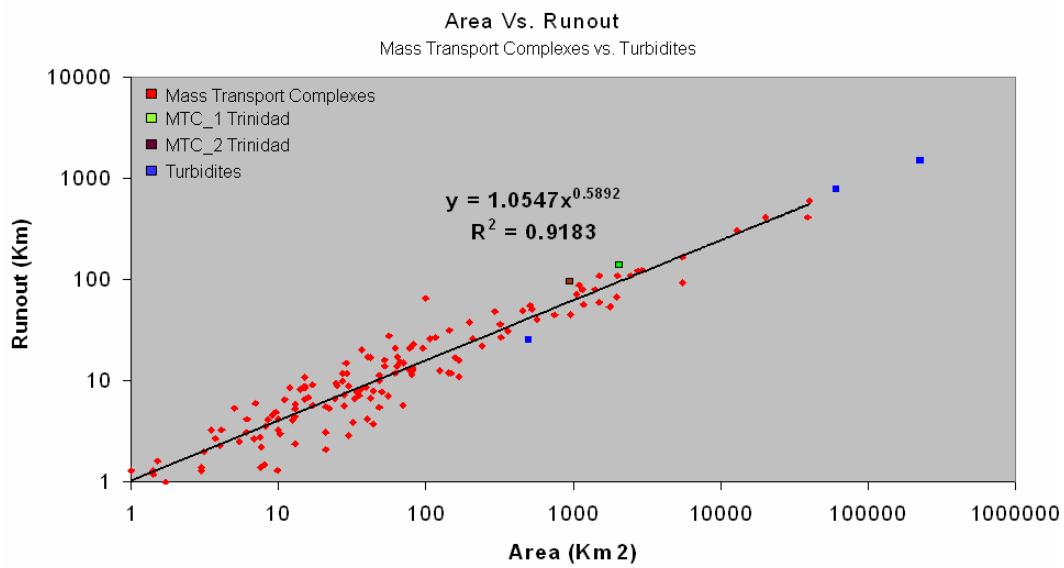


Figure 2. Log-log plot illustrating relationship between run-out distance and area within a series of MTC's around the world (Storegga, Oregon, California, New Jersey, GOM, Canary and El Hierro Islands, Ebro Spain, Fjord Canada and Trinidad)

Turbidity Current Generation from Submarine Debris-Flows: Flux Dynamics and Depositional Processes

Munachen, S.E.

Geohazard Research Centre, 38 Lincoln Way, Harlington, Bedfordshire, LU5 6NQ, United Kingdom.

Submarine landslides and debris-flows are some of the most prominent and effective mechanisms of sediment transport from continental shelves to deep ocean basins. They are particularly common along glaciated margins that have experienced high sediment flux to the shelf break during and after glacial maxima, and are important not only for the potential environmental hazard they pose, but also because their deposits can host significant volumes of hydrocarbons. Recent seismic surveys of the seafloor near continental margins have revealed complex morphological features associated with mass flow deposits. In proximal zones, facies tracts tend to be characterised by poorly sorted, massive sands, interpreted as deposits of dense, inertial flows, which are replaced, in distal regions, by finer-grained laminae that have aggraded progressively beneath relatively dilute gravity currents. This stratigraphy is consistent with deposition from bipartite flows in which sediment, eroded from the leading edge of surge fronts as ambient fluid is deflected from their paths, is entrained into the overlying water column generating subsidiary turbidity currents. Although there appears to be a general consensus that many turbidites originate from the gradual transformation of sand-rich debris-flows into turbidity currents, very little research has been specifically directed at quantifying these processes in order to understand the basin-ward variation of deposit composition and architecture.

This paper examines the influence of clay-sand mass fraction on the dynamics of submarine debris-flows, with particular emphasis on the formation of subsidiary turbidity currents from impulsive failures of continental slope deposits. Results from a series of highly instrumented flume tests are used to constrain the mechanics governing post-failure flow transformation in order to develop a quantitative framework in which to interpret process-oriented facies tracts. Flow processes are explored as functions of the original sediment composition and transport of the dense parent phase. Through the simultaneous measurement of internal velocity and concentration gradients, both the volume fraction of sediment reworked into an overriding turbidity current and the degree to which the original dense flow is diluted through ingestion of ambient seawater are determined. This information is necessary input data for many theoretical models of seascape evolution and is, therefore, prerequisite for predicting the complex interactions and feedback mechanisms involved in turbidity current generation.

Flux mechanics were strongly tied to the coherence of the debris-flow, that is, the ability of the slurry to resist erosion and fracture during transit. Weakly coherent flows, characterised by high water contents and low clay fractions, exhibited intensively fluidised surge fronts in which the entire head fragmented into a turbulent bore, producing significant, low-concentration, turbidity currents. A dense substratum formed directly behind the heads as sand grains dropped out of suspension during the flow to create a depositional layer. The highest mobility was found for slurries with low yield strength combined with sufficient competence to allow moderate settlement of sand particles. Conversely, strongly coherent flows were enhanced by hydroplaning, a process in which the dynamic overpressure at the leading edge of the debris-flow front balances the weight of the superincumbent sediment. Ambient water mixed with eroded material from the underside of the head formed a low viscosity, lubricating slurry which decoupled the sediments from the bed, inhibiting the transmission of shear stresses and increasing surge front velocity. These high velocities promoted sediment suspension and turbidity current formation, and can cause autocephalation, a process whereby the heads of debris-flows accelerate away from their bodies to the point of complete detachment. Comparison of the observed velocity profiles with rheological measurements of the pre-flow slurries demonstrates that strain-induced wetting can substantially soften the basal shear layer, without effecting the plasticity of overlying plug.

Three modes of sediment transfer from a parent debris-flow were observed; grain-by-grain erosion of sediment from the leading edge, detachment of thin sheets of material due to localised shearing, and turbulent mixing of ambient fluid into the head of a parent flow causing dilution and localised transformation. All three styles of transference from the original flux to a turbidity current were focused at the heads of the parent debris-flows because this is where the large dynamic stresses developed as a result of interfacial traction with the standing water are localised. The laboratory measurements confirm that the influence of these stresses on turbidity current development depends on their magnitude relative to an effective yield strength for the parent mixture of sediment and water. The experimental data were used to constrain the critical values of the ratio of yield strength to dynamic stress at which changes in character of

the transfer processes were observed.

Detailed measurements of the spatio-temporal evolution of the vertical flow structure within turbidity currents were performed using a novel ultrasonic Doppler velocity profiling technique, permitting the holistic reconstruction of turbulent flow fields. Direct sampling using racks of vertically stacked siphons to measure both particle concentration and grain size distributions of suspended sediment revealed aspects of mixing and the progressive segregation of particles due to sedimentation within the turbidity currents. Acoustic backscatter imaging was employed to resolve the internal boundary separating the turbulent mixing zone near the front of a flow from unmodified parent material, and clearly showed that the mixing length increased, moving backward from head, as coherency of the parent flow drops. Mixing of the turbidity current with the ambient fluid occurred primarily by detrainment of suspended matter behind the head in a series of transverse vortices, creating density stratification characterised by a dense sublayer with a more dilute homogenous region above.

Late Quaternary terrestrial climatic changes recorded in deep-sea turbidites along the Toyama Deep-Sea Channel, central Japan Sea

Nakajima, T.¹, and Itaki, T.².

1. National Institute of Advanced Industrial Science and Technology (AIST), Geological Survey of Japan, C-7, 1-1-1 Higashi, Tsukuba 305-8567, Japan.

2. Department of Earth and Planetary Science, The University of Tokyo, Science Building #1, 7-3-1 Hongo, Tokyo 113-0033, Japan.

Terrestrial climate is one of the most important external controls on deep-water depositional systems especially in active margins. There sea-level control is minimized due to poorly developed shelves and sediment flux is high due to high uplift rates in the sediment source areas. This study provides an excellent case study of a deep-sea channel system from central Japan Sea where deposition has been chiefly controlled by climatic forcing during late Quaternary.

Turbidites distributed along the Toyama Deep-Sea Channel (TDSC) in central Japan Sea consist of rhythmite beds and classical turbidites which are interpreted to be hyperpycnites deposited from hyperpycnal river effluents during floods and surge-type turbidites deposited from sediment failures on deltaic slopes, respectively. Hyperpycnites constitute approximately half of turbidites and may be correlated to major historic floods in the drainage area. Hyperpycnites often show inversely graded basal motif and generally have finer grain size, higher organic carbon content and higher C/N ratio than surge-type turbidites. Frequency and thickness of both types of turbidites along the channel would reflect the frequency and magnitude of river floods and resultant sediment accumulation on deltaic slopes. Hence the temporal variability of turbidite facies, composition, frequency, and thickness would record climatic changes in the central Japan as well as sea-level changes and tectonics.

Stratigraphic variations of facies types, coarse fraction content, frequency, and thickness of turbidites in three cores collected along the down channel transect of the TDSC show consistent temporal trends with the changes in terrestrial climatic records. These temporal changes in turbidite deposition are interpreted to reflect climatic forcing in the sediment source areas for the last 70 ka. (1) During the stadials and interstadials (70–22 ka) in the last glacial when a warm current periodically flowed into the Japan Sea, the Japanese main land climate was cold and wet, resulting in occasional glacial advances in adjacent mountains. Turbidite flux and coarse fraction increased in the TDSC system during the major glacial advances because of the increased production of coarse debris and high transport potential due to high precipitation. During this period, turbidite flux and coarse fraction content also fluctuated while surge-type turbidites increased. They were probably caused by fluctuating precipitation and by fluctuation and rapid fall of sea-level in the oxygen isotope stage 3 (2) During the last glacial maximum (22–18 ka) when the Japan Sea was capped by cold, low-salinity surface water, the terrestrial climate was cold and dry due to low evaporation from the Japan Sea. As a result of low precipitation, little coarse debris was transported into deep basins. During this period, turbidite flux, coarse fraction, and relative abundance of surge-type turbidites along the TDSC were reduced. Responsible turbidity currents may have been chiefly small or medium size hyperpycnal flows with low flow competence. (3) During the last deglaciation (18–8 ka), precipitation and storms in central Japan increased due to intensified summer monsoon. This resulted in destabilization of mountain slopes and increased transport of detritus to the lowlands. Consequent turbidity currents may have been large hyperpycnal and surge-type flows. As a result, turbidite flux and coarse fraction content along the TDSC system increased. (4) After the warm current flowed into the Japan Sea at ca. 10 ka, the land climate became warm, wet, and stable. Enhanced vegetation and re-stabilized mountain slopes reduced sediment input to the TDSC system since 8 ka. Consequently, turbidite flux and coarse fraction content decreased along the TDSC.

Tectonic, volcanic, sedimentary, climatic, sea level, oceanographic, and anthropogenic controls on turbidite systems

Nelson, C.H.¹, Escutia, C.¹, Goldfinger, C.², Gutiérrez-Pastor, J.¹, Karabanov, E.³.

1. C.S.I.C.- Universidad de Granada. Instituto Andalúz de Ciencias de la Tierra. Campus de Fuentenueva. 18002 Granada, Spain (odp@ugr.es).

2. COAS Oregon State University 104 Ocean Admin Bldg. Corvallis, OR 97331.

3. Geology Department, U of S. Carolina, Columbia, SC.

A wide variety of controlling factors combine to influence the development of turbidite systems, and these vary with location and time in each turbidite system. For example, Cascadia Basin, underlain by the Cascadia Subduction Zone, exhibits the climatic and sea level control of the Pleistocene lowstands, the tectonic control of earthquake triggering of turbidites during the Holocene, the volcanic effects of the Mt. Mazama catastrophic volcanic eruption, and finally the anthropogenic control of the sediment supply for the last century. Lake Baikal shows how the rift basin tectonic setting controls the number of sediment inputs, amounts of sediment supply and types of turbidite systems developed, whereas climatic changes controlled the deposition of thick robust turbidite sands during the Pleistocene. The Ebro turbidite system in the Mediterranean exhibits Messinian salinity crisis, climatic, oceanographic current and anthropogenic controls on the sediment supply and resulting turbidite system development.

Astoria Fan in Cascadia Basin was the first location in which thick robust sands deposited during Pleistocene glacial and lowstand times were observed. Pleistocene turbidites were mainly funneled to outer fan lobes where the highest sand:shale ratios are found. In contrast, during the Holocene higher sea levels, warmer climate and significant Pacific Northwest forestation, turbidite deposition is confined to channel floors and consists mainly of thin-bedded turbidites (5-10 mm). The exceptions to this are the thick (30-100 cm) tuffaceous turbidites deposited in Cascadia Basin channels after Mt. Mazama ash (Crater Lake, Oregon) blanketed the Columbia River drainage with 50 km³ of volcanic debris in 7626 yr B.P. The volcanic glass washed down drainages to the ocean, mixed with Columbia and Rogue Canyon sands when Cascadia Subduction Zone earthquakes triggered turbidity currents, and was transported for hundreds of kilometers down channel systems. Correlation of this marker bed shows that overbank suspension flows, rich in volcanic glass, deposited thin-bedded turbidites in interchannel areas of the upper and middle Astoria Fan, thus proving that thin-bedded turbidites do not equal distal turbidites; also poorly sorted, high matrix (20%) and wood-rich deposits of the canyon mouth evolved 150 km downstream to well sorted, low matrix (5%) graded sands with a complete Bouma sequence. In addition, the first occurrence of the Mazama turbidite in submarine fan, deep-sea channel and base of slope apron turbidite systems in Cascadia Basin, permits us to correlate ~ 13 post-Mazama Holocene turbidites that are synchronously triggered by great earthquakes of the Cascadia Subduction Zone. Using Mazama ash stratigraphic correlation, ¹⁴C ages, hemipelagic sedimentation rate ages, and physical property stratigraphic correlation it can be shown that most of the Cascadia basin turbidites correlate along much of the margin, and pass several relative dating tests of synchronous triggering. Of 23 correlated events, 17 of them suggest rupture of at least ~ 800 km of the megathrust, while the remaining 6 events show partial rupture. The robust stratigraphic correlations suggest that the rupture of the margin (probably similar to the ~300 second Sumatra event) creates a unique set of coarse-grained pulses that are retained in turbidites. In sum, as described in additional posters, Cascadia Basin shows the detailed earthquake control on timing, periodicity and cycles of Holocene turbidite deposition. In contrast, the controls of climate change and lowered sea levels of the Pleistocene result in robust turbidity currents that erode channels and destroy the record of earthquake controls.

Tectonically caused half-graben morphology controls the amount and type of sediment supply and consequent type of late Quaternary turbidite systems developed in the active rift basins of Lake Baikal, Russia. Steep border fault slopes (footwall) along half-graben basins provide multiple small sources of gravel/sand to feed small (<10 km diameter) sublacustrine base-of-slope aprons on the lake floor. Gradual slopes of the southeastern ramp margins (hanging wall) of the lake basins, conversely, feed finer grained sediment from larger drainages into two different types of channelized turbidite sublacustrine fan systems: (1) small (5-20 km) laterally fed sand-rich fans sourced by local rivers, often originating from glaciated valleys; and (2) large (> 65 km) axially-fed, elongate silt-rich fans sourced by regional exterior drainage of the Selenga River. Low sedimentation rates and thin-bedded mud and silt turbidites are characteristic of Holocene time whereas high sedimentation rates, thick sand turbidites and over-sized fan channels are characteristic of Pleistocene glacial times. As glaciers receded, fan lobes back stepped and thinner and finer grained turbidites deposited. Because there have been no significant lake level variations from Pleistocene to Holocene time and sediment always has direct access down the steep walls to lake floor turbidite systems,

climatic changes and glacial sediment sources alone control turbidite system growth rates that are equal to those in marine basins. This isolates Pleistocene climatic change as a major factor controlling sediment supply in contrast to the conceptual idea that lowered sea level and erosional base level of drainages mainly control sediment supply and turbidite system growth rate.

The subaerial drainage system, formed during the Messinian dessication in the Mediterranean, exerts control on Ebro turbidite systems. For example, the 20 km wide and 2,500 m deep Messinian Canyon of the Ebro rapidly filled with Pliocene mud and now is dominated by sediment failures that prevent turbidite system development in this area. The Messinian and other Pliocene, Pleistocene and Holocene surfaces also can be used to estimate the Ebro River sediment supply to highstand deltaic and lowstand turbidite systems. The general highstand conditions of the Pliocene, similar to the Holocene, resulted in a low discharge of Ebro River sediment (~ 6.5 million tonnes/yr) and a sediment drape across the margin that deposited at rates of ~ 24-40 cm/ky. In contrast, sediment supply increased two-to-three times during the Pleistocene, the margin prograded rapidly and deposition occurred at rates of 101-165 cm/ky on the outer shelf and slope, but basin floor rates remained anomalously low (21-26 cm/ky) because sediment is drained along relict Messinian pathways and broadly dispersed eastward in Valencia Trough. Throughout high and low sea levels, westward oceanographic currents have caused a progressive progradation of Ebro prodeltaic and turbidite systems. During the late Pleistocene rise of sea level, the main depocenters progressively shifted shoreward and sedimentation rates greatly decreased from 175 cm/ky on the upper slope during the early transgression to 106 cm/ky on the outer shelf and then to 63 cm/ky on the mid-shelf during the late transgression as the river sediment discharge dropped to half by Holocene time (~ 6.2 million tonnes/yr). Maximum sedimentation rates occur in active depocenters such as the Holocene delta (370 cm/ky) or the youngest Pleistocene Oropesa channel-levee complex (750 cm/ky) where deposition rates are more than an order of magnitude greater compared to average Ebro prodeltaic (38 cm/ky) or turbidite system rates during the Pleistocene (21 cm/ky). The sedimentation rates verify the importance of sea level control on the progressive change in location of depocenters and amount of sediment supply, but Pleistocene climatic change and deforestation alone can be observed to double river sediment discharge. Climatic change helps explain the anomalously high deposition rates in Pleistocene turbidite systems compared with older systems that may be controlled more by tectonic and sea level changes alone. During the past 2,000 years, in contrast, humans have controlled deposition in the Ebro margin system; first, by deforestation that more than doubled river sediment discharge and shelf deposition rates to equal those of Pleistocene time; second, by river dam construction that reduced sediment discharge to less than 5% of normal Holocene discharge. Similar recent discharge reductions from the Nile, Po and Rhone Rivers suggest that during the past century there has been a significant loss of river sediment supply for the deltaic and turbidite depositional systems in the Mediterranean Sea.

Mass balance controls on offshore sediment delivery: experimental results

Paola, C.

*St. Anthony Falls Laboratory
Minneapolis MN 55414*

The large-scale, continuous extraction of sediment mass from transport that characterises depositional systems is one of the dominant controls on local stratal architecture and properties. The degree to which local variability can be accounted for using depositional mass balance is especially clearly revealed using basin-scale experiments, where the entire linked depositional system is accessible for study. We show how the mass balance can be expressed in terms of either a dimensionless extraction fraction or a dimensionless bypass ratio. We then show how using this framework to account for mass balance effects reveals similarity in dip and strike section stratal architecture, using experimental and field examples. Finally, we will look at how the depositional mass balance is controlled by external forcing (eustatic sea level), subtle changes in supply grain size (deepwater systems), and transport conditions at critical points ("choke points") in linked depositional systems.

How do sediment flux and sea level changes control deepwater deposition? Implications from Eocene Central Basin of Spitsbergen

Plink-Björklund, P.

Department of Geology and Geological Engineering, Colorado School of Mines, Golden, CO, 80401, USA.

Basin-floor, as well as slope turbidite systems have been documented on Spitsbergen shelf margins. The former are associated with incision of canyons at the shelf edge, whereas the latter were fed by shelf-edge deltas. However, both these systems are associated with relative sea-level falls below the shelf edge, and a higher sediment fallout rate during the falling stage, rather than sea-level fall amplitude, has been documented to delay and prevent major shelf-edge incision.

The Spitsbergen turbidite systems are dominated by hyperpycnal flow turbidites, as the sediment was fed directly by river effluent onto the deepwater slopes. The following observations collectively suggest that hyperpycnal flows generated most of the Spitsbergen turbidites: (1) physical connection between fluvial channels on the shelf edge and turbidite channels on the upper slope, (2) general abundance of thick turbidite sandstone beds, (3) generally sand-prone character of the turbidite systems, (4) downslope changes of individual turbidite beds and identification of their collapsed pinch-outs, (5) great abundance of relatively delicate, terrestrial material (leaves, coal) in turbidite beds, (6) low abundance of associated slumped or debris-flow beds, and (7) the occurrence of turbidites in systematically accreted shelf-margins.

Four basin-floor fans were studied by measuring detailed vertical sections, walking-out stratigraphic units and correlating photomosaics on dip-direction Pallfjellet exposures, Van Keulenfjorden. The basin-floor fans have a three-fold architecture. (1) The lowermost, Stratigraphic Unit 1 (SU 1) consists of low-angle, basinwards prograding clinofolds that downlap into underlying marine shales. Individual clinofolds are dominated by upwards coarsening and thickening packages of dominantly thin, surge-type flow turbidite beds. (2) The middle, Stratigraphic Unit 2 (SU 2) is based by an erosion surface that can be traced across the ca 5 km long exposures of the basin-floor fans. The SU 2 reaches farthest out into the basin, and is dominated by thick and sandy, sustained-flow beds. (3) The upper, Stratigraphic Unit 3 (SU 3) is based by a 'flooding' surface that brings mud rich turbidites at the top of the sandy turbidite beds of the SU 2. The SU 3 consists of retrogradationally stacked turbidite beds. The retrogradation is seen by the landwards-stepping of pinch-outs in the successively higher stratigraphic levels in the distal end of the fans. The landwards pinch-outs at the base of slope do not onlap onto the slope, as they merge into an erosion surface instead.

The progradational, lower stratigraphic unit is interpreted to be deposited during relative sea-level fall. The turbidite beds were prograding, as the rivers were forced out towards the shelf edge. The middle, sand-prone stratigraphic unit is interpreted to be deposited during the early lowstand, when the feeding river system was at the shelf edge, and sediment was delivered directly onto the slope. The middle Stratigraphic Unit 2 represents maximum progradation of the system. The erosion surface below the SU 2 is interpreted as the sequence boundary, as it was eroded by increasingly denser and faster turbidity currents during relative sea-level fall, while the fluvial feeder system was shifting gradually closer to the shelf edge and delivering gradually more sediment into the deepwater slope. Sequence boundary is placed at the regional erosion surface, rather than at the base of the fans, because (1) this surface was eroded throughout the falling-stage, and corresponds to the lowest sea level at the shelf edge, (2) this surface correlates into main canyon base, feeding the basin-floor systems, (3) SU 2 above the sequence boundary reaches furthest out into the basin, whereas SU 1 pinches out further landwards. The retrogradational, SU 3 is interpreted to be deposited during late lowstand, when relative sea-level rose slowly.

Sea-level changes clearly control deepwater deposition on the Eocene shelf margins on Spitsbergen, especially the internal architecture, stacking pattern, and sand/shale ratio within the basin-floor fans (as well as the slope turbidite systems). The location of turbidite systems on the slope or basin floor, and their attachment or detachment to the shelf-edge feeder system, nevertheless, is controlled by the sediment fallout rate during the falling stage.

Facies architecture and sediment composition of Middle-Upper Jurassic base-of-slope successions, central Apennines, Italy

Rusciadelli, G.

Dipartimento di Scienze della Terra, Università "G. d'Annunzio" di Chieti, Via dei Vestini, 30, 66013 Chieti Scalo, Italy.

Carbonate slopes are sinks for much of the excess sediment produced by the carbonate factory, which is susceptible to chemical and physical conditions, achieving the few tens of meters below the sea level. Carbonate platforms compete with sea level variations and rapidly respond to environmental changes by varying the production potential, the type and amount of sediments exported downslope. Carbonate slopes thus contain a record of these changes in their stratigraphic architecture, which is highlighted by the vertical distribution of platform-derived deposits interbedded with pelagic limestones.

A northern margin portion of the Apulia Carbonate Platform and its adjacent slope and base-of-slope are exposed along a north-west/south-east transect of approximately 20 km, on the western flank of the Morrone Mountain, a thrust-related anticline of the outer central Apennines fold-and-thrust belt. Middle-Upper Jurassic slope and base-of-slope successions outcropping in the northern sector of the Morrone anticline, represent a suitable example to investigate depositional architectures produced by the off-shorewards exportation from the adjacent carbonate platform. Quantitative compositional analysis allows the type of grains exported from the platform to be defined, and provides evidence of important vertical changes in the sediment composition.

Two major large-scale units have been identified based on facies and stratal stacking pattern and sediment composition. Their internal architecture is defined by an overall coarsening and thickening upward stratal stacking pattern, which records the progressive upward increase of platform-exported sediments. Superimposed units are differentiated by abrupt facies contrasts across mappable surfaces, which separate thick stratal packages with dominant calcarenites and calcirudites from pelagic limestone intervals.

Sediment composition of platform-derived grains greatly varies between the two identified large-scale units. Non-skeletal grains largely dominate the lower large-scale unit, with percentages generally higher than 60%, whereas skeletal grains dominate the upper large-scale unit, with percentages higher than 70%. Important changes between the two large-scale units are also recorded by compositional differences in skeletal associations. Variations in grain composition also characterize the development of smaller-scale units within large-scale ones. Higher percentages of non-skeletal grains characterize strata interbedded with frequent micritic limestones, in the lower part of small-scale units, whereas skeletal grain percentages tend to increase upward, within stratal packages with more and thicker resedimented deposits, at the top of small-scale units.

The compositional differences of platform-derived grains and skeletal associations through the two studied large-scale units reflect variations in the dominant type of carbonate-producing biota, independently of the changes in accommodation. Conversely, internal depositional architectures of large and small-scale units and variations of sediment composition within small-scale units, are thought to be more consistent with processes related to different orders of sea level changes.

Integrating basin-scale forcing parameters in density currents process-based modeling

Salles, T., Lopez, S., Euzen, T., and Eschard, R.

IFP, 2&4 avenue de Bois-Préau, 92852 Rueil-Malmaison Cedex, France.

Using the cellular automata paradigm, we implemented a process-based model of multi-lithology submarine density currents. It takes into account both gravitational and inertial effects when computing the flow over a given submarine topography. It includes ambient fluid entrainment and lithology dependent erosion/deposition rules to progressively build a full three dimensional geological architecture. It produces sedimentary objects such as erosive channels, overflow levees and depositional lobes with features such as grainsize segregation. To achieve an operational model over geological time scale, turbiditic deposits were considered to be the results of a succession of quasi steady state events for which sediment transport had permanent values.

With this model we propose to explore the linkage between basin scale forcing parameters and typical oil reservoir scales. Our starting point was the basin-scale simulations of the Lower Pab basin floor fan and the Upper Pab sand-rich slope fan (Pab Fm., Pakistan) which were obtained using the diffusion oriented software Dionisos (Eschard et al., this conference). Stratigraphic basin modeling over large time scales implies averaging external forcing factors and considering their influence on the model as long trend variations that may hide considerable temporal and spatial variability. Indeed, most natural processes are highly sensitive to autocyclic and allocyclic controls, even exhibiting chaotic behaviors. Consequently long term parameters were first extracted from the Pab simulations, then given temporal variability and used to design several numerical experiments with different sets of hydrodynamic and sedimentary fluxes boundary conditions.

Climate related short term cyclicity

A preliminary step of our model consists in defining a succession of quasi steady-state events representing what is thought to be the averaged basin-scale geological history. Then, some spatial and temporal variability is introduced both in the occurrence and magnitude of these events. Combining them differently in time, various 3D architectures are obtained. For example, the effects of frequent short sedimentary pulses are compared to those of rare but long events. These different temporal distributions of events may be linked to different climatic contexts or triggering processes (hyperpycnal versus surge-type).

Sedimentary source and flow composition

The role of suspended sediment concentration and grain-size distribution on the transport efficiency of the flow was also investigated. The varying compositions of the flow may not only reflect climatic variations, but also the effects of upstream basin physiography possibly trapping the largest grainsize lithologies. We observe that according to the value of the chosen parameters, different sedimentary features were obtained ranging from erosive channels to depositional lobes or sedimentary levees. The relative percentage of channel fill versus overflow deposits was also compared to the total sedimentary input.

Canyon versus multiple channel feeder

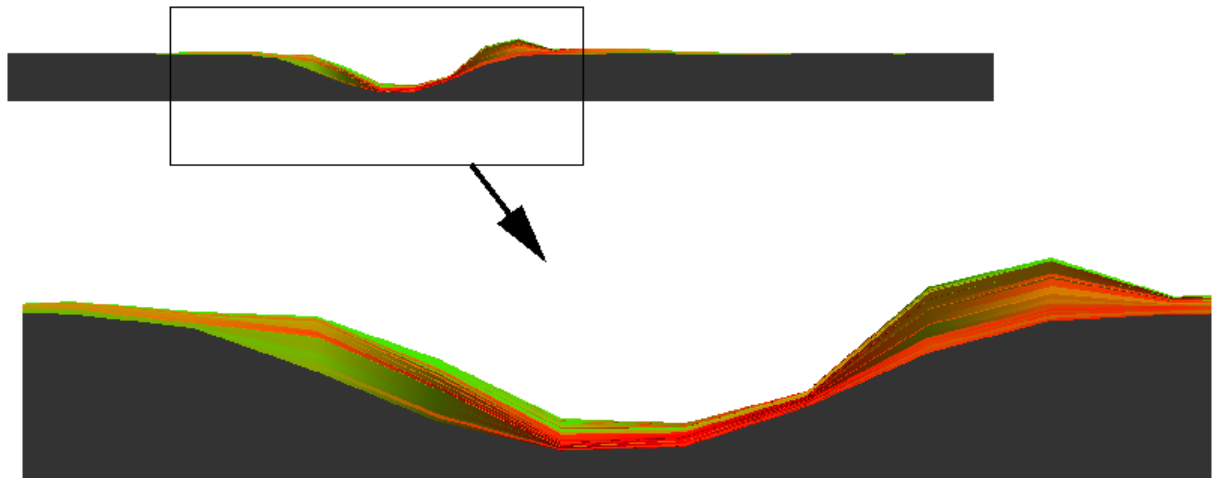
Spatial distribution of sedimentary inputs may reflect the connection or disconnection between the deep basin and the continental margin. The impact of the type of the sedimentary source has been studied comparing the differences between the Lower Pab basin floor fan and the Upper Pab slope fan. For the Upper Pab delta-fed system, a broad input zone with scattered, randomly distributed entry points was used, whereas a high discharge narrow entry zone was considered for the Lower Pab canyon fed system.

Topographic control

As the model takes into account physical laws, the interaction between the hydrodynamics of the flow and the substrate can provide insights into the impact of topographic controls on geological deposits. Grainsize segregation is observed with topographic lows trapping coarse sediments whereas the finest sediments build levees on topographic highs.

The preliminary results of the simulations were compared to field observations made in the Lower Pab and Upper Pab formations. Variations of the physical parameters may be linked to different possible external

factors that controlled the internal organization of these contrasting turbiditic systems. Finally, this process-based quasi steady approach allows a better identification and understanding of key physical parameters: we think that this will make the reservoir scale prediction more efficient in deep-sea clastic systems.



Vertical cross-section view of channel deposits at the exit of a meander bend. Sandy deposits are coded in red going through to green for fine clay deposits. The channel is about 600m wide and 25 meters deep.

The architecture of the Bengal Fan as response to tectonic and climatic changes in the Himalayan

Schwenk, T., and Spieß, V.

University of Bremen, Kagenfurter Str., 28359 Bremen, Germany.

The Bengal Fan is fed by the huge amount of suspended material transported by the Ganges and Brahmaputra rivers, which drain the Himalayan on its southern and northern flanks, respectively. Since it is thought that the build-up of the fan started immediately after the begin of the orogenesis of the Himalayan, a nearly complete record of its tectonic and climatic history should be stored within the post-collision deposited sediments of the fan.

To study the architecture and stratigraphy of the fan at different scales and different distances to the shelf, high-resolution multichannel seismic data, sediment echosounder Parasound data and swath sounder Hydrosweep were collected by the University of Bremen during RV Sonne cruise SO125 in 1997 from 4 different study areas located at 17°N at the middle fan as well as at 14°N, 11°N and 8°N at the lower fan. Additional Parasound Data were gathered on the cruises SO 93 (1993) and SO 126 (1997) in cooperation with the BGR, Hannover.

A combined analysis of the data sets from a detailed survey at 17°N turned out, that the active channel levee system on the middle fan is characterized by a high number of cut-off loops and a heterogeneous structure of the levees. The channel segments show a complex behaviour with changing ratios of vertical aggradation and lateral migration during their development. In contrast, a prominent buried system shows no cut off loops and a different, but also complex behaviour. Both, the changing behaviour of the systems and the difference between the systems, indicate that the turbidity currents building-up the systems changed in terms of loading, density and velocity which may be the result of different delivery of the feeding rivers and finally suggests changing environments in their draining areas.

A long seismic profile from the middle fan at 17°N reveal four channel-levee system complexes, separated by regional unconformities, which may partly be caused by switching of the feeding canyon or generating of non-channelized turbidity currents. The absence of hemipelagic drapes as well as mass-flow deposits indicate activity of the Bengal Fan even during sea-level rises and highstands.

In all three profiles from the lower fan, regional unconformities were found. At 8°N, unconformities have Pliocene and Pleistocene age and were interpreted to be the equivalents of unconformities found in the central Indian Ocean, which are related to deformation events of the oceanic crust and to changes of sediment character. Faults terminating within Pleistocene sediments suggesting tectonic activity at least within the Pleistocene at 8°N. The unconformities identified at 11°N and 14°N may result from tectonic events or sediment changes too. Beside these unconformities, variations of sedimentation rates in time and space determined at 8°N and the onset of channel-levee systems simultaneously to lithological changes observed at ODP Leg 116 at the lowermost fan indicating that tectonic events at the Bengal Fan and changes of sediment supply and transport occurred partly concurrently. Since sediment supply in turn depends on tectonic in the source area of the Ganges-Brahmaputra Rivers, it is reasonable that a link exists between source and sink areas of Bengal Fan turbidites, i.e. between uplift of the Himalayan and deformation events of the Indian Ocean lithosphere.

In summer 2006 an expedition will be carried out to the Bay of Bengal to collect new seismic data and sediment cores to improve the understanding of the channel-levee architecture and to link the identified unconformities. Also, a pre-site survey will be done to support the IODP Proposal 552 "Drilling in the Bengal Fan, Indian Ocean. Neogene and late Paleogene record of Himalayan orogeny and climate: a transect across the middle Bengal Fan" by France-Lanord, Spieß, Curran and Molnar. Additionally, it is proposed to collect new seismic data on the shelf and slope to support the complex IODP Pre-proposal 609 "The Himalayan-Bengal System: Studying links between Land and Ocean, Climate and Tectonics, "Source and Sink" by a multiplatform approach for drilling in the Bengal Fan" (Spieß, France-Lanord, Molnar, Curran, Kudrass, Kuehl, Goodbred & Revil).

Multi-source basins and approaches to stratigraphic prediction

Smith, R.D.A., and Burgess, P.M.

Shell International, Rijswijk, Netherlands

Sequence stratigraphy in a given basin is often made complex through the operation of multiple sediment source systems, each with different supply characteristics and different relative sea-level histories. Fine examples of such complexity are provided by the Silurian Welsh Basin and the Cretaceous-Paleocene Norwegian Sea Basin. In both cases, supply from different segments of basin margin yielded contrasting types of deep-marine turbidite systems.

Stratigraphic prediction in the subsurface must clearly take account of such complexities. Two approaches will be illustrated: 1) Shell's multi-scale basin-to-reservoir static modelling process and 2) 3D forward stratigraphic modelling using Dionisos. The first approach constructs nested quantitative static models across a range of scales, integrating available seismic, well and analogue information. The second approach deals with the uncertainty arising from multiple poorly constrained parameters by constructing multiple forward-model realizations spanning a wide range of parameter possibilities. Forward modelling results are then combined as conditional frequency maps.

Tectonic and paleotopography control on turbidite sedimentation in confined basin: the lower Messinian wedge top sedimentation of the Laga Formation (Central Italy)

Stanzione, O.¹, Milli, S.¹, Moscatelli, M.², and Falcini, F.¹.

1. Dipartimento di Scienze della Terra, Università di Roma "La Sapienza" – P.le Aldo Moro, 5 - 00185 – Roma, Italy.

2. Istituto di Geologia Ambientale e Geoingegneria CNR – Via Bolognola, 7 - 00138 – Roma, Italy.

The Laga Formation crops out in the more external sector of the central Apennine; it records the turbidite sedimentation in a complex foreland basin, characterized by the presence of an articulate substrate related to the activation of compressional structures. A recent facies and physical stratigraphic analysis, based on the measure of 45 stratigraphical-sedimentological logs for a total thickness of about 6000 m, allow us to propose a new stratigraphic framework for the lower Messinian deposits (pre-evaporitic member in literature) of the Laga Formation.

In the analyzed succession is possible to identify two superimposed units (Fig. 1), that show different vertical evolution, facies features and palocurrents distribution. The superimposition of these two units is probably related to the local depocenter migration in the appenninic foreland basin system.

The lower unit, named Laga 1, shows a general fining-upward trend. The deposits are characterised by medium-grained sandstones with a crude lamination and by fine-grained sandstones showing traction and traction-plus-fall out structures. In the northern proximal sectors of the Laga basin these deposits are organized in lenticular sand bodies forming large to medium scale channels fill, with N 170° as main direction of the paleocurrents. On the contrary, in the southern distally sectors the sedimentary bodies are generally tabular (lobes) with a more dispersed trend of paleocurrents directions from northwest, west and southwest, indicating the presence of more point sources supplying the Laga basin. The strong control exerted by the basin topography conditioned also the track of the turbidity currents which were deflected and reflected by lateral and/or frontal ramp respectively of the Gran Sasso and Montagna dei Fiori slopes. In this sector the interaction between the turbidite sedimentation and the paleotopography is also pointed out by high thickness of muddy horizons, probably related to ponding processes of the turbidite currents.

The upper unit, named Laga 2, is characterised by small coeval turbidite systems, westernly supply (paleocurrents N140°), that were deposited during the deformation of compressional structures (e.g. Acquasanta anticline). The deposits of this unit are made up of medium and fine sands, rich in coal and plant debris, generally with HCS-like lamination and climbing ripples which record the deposition of low efficient combined flows (Fig. 2). In these flows the oscillatory component could be directly related to the deflections of the flows due to rough sea floor paleotopography. Moreover, the HCS-like lamination could point out a genetic relation between the turbidite flows and hyperpicnal flows generated at river mouths during catastrophic flood events, with the oscillatory component induced by the pulsations of the river floods. In this case the deposits of this unit could point out a direct connection between turbidite systems and adjacent deltaic flood dominated systems.

Concluding, in both units the distribution of paleocurrents and the resulting facies show the interaction between the turbidite sedimentation and the seafloor paleotopography. This interaction seems to be connected to the inherited confined condition (Laga 1) and to the activation of growth structures that cause an increase in the basin articulation (Laga 2). Therefore, the recognised vertical trend of the studied succession, showing the superimposition of low efficient turbidite systems (Laga 2) on more efficient turbidite systems (Laga 1), could record the local migration of basin depocenter strictly related to thrusts propagation. According to that, we believe that lower Messinian deposits of Laga Formation could be considered as deposited in a depositional wedge-top system, probably recording the "outer stage" (or molassa stage) of the older Marnoso-Arenacea foredeep basin, whose flexure is Early Miocene in age.



Figure 1 – Panoramic view of the northern sector of the Laga basin showing the two units Laga 1 and Laga 2; these units are separated by a surface (I2), marking a clear change in the sedimentary characters and evolutive trend of the deposits.

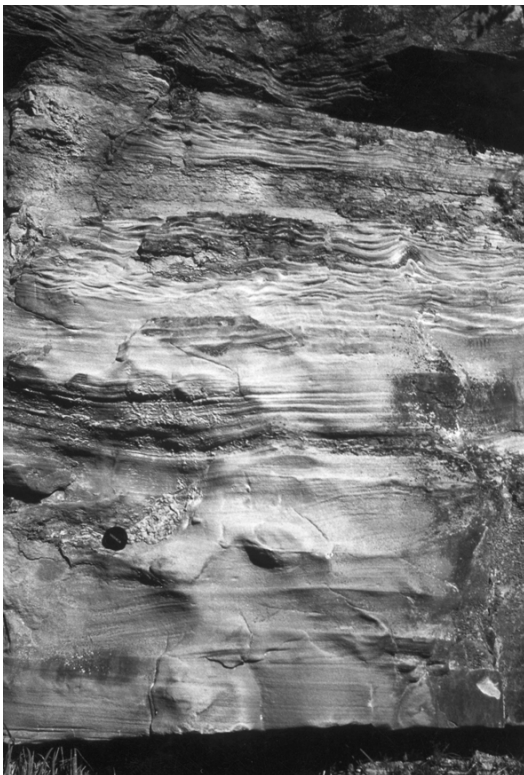


Figure 2 – Typical facies sequence of the Laga 2 deposits that shows fine sandstone with HCS-like lamination at the base, passing to very fine sandstone with climbing ripples at the top. The HCS-like lamination and the rounded shape of the ripples crest are thought to be related to the action of combined flows.

Submarine incision and renewed sediment influx during the Holocene: a case study from the Santa Monica Basin, California

Strachan, L.J.^{1*}, Schimmelmann, A.², Lange, C.³, Kneller, B.⁴, and McCaffrey, W.⁵

1. School of Earth, Atmospheric & Environmental Sciences, University of Manchester, Manchester, M13 9PL, UK.

2. Indiana University, Department of Geological Sciences, Biogeochemical Laboratories, 1001 East 10th Street, Bloomington, IN 47405-140, USA.

3. Universidad de Concepcion, Departamento de Oceanografia, Centro FONDAP, COPAS, Casilla 160-C, Concepcion, CHILE.

4. School of Geosciences, University of Aberdeen, Aberdeen, AB24 3UE, UK.

5. School of Earth and Environment, University of Leeds, Leeds, LS2 9JT, UK.

** Corresponding author : lorna.strachan@manchester.ac.uk*

Quantifying the contribution of climatic forcing on deep marine sediments is problematic because the effects of eustasy and tectonics often obscure preserved signals. Holocene sedimentary sequences however may overcome this limitation because relative sea level is well constrained and thus may facilitate the identification of a climatic signal.

This presentation uses data from the well-studied Santa Monica and Santa Barbara Basins located offshore California in an attempt to establish the evolution and development of the fluvial-turbidite system during the Holocene and relate it to climatic forcing.

Insights into the principal controls of the depositional system are derived from published seismic data, correlated and dated ODP cores and both published and unpublished shallow sediment core data from the contiguous and we suggest depositionally linked basins of Santa Monica and Santa Barbara. In particular, the availability of well-dated sediment cores from the Santa Barbara Basin allows the temporal correlation of Santa Barbara Basin flood plume deposits and turbidites with Santa Monica Basin turbidites and conspicuous erosive seismic reflectors located on the shelf and slope.

Compositional and textural variations in Santa Barbara Basin turbidites reveal two distinct types, these are interpreted as: seismogenic turbidites and flood generated hyperpycnal turbidites. Santa Barbara Basin turbidites together with flood plume deposits form an important archive of earthquakes and flood events that have been chronologically linked to dated turbidites and seismic reflectors in the Santa Monica Basin.

Calibration of ODP core and seismic data in the Santa Monica Basin reveal formation, through incision, of the modern day Hueneme submarine Channel c.3.5 ka. This date correlates closely to the end of a c.2.3 kyr period of increased climatic instability or storminess recorded as hyperpycnal turbidites in the Santa Barbara Basin. We therefore infer that Hueneme submarine Channel incision was driven by hyperpycnal turbidity current substrate erosion driven by enhanced climatic instability over a protracted period of c.2.3 kyrs. In addition, by correlating older seismic reflectors from shelf and slope areas to dated ODP core it becomes apparent that the present day Hueneme Canyon did not exist until after the Younger Dryas period. It is surmised, therefore, that the formation of this significant feature was likely also linked to this period of enhanced climatic instability.

The formation of the submarine Hueneme Canyon and Channel system is intrinsically linked to climatic forcing, the main driver for generating turbidity currents between c.5.4 and c.3.1 ka, and does not conform to typical Holocene transgressive systems from active margins.

Shelf Margin Systems: Interface between Shallow Water Sediment Sources and Deep Water Sinks

Suter, John R.

*Sedimentary Systems
Subsurface Technology
ConocoPhillips
Houston, TX*

Shelf Margins are the critical interface between shallow water, traction-dominated shelf and nearshore environments and the gravity-flow dominated environments of the slope and deep water basins. Shelf margins, like most geological systems, are manifestations of multiple controlling factors, including tectonic setting, transition between continental and oceanic crust, type of substrate, rate of supply and caliber of sediments, base level changes, and dynamic process environments. The nature of the shelf margin can be both a key control on sediment delivery to deeper water environments and a clue to types of deposits that may occur in deeper water sinks. Progradational shelf margins, typified by shelf margin deltaic systems, provide coarse-grained sediments to deep basins by a variety of mechanisms. On stable prograding margins, during lowstands in which shorelines are located near the shelf margin, sediments may be directly supplied to the upper slope by sustained hyperpycnal flows from deltaic distributaries, or by longshore drift, storm, and/or tidal processes. Enhanced deposition may locally oversteepen the shelf margin, resulting in failures and delivery of sediments by slumping, sliding and ignition of gravity flows. Unstable progradational margins involved with mobile salt or shale substrates are also subject to a variety of larger scale collapse features, resulting in massive reconfiguration of the margin and consequent effects on deep water sediment delivery. Stacking patterns on seismic profiles can be extremely useful in recognizing the nature of these systems and likely types of deep basin sediments.

Non-depositional shelf margins supply sediment to deeper water basins by different mechanisms. Large scale failures, resulting from instabilities triggered by tectonic events and changing base level are likely to be primary sediment suppliers, but other mechanisms are operative. On higher gradient, narrow margins, fluvial systems may be better able to generate hyperpycnal flows and deliver sediments to the upper slope and basin than on lower gradient progradational margins. Given sufficiently narrow shelves, longshore drift fed systems may supply sand directly into headward-eroding canyons, or interact with tidal and storm currents to provide sources of clean sands to slope and basin systems. Conventional sequence stratigraphic models emphasize the importance of lowstand sediment supply to slope and basin environments, and indeed shifting the shoreline to the shelf margin facilitates the process of sediment delivery to deeper water. However, some mechanisms may actually be more effective during highstands. Longshore drift fed systems which derive sediment by erosion of highstand shorelines may well deliver less sediment at lowstand. Relict sediments on the outer shelf can be remobilized by oceanic currents and/or storm flows and delivered to the upper slope. These latter processes may be volumetrically less significant than gravity flows generated by shelf margin failures, but are probably underappreciated in exploration models as sources of reservoir caliber sediments to deep water environments.

Sediment Flux To Basin Plains, Bed Volumes, And External Controls On The Geometry Of Individual Turbidite Beds

Talling, P.J.¹, Amy, L.A.¹, and Wynn, R.B.².

UK Turbidite Architecture and Process Group (UKTAPS)

1. Department of Earth Sciences, University of Bristol, Queens Road, Bristol, BS8 1RJ, UK.

2. Challenger Division, National Oceanography Centre - Southampton, European Way, Southampton, SO14 3ZH, UK.

Deposits from individual flow events, comprising turbidity current and 'linked' submarine debris flow, have been correlated over an area of 120 x 30 km in the Miocene Marnoso Arenacea Formation in the northern Italian Apennines.

Intermediate and large volume beds within the correlated interval of Marnoso Arenacea strata contain $\gg 0.5$ km³ of sediment, and the volume of the largest beds exceeds 5 km³. Such extremely large volume flows can only have originated through submarine slope failure. Other processes that trigger turbidity currents, such as flood discharge from rivers, cannot have supplied such large sediment volumes. Even the highest mean annual sediment discharge of any river on Earth, 1,200 million tonnes from the Amazon (Milliman and Meade, 1990), would represent less than 1 km³ of rock, assuming a sediment density of 2,600 kg m⁻³ and relatively high porosity of 0.5.

Carbonaceous flakes are commonly seen dispersed within large-volume sandstone intervals, especially within the finest parts of some sandstone intervals. Abundant carbonaceous material suggests widespread failure of sediment associated with a delta or other fluvial input to the continental shelf. As the organic matter has not been oxidised, it must have resided in the uppermost part of the sediment column for a limited period of time.

Sediment deposition within the interval of correlated beds was dominated by a small number of large volume events. Approximately half of the strata, within the largest 56 beds, was deposited by 5 turbidity currents (Fig. 1). This may be a general feature of basin plains fed by infrequent flows generated by large submarine slope failures.

Volumes of beds, and sandstone or mudstone intervals within the beds, have an approximately log-normal frequency distribution. This type of frequency distribution commonly results from multiplication of a series of parameters that are randomly (normally) distributed. It has previously been suggested that volumes of submarine slope failures, and associated turbidites, follow a fractal (power law) distribution.

Large-volume turbidites potentially record the dynamics of their parent slope failure. Two beds comprise multiple sandstone intervals with intervening turbidite mudstone. This bed geometry suggests that parent slope failures occurred in multiple stages separated by days to months. Almost all the other large-volume beds locally contain an internal erosion surface underlain by inversely graded sandstone. This geometry indicates deposition from a turbidity current that waxed and then waned. These beds are simply too voluminous to have been formed by hyperpycnal flood discharge. Such waxing and waning flow was presumably generated by the initial slope failure.

A consistent bed shape is observed for small (< 0.7 km³), intermediate (0.7 to 2.5 km³), and large (2.5 to 7.0 km³) volume beds. Three intra-basinal highs are associated with subtle thickening of sandstone intervals. However, similar deposit shapes are observed for flows that traversed the basin plain from opposite directions. This suggests that intra-basinal topography was not the dominant control on deposit shape. A single composite shape is defined for turbidite sandstone deposits, in which the effects of the intra-basinal highs are removed.

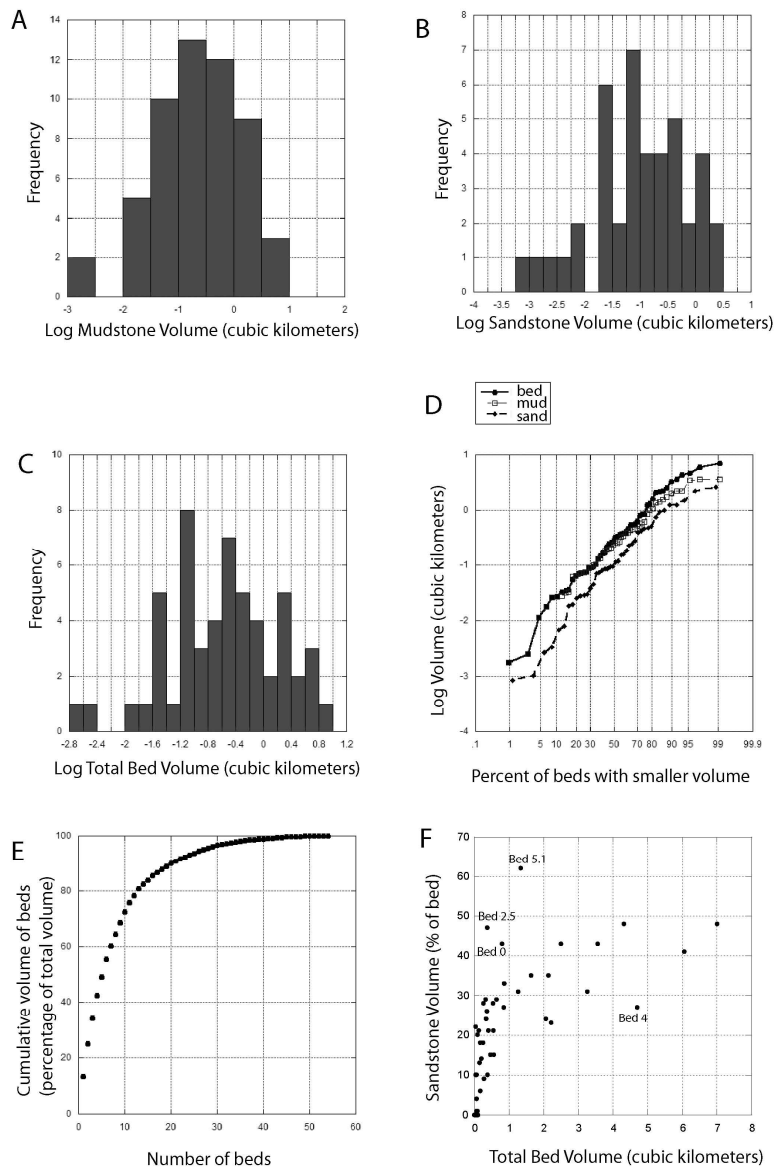


Figure 1: (A) Frequency distribution of mudstone volumes within beds. (B) Frequency distribution of sandstone volumes within beds. (C) Frequency distribution of total bed volumes. (D) Probability plots showing total bed, sand and mud volumes. (E) Cumulative volume of strata plotted against number of beds. A small number of large volume beds dominate the cumulative volume. (F) Plot of total bed volume against the volume percentage of sandstone within that bed.

The effects of submarine canyon and proximal fan processes on the depositional systems of the distal Mississippi Fan

Twichell, D.C.¹, Schwab, W.C.¹, Nelson, C.H.², and Kenyon, N.H.³

1. US Geological Survey, Woods Hole, MA, USA.

2. CSIC University of Granada, Granada, 18002, Spain.

3. National Oceanographic Center, Southampton SO14 3ZH, UK.

The Mississippi Fan is a Plio-Pleistocene deposit that covers most of the eastern half of the deep Gulf of Mexico Basin. Sidescan sonar imagery, high-resolution seismic profiles, and short cores have provided insight into the processes that have shaped the surface of this fan since the latest Pleistocene (Nelson et al., 1992; Twichell et al., 1992). Mapping and integration of these data indicate a three-staged progression since the last lowstand of sea level: (1) deposition of turbidites and debris flow deposits on the distal fan that were derived from the shelf edge during the last lowstand and the initial stage of the Holocene transgression, (2) failures in the Mississippi Canyon and on the adjacent continental slope during the Holocene transgression that buried large areas of the surface of the proximal Mississippi Fan including the channel that had previously supplied sediment to the distal fan, and (3) continued reworking of the surface of the fan and the overlying hemipelagic cover by bottom currents (Fig. 1).

During the latest Pleistocene, turbidity currents and debris flows passed through sinuous channels to the distal fan where they were deposited as elongate sandy beds or clast-rich mud beds parallel to channel axes (Fig. 1A). Active shifting of distal fan channels, resulting from localized levee failures, has resulted in laterally discontinuous facies at the distal edge of the fan. These distal fan deposits are overlain by hemipelagic sediment and age dates show that turbidite and debris flow deposition ceased about 11,600 yr BP (Schwab et al., 1996).

Drilling in the Mississippi Canyon indicates that sediment failures exhumed the upper canyon several times between 15,000 and 7,500 BP (Goodwin and Prior, 1989). These failures have been attributed to instabilities associated with rapid sediment loading during the last lowstand of sea level and the initial part of the Holocene transgression. The deposits from these failures cover large parts of the proximal fan, and completely bury much of the channel that delivered flows to the distal fan (Fig. 1B). While the timing of the onset of hemipelagic sedimentation on the distal fan is similar to the timing of the last meltwater discharges into the Gulf of Mexico (Laventer et al., 1982; Flower et al., 2004), we propose an alternative explanation for the shift from turbidite to hemipelagic sedimentation on the distal fan. The shift is probably due to slope failures choking the channel system thus isolating the distal fan from its sediment source rather than its being directly tied to an external climate or river discharge event.

Once the distal fan was isolated from turbidity current and debris flow sedimentation, hemipelagic sedimentation became the dominant depositional process. However, the presence of dune-like features and northeast trending linear furrows indicate active reworking of these deposits by northwest flowing bottom currents (Fig. 1C; Kenyon et al., 2002).

Since this progression in depositional styles is not recorded in any one place on the fan; a regional synthesis of stratigraphy and processes is needed to decipher these three stages that have shaped the surface and shallow subsurface deposits of the Mississippi Fan.

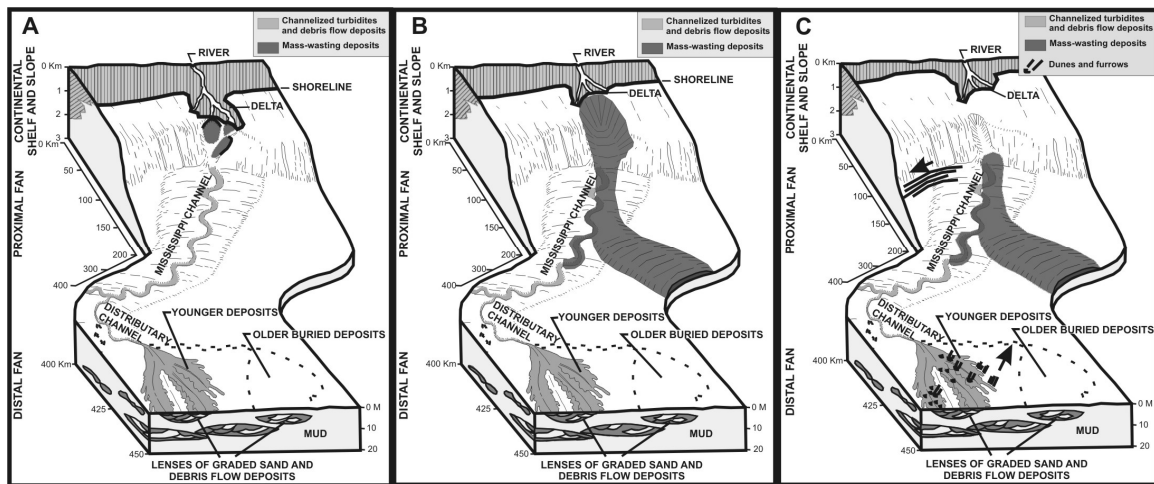


Figure 1. Summary diagram showing the progression from (A) turbidite and channelized debris flow deposition on the distal fan to (B) mass-transport deposition on the proximal fan which choked the channel, and (C) reworking of the seafloor by bottom currents (arrows show current direction inferred from bedforms).

- Flower, B.P., Hastings, D.W., Hill, H.W., and Quinn, T.M., 2004, Phasing of deglacial warming and Laurentide ice sheet meltwater in the Gulf of Mexico: *Geology*, v. 32, p. 597-600.
- Goodwin, R.H., and Prior, D.B., 1989, Geometry and depositional sequences of the Mississippi Canyon, Gulf of Mexico: *Journal of Sedimentary Petrology*, v. 59, p. 318-329.
- Kenyon, N.H., Akhmetzhanov, A.M., and Twichell, D.C., 2002, Sand wave fields beneath the Loop Current, Gulf of Mexico: Reworking of fan sands: *Marine Geology*, v. 192, p. 297-307.
- Laventer, A., Williams, D.F., and Kennett, J.P., 1982, Dynamics of the Laurentide Ice Sheet during the last deglaciation: Evidence from the Gulf of Mexico: *Earth and Planetary Science Letters*, v. 59, p. 11-17.
- Nelson, C.H., Twichell, D.C., Schwab, W.C., Lee, H.J., and Kenyon, N.H., 1992, Late Pleistocene turbidite sand beds and chaotic silt beds in the channelized distal outer fan lobes of Mississippi Fan: *Geology*, v. 20, p. 693-696.
- Schwab, W.C., Lee, H.J., Twichell, D.C., Locat, J., Nelson, C.H. McArthur, W.G., and Kenyon, N.H., 1996, Sediment mass-flow processes on a depositional lobe, outer Mississippi Fan: *Journal of Sedimentary Research*, v. 66, p. 916-927.
- Twichell, D.C., Schwab, W.C., Nelson, C.H., Lee, H.J., and Kenyon, N.H., 1992, Characteristics of a sandy depositional lobe on the outer Mississippi Fan from SeaMARC IA sidescan sonar images: *Geology*, v. 20, p. 689-692.

Modelling Long Term Climate Change

Valdes, Paul

*Geographical Sciences
University of Bristol, UK*

The talk will review our current understanding, and ability to model, climate change on geological time scales. Computer models of the Earth System play a vital role in such work. These have developed from early models, which were highly empirical and considered changes in atmospheric circulation only, to the current state-of-the-art Earth system model which includes a process representation of the atmosphere, ocean, vegetation and ice sheets. Lessons learnt from these models will be described, using examples from the late Cretaceous, Eocene and Oligocene.

Sedimentary processes throughout the North Atlantic. Glacial versus interglacial controls and comparisons between the eastern and western North Atlantic

Weaver, P.P.E., and Benetti, S.

National Oceanography Centre, Southampton, UK.

The seabed of the North Atlantic continental margin displays a wide range of sediment transport processes including both alongslope and downslope processes. There are strong similarities between the eastern and western margins but also some important differences. Each margin can be divided into three primary margin types reflecting to the influence of glacio-eustatic processes: (1) glaciated margin dominated by processes that occurred during glacial times when ice extended across the continental shelf; (2) glacially influenced margin influenced by higher sediment supply at the shelf edge during glacial periods; (3) non-glaciated margin largely unaffected by glacial sediment supply. Some spatial control on sedimentation may result from the regional tectonic setting, but a temporal control results from the cyclicity of major paleoclimatic and paleoceanographic events (i.e. glaciations, sea level oscillations, and changing current patterns or water masses).

The glaciated margin North of 56°N in the east and 41°N in the west the margin is heavily influenced by glaciomarine processes during glacial times, which build glacial trough-mouth fans such as the North Sea Fan and leave iceberg scour marks on the upper slope and shelf. During interglacials the Norwegian margin has been greatly influenced by alongslope currents, with less influence by turbidity currents than on the lower latitude margins. Landsliding is a prominent feature off Norway and the Faeroes but less so on the Canadian margin. Some of these landslides have occurred during the Holocene, though high glacial sedimentation rates may have contributed to the instability. In general, the glaciated margin of the western North Atlantic shows much more evidence for an important role for glacial meltwater in both erosion and deposition. Along the margin of southern Canada, large turbidite systems, more similar to mid-latitude submarine fans, were developed and the slope was incised by muddy turbidity current generated by plume fall-out, hyperpycnal flows from the ice margin and slumping of proglacial sediments.

The glacially influenced margin On both sides of the Atlantic canyons dominate across a latitudinal range where there was elevated sediment supply during glacials, but where the ice did not reach the shoreline. On the western side this was from 33-41°N whilst on the eastern side canyons range from 26-56°N. During low sealevels these canyons were very active though many are now inactive. Fans are common in the east but less so in the west presumably due to strong bottom currents such as the WBUC. In the east the Mediterranean outflow is a particularly strong bottom current in the Straits of Gibraltar and Gulf of Cadiz. Landslides are widespread on the western margin but not on the east. Small slumps are related to canyon incision and widening, while large slide complexes originate from a combination of intrastratal deformation, salt intrusion, melting of gas hydrates and earthquake triggering.

The non-glaciated margin. These margins do not compare so well due to their setting. Off most of the NW African margin, south of 26°N, upwelling produces elevated accumulation rates, though there is little fluvial input. This area is subject to infrequent but large-scale landsliding, giving rise to debris flows and turbidity currents. The latter traverse the slope and deposit thick layers on the abyssal plains, whilst debris flows deposit on the continental slope and rise. On the western margin, south of 33°N, three distinct depositional environments can be identified: (1) a sediment-starved eastern Florida margin, (2) the carbonate-dominated Bahama platform and surrounding areas, and (3) the active margin of Puerto Rico. Sea-level fluctuations affect biogenic production on carbonate banks and downslope deposition results. This is enhanced during highstands when the banks are flooded. Downslope processes, however, occur at a much smaller scale than further north or on the eastern Atlantic margin.

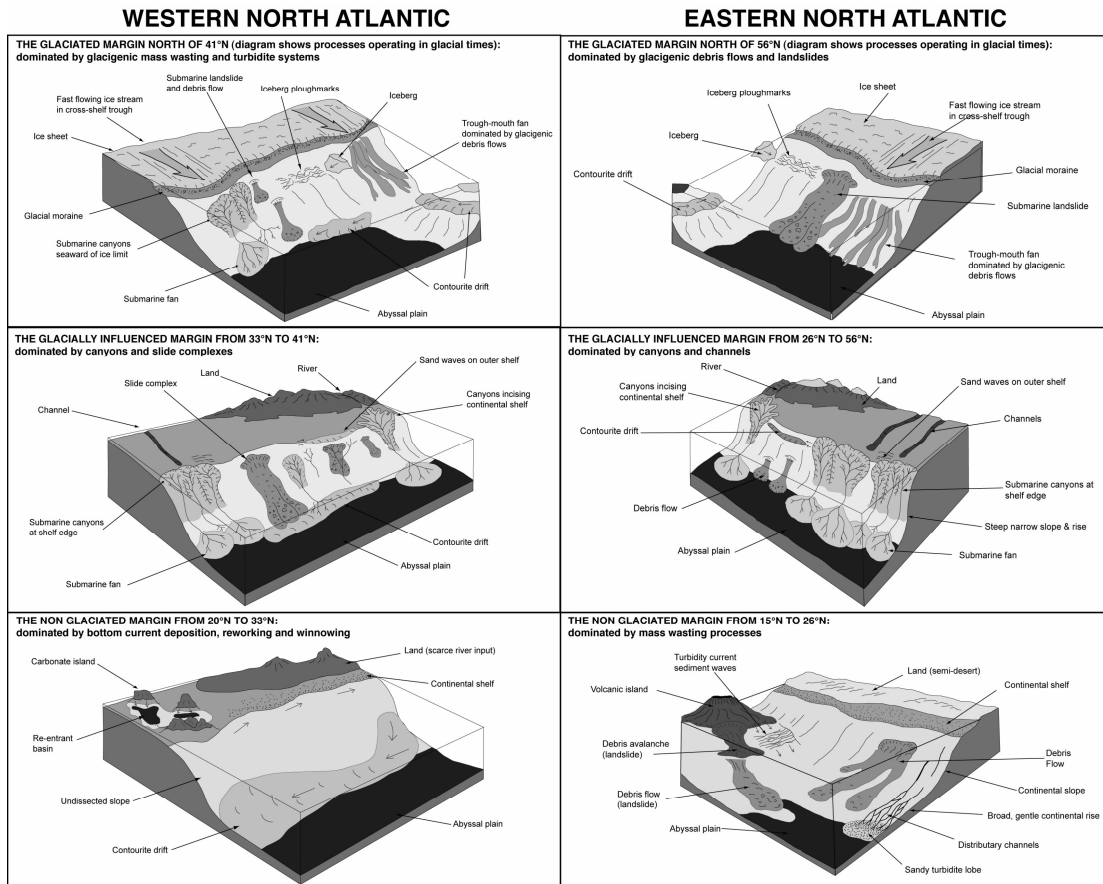


Figure 1. The main sedimentary characteristics of the North Atlantic margin.

Influences on deep-marine sedimentation along the continental margins of northeastern South America: Orinoco and Amazon systems

Wood, Lesli J., and Moscardelli, Lorena

Quantitative Clastics Laboratory, Bureau of Economic Geology, Jackson School of Geosciences, The University of Texas at Austin

The Orinoco and Amazon systems compose two of the largest source-to-sink sedimentary systems in the world. Their drainages are thought to have been intimately linked in the Quaternary through the interaction of source area tectonics, and their sediment discharges are dominated by fine-grained sediments (80-90% silt and clay). Likewise, these systems have undergone identical eustatic sea-level changes throughout their history. However, the continental margins into which they discharge and across which shelf to deep-marine sedimentation occurs have very different tectonic regimes, a variable that causes a great difference in the nature of deep-marine sedimentation in these systems.

The Amazon River exhibits the largest fresh-water discharge and maintains one of the three largest sediment discharges in the world. Under conditions of sea-level highstand it is thought to provide, through longshore transport, nearly 50% of the sediments deposited along the northeastern South American coast. However, at times of lowstand, sediments funnel directly into the deep sea fan of the Amazon. Importantly, the Amazon discharges into a tectonically stable shelf and shelf margin. Although minor mobile shales have been reported to the south of the main outlet, they have little effect on the nature of sediment sinks in the offshore. It has been proposed by recent authors that several mass transport complexes reported in the Amazon can be directly linked to changes in climate in the Amazon's source area, a concomitant increase in sediment supply, and resultant slumping and shelf failures due to overloading of the shelf edge.

The Orinoco system, in contrast to the Amazon, discharges into a tectonically active transpressional margin associated with its location along the boundary of the Caribbean and South American plates. The Orinoco River produces the world's third largest discharge but exhibits only the eleventh largest sediment discharge. Large transpressive ridges, buckle folding, and active mud diapirism and volcanic activity strongly influence gravity sediment pathways in the shelf edge, slope, and proximal basin floor. In more distal areas, as sediments proceed toward the Orinoco fan they must negotiate a tortuous pathway of accretionary thrusts, gateways between uplifting ridges and continued mud volcanism. Sediments in the Orinoco are destabilized at the shelf edge by active tectonics, and large progradational overloading of the shelf is driven more by phases of mountain building in the downstream reaches of the Orinoco River than by hinterland basin climate change, as proposed in the Amazon. Mass transport complexes reach as much as 250 meters in thickness, and flow paths are strongly directed eastward owing to uplift along the plate boundary. Leveed channels exhibit asymmetric levee growth that is higher to the south, away from the plate uplift. Channels form moats around collapsing diapirs and may show localized migration upslope in response to local tectonic forces.

Although these two major sedimentary systems are geographically proximal and share common drainage histories, sediment types, and sea-level histories, the difference in their tectonic settings results in completely different sediment drivers and different deep-marine basin fills. The architecture of these two systems is dramatically different, as are the distribution and nature of gravity deposits.

Timing and relation to climate/sea-level of giant landslides and turbidity currents on the Northwest African continental margin, from Morocco to Senegal

Wynn, R.B.* and the UK-TAPS group

National Oceanography Centre, European Way, Southampton, SO14 3ZH, UK

** Corresponding author : rbwl@noc.soton.ac.uk*

The Northwest African continental margin is an ideal location for studying the impacts of climate and sea-level change on deep-water gravity flow deposition (e.g. Weaver et al., 2000). In this contribution, we provide an overview of giant landslides and turbidity currents that have been deposited during the last 200,000 years on this margin, and relate their emplacement to glacial-interglacial cycles.

The largest turbidite system on the Northwest African margin is the Moroccan Turbidite System (Wynn et al., 2000; 2002), which receives sediment from the Moroccan margin and the volcanic Canary Islands. This turbidite system comprises three interlinked deep-water basins: the Agadir Basin and the Seine and Madeira Abyssal Plains. The largest turbidity currents from either source can reach all three basins, covering a distance of over 1500 km (Wynn et al., 2002). In late 2004 a UK-TAPS research cruise collected 50 new piston cores and a suite of geophysical data from the proximal part of the system, which includes the Agadir Canyon and Basin. This dataset has been integrated with previous studies carried out on the abyssal plains, and has provided new insights into the timing, processes and deposits of giant turbidity currents.

Over the last 200,000 years a total of about ten large-volume turbidity currents have contributed to the fill of the Agadir Basin, with eight sourced from the Moroccan margin and two from the flanks of the Canary Islands. The two largest volume Moroccan margin flows (turbidites 5 and 12) were deposited during glacial-interglacial transitions at oxygen isotope stage boundaries, with turbidite 5 emplaced between stages 3 and 4, and turbidite 12 deposited between stages 5 and 6. It is thought that sediment flux to the outer shelf and upper slope off Morocco markedly increased during glacial periods (due to increased upwelling and fluvial discharge), and this provided the sediment volume required for such large flows. The subsequent triggers for these events appear to be linked to the late/post-glacial rise in eustatic sea-level, but the reasons for this remain unclear. The large volume and increased erosive capacity of turbidite 5 is thought to be the major factor in its unique development as a linked turbidite-debrite unit in the Agadir Basin (Talling et al., 2004).

The most recent large-volume turbidite (turbidite 2) derived from the Canary Islands source is linked to the major El Golfo landslide on the flanks of El Hierro (Wynn and Masson, 2003; Masson et al., in review). This event occurred between oxygen isotope stages 1 and 2, which is also a glacial-interglacial transition, again suggesting a link to eustatic sea-level change.

Further south, off Western Sahara and northern Mauritania, the margin morphology and climate is markedly different. Large sections receive little or no clastic sediment for long periods due to the presence of the Sahara Desert, and as a consequence canyons and channels are rare and giant landslides become dominant. The Sahara Slide appears to be contemporaneous with turbidite 5 in the Agadir Basin, while the Mauritania Slide (Henrich et al., in review) occurred at a similar time to the El Golfo landslide/turbidite 2 event in the Agadir Basin. Both landslides therefore also occurred during periods of sea-level rise at glacial-interglacial transitions, with crustal loading and localised earthquake triggering possibly being a contributing factor.

In summary, even allowing for error margins in dating techniques, there is sufficient evidence to show that giant landslides and turbidity currents on the Northwest African margin definitely do not follow the standard 'lowstand emplacement' model found in many deep-water gravity flow systems around the World. Instead the largest events appear to occur during late/post-glacial periods of rising sea-level. This is probably due to a variety of factors, including the relatively low clastic input and low frequency of events in this passive margin environment.

Wynn, R.B., Masson, D.G., Stow, D.A.V., and Weaver, P.P.E. (2000) The Northwest African slope apron: a modern analogue for deep-water systems with complex seafloor topography, *Marine and Petroleum Geology*, v.17, 253-265.

Weaver, P.P.E., Wynn, R.B., Kenyon, N.H. and Evans, J. (2000) Continental margin sedimentation with special reference to the Northeast Atlantic margin, *Sedimentology*, v.47 (Supplement 1), 239-256.

Wynn, R.B., Weaver, P.P.E., Stow, D.A.V., and Masson, D.G. (2002) Turbidite depositional architecture across three interconnected deep-water basins on the Northwest African margin. *Sedimentology*, v.49, 669-695.

- Talling, P.J., Amy, L.A., Wynn, R.B., Peakall, J. and Robinson, M. (2004) Beds comprising debrite sandwiched within cogenetic turbidite: origin and widespread occurrence in distal depositional environments. *Sedimentology*, v.51, 163-194.
- Wynn, R.B. and Masson, D.G. (2003) Canary Islands landslides and tsunami generation. In: Proc. 1st Int. Symposium on Submarine Mass Movements and their Consequences (Ed. by J. Mienert and J. Locat), Kluwer, Dordrecht, 325-332.
- Henrich, R., Hanebuth, T.J.J., Krastel, S. and Wynn, R.B. Architecture and sediment dynamics of the Mauritania Slide Complex. *Sedimentology*, in review.
- Masson, D.G., Harbitz, C.B., Wynn, R.B., Pedersen, G. and Løvholt, F. Submarine landslides – process, triggers and hazard prediction. *Phil. Trans. Roy. Soc.*, London, in review.

POSTER ABSTRACTS

Climate control on the Pliocene deepwater deposits of the Periadriatic basin, central Italy

Albianelli, A.¹, Cantalamessa, G.², Di Celma, C.², Didaskalou, P.², Lori, P.², Napoleone, G.¹, and Potetti, M.².

1. Dipartimento di Scienze della Terra, Università di Firenze, 50121 Firenze, Italy.

2. Dipartimento di Scienze della Terra, Università di Camerino, 62032 Camerino, Italy.

The middle to late Pliocene fill of the Periadriatic basin, the Plio-Pleistocene foreland basin developed on the flexural Adria Plate, in central Italy consists of several conglomerate and sandstone beds that occur as individual or composite wedges encased within a considerably thicker succession of hemipelagic mudstones. A detailed facies analysis of two of these composite wedges and encasing sediments exposed in the Monte dell'Ascensione and Offida areas (Fig. 1), suggests deposition within an overall base-of-slope setting and reveals that most of the sediments were deposited by a wide spectrum of subaqueous sediment gravity flows, such as muddy slumps, non-cohesive debris flows, cohesive mud flows, and turbidity currents. Component facies are superposed in fining-upward trends and their vertical stacking imparts a strong cyclic architecture to the studied successions. Each cycle, 20 to 65 m thick, comprises basal non-cohesive debris-flow conglomerates, which grade downstream into turbiditic sandstones, overlain by cohesive mud-flow pebbly mudstones and slumped muddy horizons. The boundaries between successive cycles are expressed by erosional surfaces across which a relatively coarse-grained interval overlies a relatively fine-grained interval. This relationship, commonly used as evidence for a basinward shift in facies, suggests that the coarse-grained basal deposition was associated with the formation of the erosional unconformities and occurred when sediment flux to the base-of-slope setting increased in response to relative sea-level lowering. Inversely, deposition of the overlying mud-prone interval occurred during the ensuing relative sea-level rise when clastic material was preferentially stored on the shelf and a negligible volume of coarse-grained deposits entered the deep basin. On these basis, we interpret each cycle as a depositional sequence and the component coarse-grained and fine-grained intervals as the lowstand systems tract and the transgressive-to-highstand systems tract, respectively. As a consequence, the two composite wedges studied at Monte dell'Ascensione and Offida, each resulting by the stack of five of such a sequence, have been interpreted as two low-frequency lowstand sequence sets, each composed of stacked higher-frequency sequences dominated by their lowstands.

The tight biostratigraphic and magnetostratigraphic control available on this clastic succession reveals that the markedly cyclic arrangement of the composite wedges developed in response of periodic changes of climate due to obliquity-driven, sixth (~40ka)-order Milankovitch cycles and allows a precise correlation of high-frequency sequences with the middle to late Pliocene oxygen isotope curve. The key palaeomagnetic tie-points used for pinning the isotope record to the studied succession are the Gauss/Matuyama boundary (2.58 Ma), the Reunion Subchron (2.15–2.14 Ma), and the Olduvai Subchron (1.94–1.76 Ma), which have been correlated to the magnetic polarity time scale using several biostratigraphic constraints.



Figure 1. Representative outcrop photos. A) Northward panoramic view of Monte dell'Ascensione showing the stack of five conglomerate packages and the encasing mudstones. B) General view of the fourth and fifth conglomerate packages near Offida. The recessive intervals consist of cohesive mud-flow pebbly mudstones and slumped muddy horizons.

Glacial-interglacial sedimentation in the deep continental margin off Portugal

Arzola, R.

NOC

The sedimentary processes and dynamics that go on at continental margins are poorly understood, mainly because of the difficulties involved in sampling at these deep-sea locations of varying bathymetry. However, not only are continental margins sites of high biodiversity and organic carbon burial, they are also locations of hydrocarbon recovery, telecommunication cables and pipelines, and building of large infrastructures such as oil rigs, which give continental margins a large economic as well as biological importance. Because sedimentary processes affect all of these things, learning more about what controls sedimentation at these locations is of vital importance. The Portuguese margin has been chosen for this investigation because of its complexity as a canyon-dominated margin with a high fluvial sediment input.

Multi-Sensor Core Logging and mineralogical analyses were used to identify different types of deposit within the five piston cores used in this study, these being turbidites, hemipelagite and ice-rafted deposits. $\delta^{18}O$ and foraminifer species counts allowed the stratigraphy to be obtained for the sediment record. From this, it can be determined whether each type of deposit was laid down during a glacial or an interglacial.

The results suggest that the general sedimentation pattern in the Portuguese continental margin is climatically controlled. Turbidity currents occur throughout the Quaternary, although mainly during the glacial periods when lower sea levels allowed increased sediment input by rivers. Heinrich Layers are found as distinct peaks in magnetic susceptibility, P-wave velocity and density, which are composed of a coarse-grained, iron-rich mineralogy – they are the deposits of ice-rafting Heinrich Events that were caused by periodic ice sheet collapses in the North Atlantic during glacial periods. The magnetic susceptibility profiles show that interglacials have low values, and this is due to dilution by non-magnetic $CaCO_3$, which is controlled by the calcite compensation depth and therefore climate. Although glacial periods have high peaks caused by the Heinrich Events, the overall profile is consistently low for both glacials and interglacials. This study suggests that the reason for the observed low magnetic susceptibility profile throughout the Quaternary is that something is diluting the signal. A likely source for this is low magnetic susceptibility turbidity currents, which are common in the Portuguese continental margin and especially during times of low sea level.

Statistical analysis of stratal patterns and facies changes: deconvolving controls on the depositional architecture of deep-sea confined clastic units

Bersezio, R., Felletti, F., Micucci, L., and Riva, S.

Dipartimento Scienze della Terra, Università di Milano, via Mangiagalli 34, 20133 I-Milano, Italy.

The turbiditic sand-lobes hosted within confined basins at the active margins provide interesting analogues of some deep-sea clastic reservoirs. Their depositional architecture derives from the complex interplay of external forcing vs. intrabasinal and autocyclic controls on sedimentation. Therefore, knowing to which factors responds any measurable depositional variable should help to quantify and to forecast facies changes and stacking pattern styles throughout a turbiditic reservoir; vice versa the statistical knowledge of sedimentary trends could help to infer the most influent controls on deposition. At this purpose, we applied a simple statistical analysis to the study of the well-known and well-exposed Cengio Turbidite System (CTS; Late Oligocene, episutural Tertiary Piedmont Basin, Northern Italy). It consists of several stacked sandstone bodies ("lobes") which were deposited within a narrow and confined structural depression. At present the CTS succession is exposed over a 14 km² wide area, where it can be as thick as 170 m. The outstanding features of the CTS are: 1) stacking of several almost tabular sandstone-mudstone bodies, thin to medium bedded and metres to decametres thick, that pinch out onlapping the marginal slope mudstones. Progressive filling of the basin determined widening of the depositional area through time, as it is shown by shifting of onlap terminations; 2) coupling of thick-bedded and amalgamated sandstone units, that are flat-shaped and metres to decametres thick, with the sandstone-mudstone units, mostly in the lower part of the CTS; 3) occurrence of different facies trends from the depocentres towards the distal sectors and towards two different types of terminations (i.e. "mild onlaps", almost parallel to palaeocurrent trends and "abrupt onlaps", almost normal to the same). A simple uni- bivariate statistical analysis was performed to quantify facies associations and describe the behaviour through space and time of several sedimentary variables: grain-size, bed thickness, sand/mud ratio, frequency of facies, percentage of amalgamated bed vs. total number of beds, graded/massive facies ratio, laminated/massive+graded facies ratio. The relationship between basin confinement and size and efficiency of sediment flows was explored by the analysis of bed thickness distribution (thickness of beds vs. facies, frequency distribution of bed thickness). This analysis helped to separate the influence of basin morphology and of the changing degree of confinement (that is the most influent local factor, linked to intrabasinal tectonics) from the external controls on volume and type of sediment load of the turbiditic flows entering the basin. The outstanding feature is the different behaviour of the considered variables throughout the sandstone-mudstone units and the amalgamated sandstone bed-sets, moving away from the onlap terminations. In fact, the statistics of facies variation of the sandstone-mudstone units provided evidence of flow transitions occurring downcurrent with respect to the depocentre and onlap areas. By contrast the thick-bedded and amalgamated sandstone bed-sets showed some changes only close to their terminations. The cumulative frequency distribution of bed thickness follows a segmented power-law with two steps, corresponding to deviations from the power-law trend, that occur for bed thickness respectively larger than 32 cm and 134 cm. The correspondence between thickness of beds and facies suggests that the first step can be interpreted as a consequence of the down-current transition from high-density flows to low-density turbulent flows. It occurs within the population of beds forming the sandstone-mudstone units. The thick beds of the amalgamated sandstone bed-sets contribute almost exclusively to the second step. Therefore it presumably indicates the critical thickness of the largest beds that could spread throughout the entire basin. These facts can be interpreted considering the differences of flow volume and efficiency that characterize the deposition of the two types of sandstone bodies, with respect to basin morphology. It seems reasonable that, even if the basin was widening due to progressive filling, the large-volume and poorly efficient, sand-laden sediment flows of the amalgamated sandstone bed-sets were fully contained within an area of enclosed bathymetry, that was also too small to permit the development of flow transitions. Differently, the turbidity flows that formed the mudstone-sandstone bodies were small and efficient enough, with respect to the basin width, to be able to segregate downcurrent textures and facies. The striking difference between the two types of turbiditic units may be attributed to the repetitive increase of volume of the sediment gravity flows entering the basin that forced the depositional system to fill the available room and then to aggrade. The progressive widening of the depositional area made this mechanism less efficient through time, as it is witnessed by the disappearance of the massive and amalgamated sandstone units in the upper part of the CTS and through the overlaying turbiditic units. Yet, whether the external control capable to force the repetitive changes of flow volume and density was climate cyclicality or something else, like a sequence of tectonic pulses, remains unclear.

Morpho-sedimentary features of the distal Cap Ferret Fan (Bay of Biscay, NE Atlantic Sea)

Ercilla, G., and Marconi Team

Instituto Ciencias del Mar, CSIC, Paseo Marítimo de la Barceloneta, 37-49, 08003 Barcelona, Spain.

High resolution acoustic data (TOPAS and airgun seismic records, and multibeam bathymetry) were acquired for knowing the stratigraphic architecture and geological features of the East Cantabrian continental margin (Spain) and Biscay Abyssal Plain. These data have allowed the mapping of the sea-floor and near surface features of the Cap Ferret Fan on the eastern Biscay Abyssal Plain (at > 4000 m water depth). This system is fed by the Cap Ferret Canyon that evolves basinward to the Cap Ferret Channel, both on the French continental margin (Cremer, 1983; Faugères et al., 1998). This channel runs and transports the sediment down to the Biscay Abyssal Plain. Here, new sediment sources coming from the Spanish continental margin also feed the turbidite system; sediment is transported by the Cap Breton, Santander, Torrelavega, Lastres and Llanes canyons. The convergence of sediment coming from French and Spanish continental margins contributes to develop the distal sector of the Cap Ferret Fan (Ercilla et al., 2005).

The main morpho-sedimentary elements that comprise this sector of the fan are the followings: the Cap Ferret leveed channel, small-scale turbidite channels, sediment waves, scours of channel-lobe transition (Fig. 1), mass-flow deposits, and distal sheetlike turbidites. The Cap Ferret leveed channel here mapped corresponds to the northern Cap Ferret channel of Faugères et al (1998). In fact, those authors differentiate two turbidite channels in the study area, northern and southern. But, the new data, especially those obtained with the swath bathymetry shows that only one channel (the northern channel) occurs on the distal part.

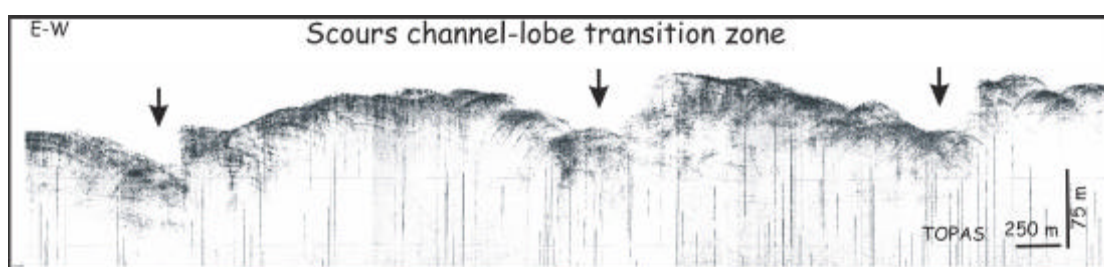


Fig. 1. - TOPAS seismic profile showing the scours identified immediately downslope the Cap Ferret channel mouth.

The small-scale turbidite channels refer to those channels that represent the seaward continuation of the talwegs eroding the Torrelavega and Santander canyons. These channels display a scale of hundreds of meters and have a sinuous pattern. The sediment waves occur on the external face of the Cap Ferret levee. The crests of these waves are sinuous with bifurcations and roughly parallel to the regional slope. In spite that there are not seismic lines that cut perpendicularly to crestlines, the morphological measurements made on waves indicates that their dimensions are variable, ranging wave height between 1 and 25 m, and wave length between 534 and 2600 m. The scours occur in the Cap Ferret channel termination, immediately downslope when this channel is not confined by the Aquitania High. The scour area extends about 107 km in a channel-lobe transition zone. They have dimensions about 5 km wide, 20 m relief, and up to 15 km long. Mass-flow deposits and distal sheet-like turbidites represent the predominant basinal recent deposits on the abyssal plain. Their presence suggest that sediment flow processes are the mechanisms responsible of formation of the main morpho-sedimentary features of the distal Cap Ferret submarine fan, and they come from the large canyons on the French and Spanish continental margins, that represent the major sediment pathways for the fan.

Cremer, M. 1983. *Approches Sedimentologique et Geophysique de Accumulations Turbiditiques. L'Eventail Profond du Cap-Ferret (Golfe de gascogne), La serie des Gres (Alpes de Haute Provence).* Ph.D. University of Bordeaux, 344 pp.

Ercilla, G., Casas, D., Estrada, F., Farran, M., García, M., Alonso, B., Vázquez, T., Pérez, C., Sayazo, M., Maestro, A., Acosta, J., Gómez, M., Gómez, R., Gallart J., 2005. Submarine erosion on the Cantabrian continental margin and Biscay abyssal plain (Atlantic N Iberian). EGU General Assembly 05, Viena 24-29 Abril. Geophysical Research Abstracts. Vol.7, 03445.

Faugères, J.C., Imbert, P., Mézerais, M.L., Crémer, M., 1998. Seismic patterns of a muddy contourite fan (Vema Channel, South Brazilian Basin) and a sandy distal turbidite deep-sea fan (Cap Ferret system, Bay of Biscay) : a comparison. *Sedimentary Geology*, 115: 81-110.

The Plio-Quaternary Magdalena Turbidite System

Estrada, F.*, Alonso, B., and Ercilla, G.

*CSIC, Instituto Ciencias del Mar, Passeig Maritim de la Barceloneta, 37-49, 08003 Barcelona, **
Corresponding author : festrada@icm.csic.es

The Magdalena Turbidite System (MTS) is the second largest modern turbidite system of the South American subcontinent (Fig. 1), however little is known about its stratigraphic architecture. It develops on the Caribbean Margin of Colombia, in the area of oblique convergence between the South American and the Caribbean tectonic plates. Major fan development occurred after the Miocene, forming a sedimentary wedge that remains practically undeformed in spite of the active tectonics of the area.

The MTS development during the Plio-Quaternary time is characterized by three main periods of sedimentary evolution (Fig. 2): i) Pliocene-Early Pleistocene; ii) Early-Late Pleistocene; and iii) Holocene.

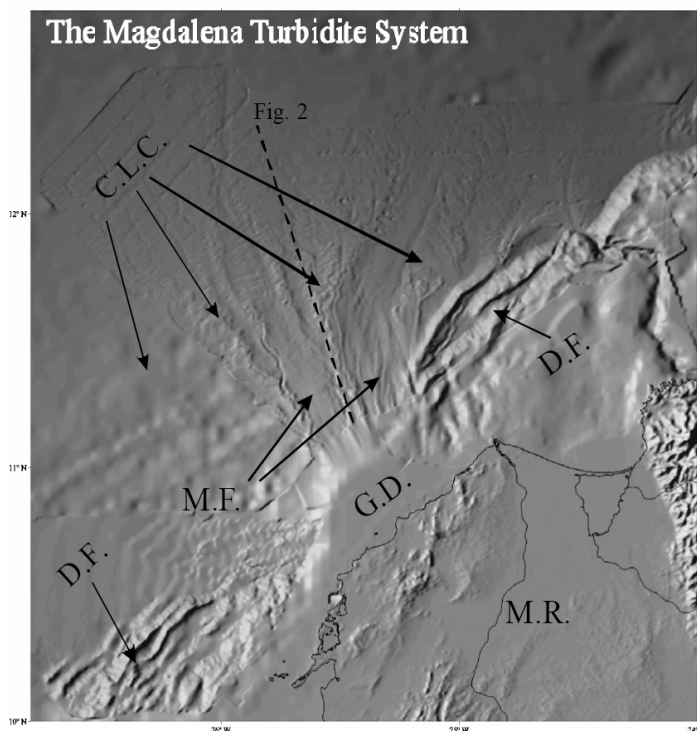


Figure 1. - Shaded relief map of the Magdalena Turbidite System. Legend: (M.R.) present day Magdalena River; (G.D.) Galerazamba Delta; (C.L.C) channel-levee complexes; (M.F.) mass-flow deposits; (D.F.) deformational front.

During Pliocene-Early Pleistocene the fan construction was predominantly controlled by mass-flows, a broad drainage network of erosive turbidity channels characterized by cut-and-fill features, and apron deposits. The generalized instability of the margin obeys to a period of intense tectonic activity (Andean orogeny) which produced a deformational front that seems to be less active in recent times (Fig. 1). The sedimentary sequence is characterized by mass-flow deposits which form chaotic wedges on the continental slope and subtabular to lens shaped bodies on the continental rise (Fig. 2). In addition, in the area where the MTS remains practically undeformed, there are several levels of erosive channel networks and apron deposits (Fig. 2). During Early-Late Pleistocene fan construction resulted from the lateral switching of fan depocenters and margin tectonics affected the position of the Magdalena River with consequent formation of several canyon-channel systems along the margin (Fig. 2). These systems are characterized by short and small canyons connected to channel-levee complexes initiated in the upper reaches of the continental slope, and evolve downslope to a radial dendritic pattern with a lobe associated to each channel mouth (Fig. 1). The canyon-channel emplacement seems to be conditioned by the original abrupt physiography of the margin and by the rapid progradation, directly onto the continental slope, of the Galerazamba Delta, what also favours the occurrence of mass-flow deposits mainly on the continental slope. The channel-levee complexes located

close to the deformational front are slightly folded and onlapped by mass-flow deposits, indicating recent tectonic activity.

Finally, during the Holocene time the Magdalena River has shifted till the present day position. The continental shelf is practically inexistent and the delta progrades onto the continental slope where several canyons develop and cut the deformational front (Fig. 1), as a consequence the sediments are trapped between the structural highs. Two main areas of mass wasting deposits occur in the abandoned Pleistocene channel-levee complexes, probably related to recent uplifting of the Galazeramba Delta and the shallower water position of the shelf-break (50 m). These mass-flows evolve downslope to unchanneled turbidity currents that result in a broad sediment wave field that covers the distal parts of the MTS (Fig. 2).

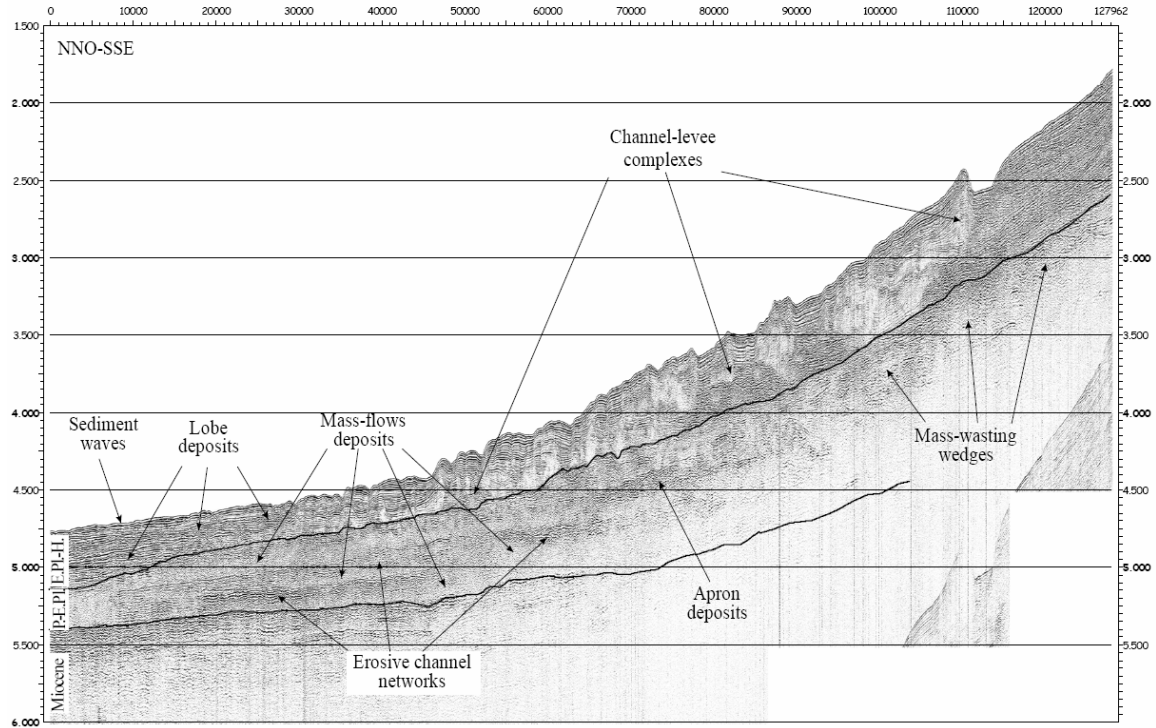


Figure 2. - Airgun seismic profile along the Colombian margin. Legend: (P-E.Pl) Pliocene to Early Pleistocene; (E.Pl.-H) Early Pleistocene to Holocene. See location on figure 1.

Sources and timing of the Agadir Basin turbidite fill, NW Africa

Frenz, M., Wynn, R.B., and Masson, D.G.

National Oceanography Centre Southampton (NOCS), European Way, Southampton SO14 3ZH, UK.

The Agadir Basin is a relatively small deep-sea basin (~4500 m water depth) situated off NW Africa, between the Canary Islands to the south and the Madeira archipelago to the north. The recent (~200 ka) sedimentary fill of the basin consists of hemipelagic mud (dominantly coccolith and foraminiferal ooze) separated by numerous turbidites up to ~3 m thick. The turbidites are derived from two principle sources: the Moroccan continental margin and the volcanic Canary Islands. The sources of the individual turbidites can be easily distinguished on the basis of their magnetic susceptibility (MS) signature. Moroccan Margin turbidites show low MS due to a lack of heavy minerals/volcaniclastic components in the dominantly siliclastic source area. In contrast, Volcaniclastic Canary Island turbidites, rich in basalt fragments and volcanic glass, show exceptionally high MS.

Moroccan Margin turbidites are supplied to the Agadir Basin via the Agadir Canyon-Channel System; they then pass along the Agadir Basin and eventually deposit considerable amounts of mostly fine-grained material in the Madeira and Seine Abyssal Plains, up to 1500 km from source. A variety of techniques can be applied allowing correlation of the largest turbidites between all three basins (Weaver and Rothwell, 1987; Wynn et al., 2002). Although many turbidite systems show increased activity during sea-level lowstands, the timing of large Moroccan Margin turbidites appears to coincide with periods of changing sea level, and there is some evidence that sea-level changes of higher magnitude seem to trigger turbidity currents of higher volume (Weaver and Kuijpers, 1983; Weaver et al., 1992). This is presumably related to the fact that the source area has relatively minor fluvial input and therefore low sediment supply (e.g. only ~12 major turbidites have come from this source in the last 200 ka), while its location offshore of the Atlas Mountains suggests that tectonic/seismic activity may be an important influence.

Volcaniclastic Canary Island turbidites are triggered by major Canary Island landslides. Over the past one million years, Canary Island landslides occurred, on average, about once every 100 ka (Masson et al., 2002). Landslide-derived turbidites deposited in the Agadir Basin during the last 200 ka include Bed 2 (emplaced at ~15 ka and linked to the El Golfo landslide on El Hierro) and Bed 14 (emplaced at ~180 ka and linked to the Icod landslide on Tenerife). Besides slope instabilities caused by sea level changes (see Moroccan Margin turbidites), volcanic activity may be an important additional trigger for these landslide-derived flows. The exact linkage between landslide and turbidity current is still under investigation, but it is hoped that study of landslide-derived turbidites may provide indications for the nature of the source landslide, which has applications when assessing the tsunamigenic potential of any future event.

Masson, D.G., Watts, A.B., Gee, M.R.J., Urgeles, R., Mitchell, N.C., Le Bas, T.P. and Canals, M. 2002.

Slope failures on the flanks of the western Canary Islands. *Earth Science Reviews*, 57: 1-35.

Weaver, P.P.E. and Kuijpers, A. 1983. Climatic control of turbidite deposition on the Madeira Abyssal Plain. *Nature*, 306.

Weaver, P.P.E. and Rothwell, R.G. 1987. Sedimentation on the Madeira Abyssal Plain over the last 300,000 years. In: *Geology and Geochemistry of Abyssal Plains* (Eds P.P.E. Weaver and J. Thomson), Geological Society Special Publication, 31, pp. 71-86. Blackwell, Oxford.

Weaver, P.P.E., Rothwell, R.G., Ebbing, J., Gunn, D. and Hunter, P.M. 1992. Correlation, frequency of emplacement and source directions of megaturbidites on the Madeira Abyssal Plain. *Marine Geology*, 109: 1-20.

Wynn, R.B., Weaver, P.P.E., Masson, D.G. and Stow, D.A.V. 2002. Turbidite depositional architecture across three interconnected deep-sea basins on the north-west African Margin. *Sedimentology*, 49: 669-695.

Holocene turbidite history in the Cascadia Subduction Zone shows the potential to develop paleoseismic methods for the Sumatra and other subduction zones

Gutiérrez-Pastor, J.^{1*}, Nelson, C.H.¹, Goldfinger, C.², and Johnson, J.³

1. C.S.I.C.- Universidad de Granada. Instituto Andalúz de Ciencias de la Tierra. Campus de Fuentenueva. 18002 Granada, Spain.

2. COAS. Oregon State University 104 Ocean Admin Bldg. Corvallis, OR 97331-5503, USA.

3. Monterey Bay Aquarium Research Institute 7700 Sandholdt Rd. Moss Landing, CA 95039, USA.

* Corresponding author : juliagp@ugr.es

Marine and onshore paleoseismic records are being studied along the Cascadia subduction margin. Submarine channels have recorded a Holocene history of turbidites mainly triggered by great earthquakes. Cascadia subduction margin is an ideal place to develop a turbidite paleoseismologic method because: (A) a single subduction zone fault underlies the margin, (B) multiple tributary canyons and a variety of turbidite systems and sedimentary sources exist to examine for synchronous turbidite events, and (C) excellent turbidite marker beds with Mazama ash (MA) (7627 ± 150 cal yr BP)(Zdanowicz et al., 1999) are present for correlation of events in turbidite systems within the northern two thirds of the basin. We have found ~13 post-Mazama ash turbidites along the whole margin and 17 Holocene events. Synchronicity of Holocene the turbidite event record for ~800 km along the northern two thirds of the Cascadia Subduction Zone is best explained by paleoseismic triggering of great earthquakes (of ~ M 9).

We have two methods of looking at the turbidite event record: 1) ^{14}C ages to estimate recurrence times between paleoseismic events and, 2) analysis of hemipelagic sediment thickness (H) between turbidites because hemipelagic thickness (H)/sedimentation rate = recurrence time between events. Using the first method, samples are taken in hemipelagic sediment below each turbidite event and planktonic forams are dated to obtain AMS ^{14}C ages. The ^{14}C recurrence times are calculated by the subtracting between one event and a subsequent event. The H method can be used to independently evaluate the ^{14}C ages because of the following reasons: the deep sea provides an independent time yardstick derived from a constant rate of hemipelagic sediment deposited between turbidites, the hemipelagic thickness/sedimentation rate = yrs which provides a set of turbidite recurrence times and ages to compare with similar ^{14}C data sets, H data from multiples cores can be used to correct ^{14}C ages obtained from eroded hemipelagic sediment and the hemipelagic data is available for every T event from multiple cores at each key channel site compared to a single incomplete set of radiocarbon ages at each key site. Most important, the H method defines accurate minimum recurrence times for great earthquakes in the Cascadia Subduction Zone, because H erosion corrections for some ^{14}C ages increase minimum recurrence times by several hundred years when they previously appeared to be as low as ~ 100 yrs (Nelson et al., 2003). This correction method is crucial because the coastal paleoseismic stratigraphic record has no independent H method to assess reliability of minimum recurrence times based only on ^{14}C ages.

From both ^{14}C and H data, we find a repeating pattern of recurrence times in the Holocene paleoseismic history of the Cascadia Subduction Zone. The recurrence pattern consists of a long time interval followed by one to three short intervals. The pattern is shown by both ^{14}C and H recurrence times between turbidites. Utilizing the most reliable ^{14}C and H data sets from turbidites for the past ~ 5000 yr, minimum recurrence times are ~ 300 yr and maximum are ~ 1300 yr (Nelson et al., 2003 and Gutierrez-Pastor et al., 2004).

Our paleoseismic methods developed in the Cascadia Subduction Zone could be applied to the Sumatra Subduction Zone because of the similar geological setting and history of megathrust earthquakes, like the 1700 AD Cascadia or 2004 AD Sumatra event. In Sumatra, an estimated 1200 km of faultline slipped about 15 m on the interface of the subducted India and the overriding Burma plates (<http://earthquake.usgs.gov/>), comparable to the rupture length shown by the Cascadia turbidite record. In Cascadia like Sumatra, tsunamis extend over an ocean wide area. For example Satake et al, 1996 have shown that an 1700 AD earthquake from the Cascadia Subduction Zone generated a tsunami of 3 meters height along the Japanese Coast. The evidence from the most recent tsunamis generated by great earthquakes in the Sumatra and Cascadia Zones suggest that obtaining a turbidite paleoseismic record could be help define periodicity of great earthquakes in the Sumatra and other subduction zones.

Atwater BF, Hemphill-Haley E. 1997. Recurrence intervals for great earthquakes of the past 3500 years at northeastern Willapa Bay, Washington: U.S. Geological Survey Professional Paper 1576, 108
Atwater, B F, Nelson H, Goldfinger C.2004. Onshore-offshore correlation of geologic evidence for great cascadia earthquakes--permissive agreement between Washington estuaries and Cascadia Deep-Sea

- Channel: Eos Trans. AGU, 85(47), Fall Meet .Suppl., Abstract T12B-01.
- Gutiérrez-Pastor J, Nelson CH, Goldfinger C, Johnson JE. 2004. Turbidite Stratigraphy on active tectonic margins and implications for Holocene paleoseismicity of the Cascadia Subduction Zone and northern San Andreas Fault: 32 nd Int. Geol. Congr. Abs. V., pt. 2, Abs. 265-5, p.1193.
- Kelsey HM, Witter RC, Hemphill-Haley E. 2002. Plate-boundary earthquakes and tsunamis of the past 5500 yr, Sixes River estuary, southern Oregon. Geol. Soc. Am. Bull. V 114 p 298—314
- Nelson, AR, Atwater, BF, Brobowski, PT, Bradley, LA, Clague, JJ, Carver, GA, Darienzo, ME, Grant, WC, Krueger, HW, Sparks, R, Stafford, TW, and Stuiver, M. 1995a. Radiocarbon evidence for extensive plate-boundary rupture about 300 years ago at the Cascadia subduction zone. Nature, V 378, p 371-374.
- Nelson CH, Goldfinger C, Johnson JE, Gutierrez-Pastor J. 2003. Holocene history of great earthquakes in the Cascadia Subduction Zone based on the turbidite event stratigraphy: EOS Trans. AGU, 84(46), Fall Meet. Suppl., Abstract, S421-05
- Nelson CH, Goldfinger C, Gutiérrez-Pastor J, Johnson J E. 2004. Holocene turbidite recurrence frequency off northern California: insights for San Andreas fault paleoseismicity: Eos Trans. AGU, 85(47), Fall Meet .Suppl., Abstract T12B-08.
- Satake K, Shimazaki K, Tsuji Y, Ueda K. 1996. Time and size of a giant earthquake in Cascadia inferred from Japanese tsunami records of January, 1700. Nature V 379, p 246-249.
- Witter RC, Kelsey HM, Hemphill-Haley E. 2003. Great Cascadia earthquakes and tsunamis of the past 6700 years, Coquille River estuary, southern coastal Oregon. Geological Society of America Bulletin, V 115(10), p 1289-1306.
- Zdanowicz CM, Zielinski GA, Germani MS. 1999. Mount Mazama eruption: calendrical age verified and atmospheric impact assessed. Geology, V 27, p 621-624.

Plio-Quaternary development of small-scale submarine valleys in the northern margin of the Alboran Sea in relation with sea-level changes

Lobo, F.J.¹, Fernández-Salas, L.M.², Ercilla, G.³, Alonso, B.³, García, M.³, Escutia, C.¹, Maldonado, A.¹, and Gómez, M.⁴.

1. CSIC, Instituto Andaluz de Ciencias de la Tierra, Avda Fuentenueva s/n, 18002 Granada, Spain.
2. IEO, Puerto Pesquero s/n, Apartado 285, 29640 Fuengirola, Spain.
3. CSIC, Instituto de Ciencias del Mar, Paseo Marítimo de la Barceloneta 37-49, 08003 Barcelona, Spain.
4. IEO, Servicios Centrales, C/ Corazón de María, 8- 8º Pl., 28080 Madrid, Spain.

The genetic link of small-scale submarine valleys with the sea-level position and the triggering sedimentary processes are a matter of discussion (Ercilla et al., 1994; Spinelli and Field, 2001). Recent studies have documented small-scale channels and gullies as tributary systems of larger canyons in the northern Alboran Sea margin, SW Mediterranean Sea (García et al., in press). The study area is located off the Guadalfeo River prodelta, where no significant submarine canyon is recognised. Instead, several types of small-scale submarine valleys seem to have developed during the generation of the stratigraphic architecture. Eastward, the canyon heads of the Motril and Carchuna Canyons incise the shelf and feed two main turbiditic systems (Pérez-Belzuz and Alonso, 2000). This study is based on the inspection of a number of geophysical data including EM3000D multibeam echo-sounder data, very high resolution TOPAS profiles and medium resolution Sparker seismic profiles (Fig. 1).

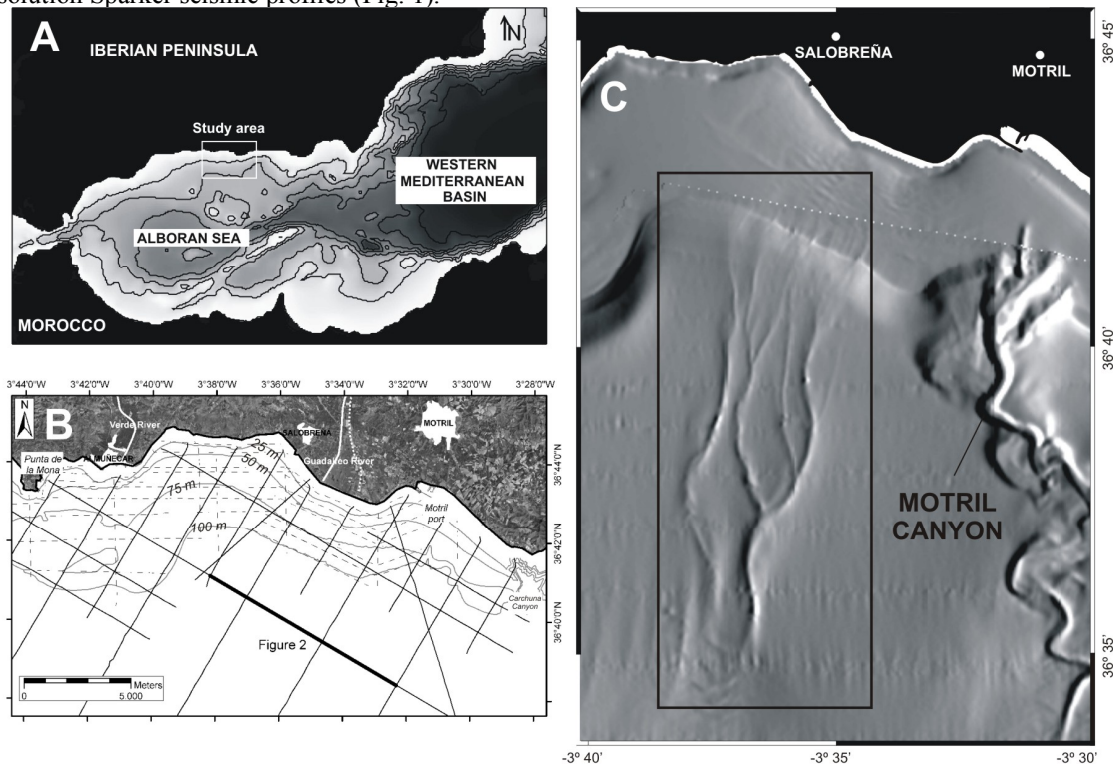


Figure 1: Geographical setting of the study area: A) location of the study area in the northern margin of the Alboran Sea; B) position of seismic profiles (TOPAS: dashed line; Sparker: continuous line); C) bathymetric shaded relief showing a network of small-scale submarine valleys starting at the outer shelf and apparently unconnected to major submarine canyons, such as the Motril canyon.

We focus on the interpretation of small-scale submarine valleys recognised on the Plio-Quaternary stratigraphic architecture, which shows three major progradational-aggradational cycles representing major sea-level falls followed by sea-level rises. In the study area, however, the aggradational unit of the second cycle is not identified. The valleys are classified according to their size and shape in: a) scours, with very low depth/width ratios; b) gullies, showing maximum widths of several hundred of meters and maximum depths less than 10 m; c) channels, more than 1 km wide and with maximum depths of several tenths of millimeters and showing an erosive character.

The Plio-Quaternary stratigraphic evolution of small-scale submarine valleys is documented on the upper

slope off the Guadalfeo River (Fig. 2). Broad scours or troughs are recognised in the lowest units (PU Alb-c and AU Alb-c). Upwards, erosive channels become the dominant feature, reaching the highest expression within PU alb-a, where a main channel with lateral small V-shaped gullies occurs. In this case, the association of channels with lateral gullies is defined as a complex channel system. Finally, gullies constitute the dominant type of small-scale submarine valley during deposition of the most recent seismic unit (AU Alb-a). The upper boundary of this unit is the present sea-floor, which also shows several V-shaped gullies at water depths higher than 220 m. Recent sea-floor gullies are also observed in multibeam bathymetric data, which show numerous straight channels on the outer shelf to upper slope.

The observed upward evolution of small-scale valleys in the Plio-Quaternary stratigraphic record developed as a response to changing depocenter location and to the progradational-aggradational pattern of the outer shelf. Gullies probably represented an embryonic stage and larger erosive channels preferentially developed during periods of sea-level fall and significant slope sediment discharge, or alternatively during long-lived lowstands. In contrast, gully generation was probably favoured under conditions of moderate slope deposition, from lowstand to highstand.

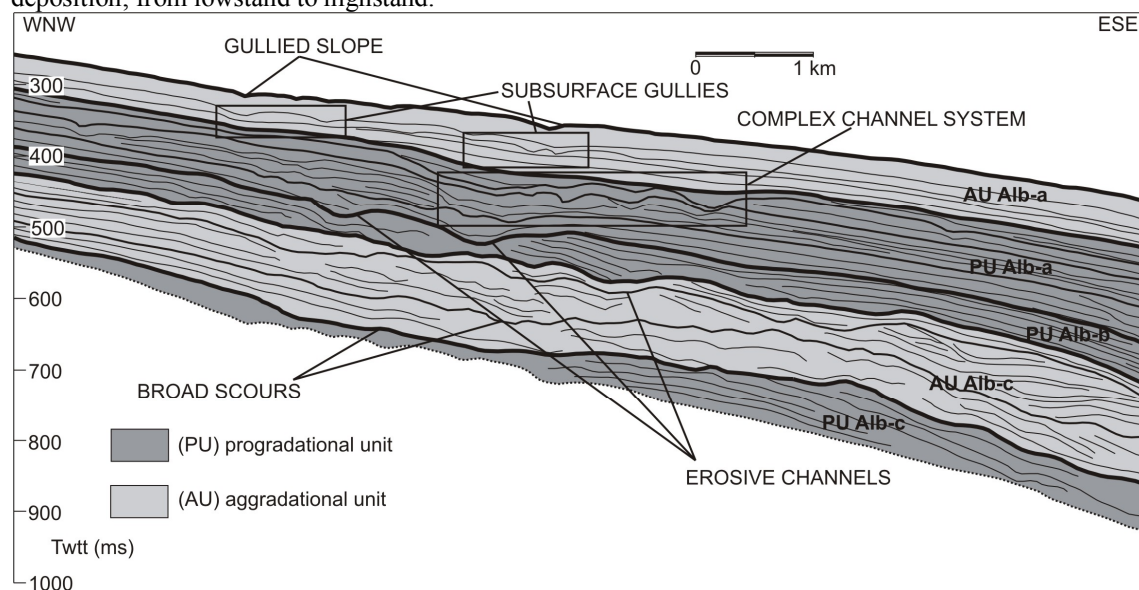


Figure 2: Interpretation of an along-slope seismic section (Sparkler profile), showing the stratigraphic evolution of small-scale submarine valleys off the Guadalfeo River.

Ercilla, G., Alonso, B. and Baraza, J., 1994. Post-Calabrian sequence stratigraphy of the northwestern Alboran Sea (southwestern Mediterranean). *Marine Geology*, 120: 249-265.

Garcia, M., Alonso, B., Ercilla, G. and Gracia, E., The tributary valley systems of the Almeria Canyon (Alboran Sea, SW Mediterranean): Sedimentary architecture. *Marine Geology*, In Press, Corrected Proof.

Pérez-Belzuz, F. and Alonso, B., 2000. Evolución sedimentaria reciente de dos sistemas turbidíticos del area de Motril (NE Alboran). Parte I: Sistema Turbidítico de Calahonda. *Geotemas*, 1: 203-206.

Spinelli, G.A. and Field, M.E., 2001. Evolution of continental slope gullies on the northern California margin. *Journal of Sedimentary Research*, 71: 237-245.

Acknowledgements: Multibeam and TOPAS data were collected in the framework of the ESPACE project (IEO). Sparkler profiles were collected by the IGME. F.J. Lobo received financial support through the Ramón y Cajal Program, 2004 call

Holocene Turbidite Paleoseismic Record Of Great Earthquakes On The Cascadia Subduction Zone: Confirmation By Onshore Records And The Sumatra 2004 Great Earthquake

Nelson, C.H.¹, Goldfinger, C.², Gutiérrez-Pastor, J.¹, and Johnson, J.E.³.

1. C.S.I.C.- Universidad de Granada. Instituto Andalúz de Ciencias de la Tierra. Campus de Fuentenueva. 18002 Granada, Spain.

2. COAS Oregon State University 104 Ocean Admin Bldg. Corvallis, OR 97331, USA.

3. Monterey Bay Aquarium Research Institute 7700 Sandholdt Rd. Moss Landing, CA 95039, USA, odp@ugr.es.

Marine turbidite stratigraphy (Goldfinger et al., 2003; Nelson et al., 2003), onshore paleoseismic records of tsunami sand beds and coseismic subsidence (Atwater and Hemphill-Haley, 1997; Kelsey et al., 2002; Witter et al., 2003) and tsunami sands of Japan (Satake et al., 1996) all show evidence for great earthquakes ($M \sim 9$) on the Cascadia Subduction Zone. When a great earthquake shakes 1000 kilometers of the Cascadia margin, sediment failures occur in all tributary canyons and resulting turbidity currents travel down the canyon systems and deposit synchronous turbidites in abyssal seafloor channels. These turbidite records provide a deepwater paleoseismic record of great earthquakes (see also Gutierrez poster). An onshore paleoseismic record develops from coseismic subsidence; by drowning forests on the coast and subsequent tsunami sand layer deposition. The recent Sumatra subduction zone great earthquake of 2004 and the 1700 AD Cascadia tsunami sand preserved in Japan (Satake et al., 1996) shows that ocean-basin wide tsunami deposits result from these great earthquakes, which rupture the seafloor for hundreds of kilometers.

The Cascadia Basin turbidites from multiple channel systems, provide the longest paleoseismic record of great earthquakes that is presently available for a subduction zone. A total of 17 synchronous turbidites have deposited along ~800 km of the Cascadia margin during the Holocene time of ~10,000 cal yr BP and ~13 have occurred since the Mt. Mazama eruption (7627 ± 150 cal yr BP) (Zdanowicz et al., 1999). Six other turbidites are more limited in extent. Because the first Mazama ash bearing turbidite marker bed was deposited ~7200 years ago and the youngest paleoseismic event in all turbidite and onshore records (Satake et al., 1996) is 300 AD, the average recurrence interval of events is ~575 yr, the same as that found in the longest onshore paleoseismic record (Witter et al., 2003). Linkage of the rupture length of these events comes from relative dating tools such as the "confluence test of Adams (1990), and from physical property correlation of individual event "signatures". We have two methods for obtaining a more detailed record of the paleoseismic recurrence history: ^{14}C ages and analysis of hemipelagic sediment thickness between turbidites (H), where $H/\text{sedimentation rate} = \text{time between turbidite events}$. Utilizing the most reliable ^{14}C and hemipelagic data sets from turbidites for the past ~5000 yr, minimum recurrence time is ~300 yr and maximum time is ~1300 yr (Nelson et al., 2003). There also is a recurrence pattern through the entire Holocene that consists of a long time interval followed by one to three short intervals that is apparent as well in the coastal records.

Both onshore paleoseismic records and turbidite synchronicity for hundreds of kilometers, suggest that the Holocene turbidite record of the Cascadia Subduction Zone is caused dominantly by triggering of great earthquakes similar in rupture length to the Sumatra 2004 earthquake. The tsunami deposit of the 1700 AD Cascadia event is estimated to result from a $M 9$ great earthquake that generated a tsunami 3 m high along the coast of Japan (Satake et al., 1996). Nanayama et al. (2003) show that historical earthquakes rupturing 100-200 km segments along the Kuril subduction zone bordering Hokkaido create tsunami deposits which extend less than 0.5 km inland from the beach; however, other pre-historic great earthquakes occurring about every 500 yr for the past 7000 yr, rupture much longer segments and create tsunamis greater than 5 m high that deposit tsunami sands more than 3 km inland. The 1700 AD and other great earthquakes of Cascadia for the past 7000 years also register an onshore record of significant coseismic subsidence and deposit tsunami sand beds along the entire Cascadia coast that extend inland as much as 10 km from the beach (Atwater et al., 1997, Nelson et al., 1995; Kelsey et al., 2002 and Witter et al., 2003). Because the ages of onshore paleoseismic events (Atwater et al, 2004) and recurrence patterns in general agree with the Cascadia turbidite paleoseismic record, and because the onshore Cascadia paleoseismic tsunami deposits are comparable to those created by great earthquakes in other subduction zones, the Cascadia onshore deposits also appear to reflect mainly a record of great earthquakes. Historic earthquakes that rupture smaller 100-200 km segments occur frequently in other subduction zones (Nanayama et al., 2003; Sieh et al. 2004), but appear to represent only six of the events in the Cascadia paleoseismic record. The perceived lack of shorter rupture length segments, thus smaller magnitude earthquakes, implied by the Cascadia record may result because

such earthquakes are not characteristic. The great earthquake tsunami deposits found around ocean basins (e.g. Japan 1700AD and Sumatra 2004), however, suggest that the similar tsunami deposits of Cascadia and synchronous turbidites for ~800 km may mainly preserve the paleoseismic record of great subduction zone earthquakes (nearly full margin rupture) and miss the record of smaller magnitude (shorter rupture length) events. The short historical record of subduction earthquakes leaves this question clouded in most locations. Consequently, the turbidite paleoseismology methods developed for the Cascadia subduction zone should be applied to better define the great earthquake history of Sumatra and other subduction zones.

- Adams J. 1990. Paleoseismicity of the Cascadia subduction zone: evidence from turbidites off the Oregon-Washington margin: *Tectonics* 9, 56-58.
- Atwater, B.F., Hemphill-Haley E., 1997. Recurrence intervals for great earthquakes of the past 3500 years at northeastern Willapa Bay, Washington: U.S. Geological Survey Professional Paper 1576, 108.
- Atwater, B. F., Nelson H., Goldfinger C., 2004. Onshore-offshore correlation of geologic evidence for great Cascadia earthquakes--permissive agreement between Washington estuaries and Cascadia Deep-Sea Channel: *Eos Trans. AGU*, 85(47), Fall Meet .Suppl., Abstract T12B-01.
- Kelsey H.M., Witter R.C., Hemphill-Haley E., 2002. Plate-boundary earthquakes and tsunamis of the past 5500 yr, Sixes River estuary, southern Oregon. *Geol. Soc. Am. Bull.* V 114 p 298—314
- Nanayamal, F., Satake K., Furukawa, R. Shimokawa, K., Atwater, B.F., Shigeno, K., Yamaki, S., 2003. Unusually large earthquakes inferred from tsunami deposits along the Kuril trench. *Nature* V 424, p 660-663.
- Nelson, A.R., Atwater, B.F., Brobowski, P.T., Bradley, L.A., Clague, J.J., Carver, G.A., Darienzo, M.E., Grant, W.C., Krueger, H.W., Sparks, R., Stafford, T.W., and Stuiver, M. 1995a. Radiocarbon evidence for extensive plate-boundary rupture about 300 years ago at the Cascadia subduction zone. *Nature*, V 378, p 371-374.
- Nelson C.H., Goldfinger C., Johnson J.E., Gutierrez-Pastor J. 2003. Holocene history of great earthquakes in the Cascadia Subduction Zone based on the turbidite event stratigraphy: *EOS Trans. AGU*, 84(46), Fall Meet. Suppl., Abstract, S42I-05
- Satake K., Shimazaki K., Tsuji Y., Ueda K. 1996. Time and size of a giant earthquake in Cascadia inferred from Japanese tsunami records of January, 1700. *Nature* V 379, p 246-249.
- Sieh K, Natawidjaja, D H, Natawidjaja, D H, Chlieh, M, Galetzka, J, Avouac, J, Suwargadi B W, Edwards R, Cheng H. 2004. The giant subduction earthquakes of 1797 and 1833, West Sumatra Characteristic couplets, uncharacteristic slip: *Eos Trans. AGU*, 85(47), Fall Meet .Suppl., Abstract T12B04.
- Witter R.C., Kelsey H.M., Hemphill-Haley E. 2003. Great Cascadia earthquakes and tsunamis of the past 6700 years, Coquille River estuary, southern coastal Oregon. *Geological Society of America Bulletin*, V 115(10), p 1289-1306.
- Zdanowicz C.M., Zielinski G.A., Germani M.S. 1999. Mount Mazama eruption: calendrical age verified and atmospheric impact assessed. *Geology*, V 27, p 621-624.

Late Quaternary (MIS 1-3) turbidite deposition in the California Continental Borderland: Comparison of closed and open basin settings

Normark, W.R.¹, Piper, D.J.W.², Romans, B.W.³, Covault, J.A.³, and McGann, M.¹.

1. US Geological Survey, 345 Middlefield Road, Menlo Park, California 94025, USA.

2. Geological Survey of Canada (Atlantic), Bedford Institute of Oceanography, P.O. Box 1006, Dartmouth, Nova Scotia, B2Y 4A2, Canada

3. Geological and Environmental Sciences Stanford University, Stanford, CA 94305, USA.

The California Borderland provides an excellent morphological and geological setting to study source-to-sink sedimentation during the Holocene. Active tectonism in and around the Borderland basins results in abundant sediment supply to the coastal areas even during sea-level highstand. High-resolution deep-towed boomer reflection profiles are used to develop a seismic-stratigraphic framework for six basins from offshore Santa Barbara to San Diego. From northwest to southeast, the basins progressively become deeper, with lower sills. The three northern basins – Santa Barbara, Santa Monica, and San Pedro -- are closed depressions that trap all turbidity-current input. In the three southern basins – western and eastern Gulf of Santa Catalina and San Diego Trough – the sills have been overtopped as the basin filled, resulting in substantial sediment transport to an adjacent, more seaward basin. To unravel the depositional history, this study utilizes 124 new radiocarbon dates from 43 USGS piston cores as well as 11 dates from ODP Site 1015 on the floor of Santa Monica Basin. For all but one of the basins (Santa Barbara), turbidite sediment funnelled to deeper water through submarine canyons forms the bulk of the basin fills.

Sea-level changes control the distribution of turbidite sedimentation within the offshore basins, by influencing the supply of sediment to submarine canyons, many of which remained (or became more) active during sea-level rise. As a result, half of the submarine canyons in the Borderland are active during the late Holocene highstand. While the inner basins may remain active during highstand, the sediment supply is generally reduced sufficiently that little coarse sediment is transported beyond to basins farther west. This study focuses on the development of turbidite facies during the late Quaternary in two of the basins: Santa Monica and San Diego Trough. Turbidite deposition in the closed Santa Monica Basin is the best documented because radiocarbon dating of ODP Site 1015 provides excellent chronostratigraphic control on the timing of turbidity current activity. The basin is principally fed by the Santa Clara River delta. In contrast, northern San Diego Trough, which also acted as an essentially closed basin in the Holocene, is fed by the beach-nourished canyons as well as the Santa Ana River delta through the Newport Canyon system. Turbulent ignitive flows initiated in beach-nourished canyon heads are highly erosive, resulting in incision of La Jolla fan valley and efficient sediment transport to southern San Diego Trough. In contrast, delta-derived systems show a more complex relationship through time between sea-level change, distributary switching, flow characteristics and resulting basinal deposits.

The Offlap Break Position Vs Sea Level: A Discussion

Tropeano, M.^{1*}, Pomar, L.², and Sabato, L.¹.

1) Dept. Geologia e Geofisica, Università di Bari, via Orabona 4, 70125 Bari, Italy.

2) Dept. Ciències de la Terra, Universitat de les Illes Balears, 07071 Palma de Mallorca, Spain.

* Corresponding author : labgeologia@geo.uniba.it

Sedimentary lithosomes with subhorizontal topsets, basinward prograding foresets and subhorizontal bottomsets are common in the geologic record, and most of them display similar bedding architectures and/or seismic reflection patterns (i.e. Gylbert-type deltas and shelf wedges). Nevertheless, in shallow marine settings these bodies may form in distinct sedimentary environments and they result from different sedimentary processes. The offlap break (topset edge) occurs in relation to the position of baselevel and two main groups of lithosomes can be differentiated with respect to the position of the offlap break within the shelf profile. The baselevel of the first group is the sea level (or lake level); the topsets are mainly composed by continental- or very-shallow-water sedimentary facies and the offlap break practically corresponds to the shoreline. Examples of these lithosomes are high-constructive deltas (river-dominated deltas) and prograding beaches. For the second group, baselevel corresponds to the base of wave/tide traction, and their topsets are mostly composed by shoreface/nearshore deposits. Examples of these lithosomes are high-destructive deltas (wave/tide-dominated deltas) and infralittoral prograding wedges (i.e. Hernandez-Molina et al., 2000). The offlap break corresponds to the shelf edge (shoreface edge), which is located at the transition between nearshore and offshore settings, where a terrace prodelta- or transition-slope may develop (Pomar & Tropeano, 2001).

Two main problems derive from these alternative interpretations of shallow-marine seaward prograding lithosomes:

1) both in ancient sedimentary shallow-marine successions (showing seaward prograding foresets) and in high resolution seismic profiles (showing shelf wedges), the offlap break is commonly considered to correspond to the sea-level (shoreline) and used to infer paleo sea-level positions and to construct sea-level curves. Without a good facies control, this use of the offlap break might cause a misinterpretation of the ancient sea-level positions and the inferred relative sea-level changes.

2) both baselevels, the sea level and the wave/tide base, govern sedimentary accumulation in wave/tide dominated shelves and, consequently, two offlap breaks may coexist (beach edge and shoreface edge) in shallow-marine depositional profiles (Carter et al., 1991). In this setting, two seaward-clinobedded lithosomes, separated by an unconformity, may develop during relative still-stand or falls of the sea-level (Hill et al., 1998; Fraser et al., 2005). In this case, the two stacked lithosomes could be misinterpreted as two different systems tracts, or sequences, and it could lead to the construction of an incorrect curve of sea-level changes.

Carter R.M., Abbott S.T., Fulthorpe C.S., Haywick D.W. and Henderson R.A. (1991): Application of global sea-level and sequence-stratigraphic models in Southern Hemisphere Neogene strata from New Zealand. Sp. Publ. IAS, 12, 41-65.

Fraser C., Hill P.R. and Allard M. (2005): Morphology and facies architecture of a falling sea level strandplain, Umiujaq, Hudson Bay, Canada. *Sedimentology*, 52, 141-160.

Hernández-Molina F.J., Fernández-Salas L.M., Lobo F., Somoza L., Diaz-del-Rio V. and Alverinho Dias J.M. (2000): The infralittoral prograding wedge: a new large-scale progradational sedimentary body in shallow marine environments. *Geo-Marine Letters*, 20, 109-117.

Hill P.R., Longuépée H. and Roberge M. (1998). Live from Canada: forced regression in action; deltaic shoreface sandbodies being formed. Abstracts, 15th Int. Cong. IAS, Alicante (Spain), 427-428.

Pomar L. and Tropeano M. (2001). The Calcarene di Gravina Formation in Matera (southern Italy): new insights for coarse-grained, large-scale, cross-bedded bodies encased in offshore deposits. *AAPG Bull.*, 85 (4), 661-689.

Sedimentary response to low- and high-frequency relative sea-level changes during the Quaternary filling of a foreland basin (Bradanic Trough, southern Italy)

Tropeano, M., Sabato*, L., Cilumbriello, A., and Pieri, P.

Dept. Geologia e Geofisica, Università di Bari, Italy

** Corresponding author : l.sabato@geo.uniba.it*

The Bradanic Trough is the Plio-Pleistocene foreland basin of the South Apennines chain (southern Italy). It is a narrow basin confined between the frontal thrusts of the chain and the exposed Apulian Foreland. Two different geodynamic stages of the foreland basin are recorded in its infilling deposits: a subsidence stage, which the basin suffered from Pliocene up to early Pleistocene, and an "anomalous" uplifting stage, which started at least during late-early - middle Pleistocene times. Both stages developed during the thrusts propagation. About 600 m of the 3-4 km basin-fill succession is exposed because of the Bradanic Trough Quaternary uplift, and this allows us to study the latest filling stages of this foreland basin.

Outcropping successions are mainly Quaternary in age and are characterised by shallow-marine deposits comprising carbonates of the Calcarene di Gravina Formation (at the base of the exposed succession on the foreland side of the basin), silty clayey hemipelagites of the Argille subappennine Formation (at the base of the exposed succession both in the depocentral part and on the chain side of the basin) and coarse-grained bodies of the "Regressive coastal deposits" (prograding from the chain onto the silty clayey hemipelagites).

The Calcarene di Gravina Formation (middle-late Pliocene to early Pleistocene in age) crops out in a backstepping configuration onto the flanks of the Apulian Foreland highs. It displays evidence of strong transgression onto a karstic region previously dissected in a complex horst and graben system. The backstepping configuration indicates deposition induced by high-frequency relative sea-level changes during a tectonically induced long-term relative sea-level rise on the foreland side of the basin. This formation simulates the transgressive systems tract of a low-order sequence developed when the subsiding basin was characterized by turbidite sedimentation in its migrating depocentre (only known by drills and seismic sections), and by shallow-marine sedimentation (on a large wedge-top area) in its chain side.

The Argille subappennine Formation (late Pliocene to middle Pleistocene in age) succeeds the carbonate sedimentation on the foreland side of the basin and represents the shallowing of the basin in the other sectors of the Bradanic Trough. Toward the Apennines chain, in the wedge-top area, the Argille subappennine Formation is very thin and laterally passes to coastal deposits; in the basin depocentre the same formation overlies turbidites. The Argille subappennine Formation may represent a regional-scale progradation of shelf systems during a tectonically induced still-stand, simulating a high-stand systems tract of a low-order sequence. High-frequency relative sea-level changes may be recorded by variation in fossil assemblages used as bathymetric indicators.

The "Regressive coastal deposits" (early to late Pleistocene in age) represent the upper part of the succession. They consist of coarse-grained wedges which lie on the hemipelagites of the Argille subappennine Formation in, alternatively, conformable or erosive contact in a downward shifting configuration, since altitude and age of these wedges decrease from the chain front up to the present-day coast. This kind of stratigraphic architecture (a downward-shifting configuration) indicates deposition induced by high-frequency relative sea-level changes during a long-term relative sea-level fall (uplift). The "Regressive coastal deposits" simulate a falling-stage systems tract of a low-order sequence.